# Distribution of STIM1 and Orai1 and associated proteins in subcellular fractions of rat liver

A thesis submitted in
fulfilment of the
requirements for the degree
of

**Doctor of Philosophy**

by

**Ka Cheung Tam**

*B.Sc., M.Sc.*


Department of Medical Biochemistry

School of Medicine, Faculty of Medicine, Nursing and Health Sciences

Flinders University

January 2015

# Table of Contents

## Declaration

I certify that the work embodied in this thesis is the result of original research Conducted while I was enrolled as a PhD student in the Department of Biochemistry at Flinders University, South Australia. This thesis does not incorporate without acknowledgment any material previously submitted for a degree or diploma in any university; and that to the best of my knowledge and belief it does not contain any material previously published or written by another person except where due reference is cited.

Ka Cheung Tam

## Acknowledgements

I would like to give my sincere thanks to my principle supervisor Professor Greg Barritt for providing me opportunity to study my PhD in his laboratory. His continuous support, guidance, and encouragement help me to overcome a lot of difficulties and let me can go through the whole journey of my PhD study and now I get there.

I would like to thank Dr. Tim Chataway and other people in proteomic laboratory. They provide me a lot of good advice and comments on my western blot and LC/MS analysis. I would like to thank Ms Jin Hau to conduct the western blot of TRMP2 and Prx4 experiments. Also thanks to Mr Eunus Ali for providing me lipid-loaded H4IIE cells for the detection of phosphorylation.

It is my pleasure that I can be one of the member in $Ca^{2+}$ signalling laboratory at Flinders university and the friendship I have in the laboratory will always be in my mind.

Finally, I want to thank all of my family members especially my parents. Without their endless support, I think I am not able to come to Australia to chase my goal. They provide me a good environment to focus on my study.

# Abbreviation List

| | |
|---|---|
| CAD: | CRAC activation domain |
| CCD: | Coiled-coil domain |
| cER: | Cortical endoplasmic reticulum |
| ER: | Endoplasmic reticulum |
| GFP: | Green fluorescence protein |
| HM: | Heavy microsome |
| $I_{CRAC}$: | $Ca^{2+}$ release-activated $Ca^{2+}$ current |
| $I_{SOC}$: | SOC current |
| IP: | Immunoprecipitation |
| $IP_3$: | Inositol- 1,4,5 trisphosphate |
| LC/MS: | Liquid chromatography tandem mass spectrometry |
| LM: | Light microsome |
| NAFLD: | Non-alcoholic fatty acid liver disease |
| RIPA | Radioimmunoprecipitation assay buffer |
| $PIP_2$: | Phosphatidylinositol 4,5-bisphosphate |
| PKC: | Protein kinase C |
| PLC: | Phospholipase C |
| PMCA: | Plasma membrane $Ca^{2+}$ ATPase |
| Prx 4: | Peroxiredoxine 4 |
| SERCA: | Sarco/endoplasmic reticulum $Ca^{2+}$ ATPase |
| SOCs: | Store- operated $Ca^{2+}$ channels |
| SOAR: | STIM1 Orai1 activating region |
| SDS-PAGE | Sodium dodecyl sulphate-polyacrylamide gel electrophoresis |
| SPCA | Secretory pathway $Ca^{2+}$ ATPase |
| STIM1: | Stromal interacting molecule 1 |
| SAM: | Sterile alpha motif |
| TRPM2: | Transient receptor potential melastatin 2 |
| OASF: | Orai1 activating small fragment |

# Summary

The activation of store-operated $Ca^{2+}$ channels (SOCs) at the plasma membrane is evoked by a decrease in the $Ca^{2+}$ concentration in the endoplasmic reticulum (ER). The pore of SOCs is formed by a multimer Orai1 polypeptides. Stromal interacting molecule 1 (STIM1), the activator of SOCs, is localised in ER. Activation of SOCs involves movement of STIM1 in the cortical ER (cER) membrane, interaction with Orai1 in the plasma membrane and opening of the channel pore. Most published results using overexpressed STIM1 and Orai1 tagged with GFP or another tag and fluorescence microscopy immunofluorescence have shown that for unstimulated liver cells and other cell types STIM1 is distributed widely in the ER and Orai1 is predominately located on the plasma membrane. Previous results from our laboratory have provided evidence that a small region of ER rather than the whole ER is required for the activation of SOCs in hepatocytes, and this region is close to plasma membrane, most likely in the cortical ER. Throughout the cell, the ER is present as either rough (ribosomes) or smooth (no ribosomes). The region of ER called cortical ER (cER) is a large network of tubule located near the plasma membrane without the attachment of ribosome, which is thought to be the region involved in protein trafficking. Taken together, these results suggest that STIM1 should predominantly be located in the smooth ER and Orai1 in the plasma membrane. Studies from other laboratories have provided evidence that other proteins, including members of the transient receptor potential family are required for either the activation or regulation of SOCs. Moreover there are many reports of proteins other than TRP which may interact with STIM1 or Orai1. Another key

finding done by other researchers from our laboratory demonstrated that the steatotic liver cells, the lipid accumulation in liver cell, causes the reduction of SOCs and the reduction can be reversed by the pretreatment of protein kinase C inhibitors. We hypothesised that the development of hepatic steatotsis is related to the phosphorylation on STIM1 and Orai1.

The overall aim of this study was to investigate the distribution of endogenous STIM1 and Orai1 in rat hepatocytes using subcellular fractions of liver. The specific aims were to determine the location of STIM1 and Orai1 in miscrosome, mitochondria and the plasma membrane fraction, to identify STIM1 binding proteins in the microsomal fractions, and to investigate phosphorylation of STIM1 and Orai1 on steatotic liver cells

Differential centrifugation and percoll gradient centrifugation were used to collect the subcellular fractions of nuclear fractions (NF), mitochondria (MT), heavy microsomes (HM)(derived from rough ER), light microsomes (LM) (derived from smooth ER), cytosol, and the plasma membrane (PM) from rat liver. The distribution of calreticulin (ER marker), Plasma membrane $Ca^{2+}$ ATPase (PMCA), STIM1 and Orai1 was determined by western blot. Immunoprecipitation combined with LC/MS or western blot were used to search the new STIM1 binding protein in heavy microsome. We employed the technique of immunoprecipitation and western blot to detect the phosphorylation of STIM1 and Orai1 from steatotic liver cells.

The results indicated that most STIM1 is found at heavy microsome (85%) with 12.5 % in light microsome. The majority of Orai1 was located in heavy

microsome (44%) and light microsome (27%) fractions with only small proportion in the plasma membrane fraction. No significant change in STIM1 and Orai1 distribution was observed after the treatment of phenylephrine to deplete $Ca^{2+}$ by activating α1-adrenergic receptor to induce activation of SOCs. The results of LC/MS and immunoprecipitation and western blot provides evidence that in heavy microsome STIM1 binds to peroxiredoxin 4. Several strategies were employed to test for the phosphorylation of STIM1 and Orai1 in steatotic liver cells. However, under the conditions of the experiments, no evidence for phosphorylation was obtained. Difficulties in using anti-phosphoserine antibodies and future alternative strategies to detect phosphorylated STIM1and Orai1 are discussed.

It is concluded that the distribution of endogenous STIM1 and Orai1 as revealed by subcellular fractionation has some important differences to that revealed using overexpressed tagged proteins: STIM1 is localised in the rough ER as well as the smooth ER and most likely has functions in the rough ER unrelated to activation of SOCE; STIM1binds to peroxiredoxin 4 in the rough ER and this may be part of a mechanism by which STIM regulates oxidation reactions or *vice versa*; the localisation of Orai1 in the microsomal fraction may reflect the role of Orai1 in regulating $Ca^{2+}$ in secretory granules as reported by others.

# Chapter I

# Introduction and Literature review

# Chapter I Introduction and Literature Review

## 1.1 Introduction

The liver is a central and important organ to perform different type of metabolisms. Various signalling molecules and pathways involve in regulating those metabolisms in the liver to maintain its normal function. $Ca^{2+}$ is one of the most important and universal signalling molecules in regulating the cellular functions including liver cells. The change of [$Ca^{2+}$] can activate or inhibite the activity of the enzymes in the metabolic reactions in liver cells. Store-operated calcium channels (SOCs) are one of the $Ca^{2+}$ -permeable channels located on the plasma membrane, which are controlled by the change of [$Ca^{2+}$] in the endoplasmic reticulum (ER). The activation of SOCs is vital for replenishing $Ca^{2+}$ to the depleted $Ca^{2+}$ store. Stromal interacting molecule 1 (STIM1) and Orai1 are the two essential molecules for determining the activity of SOCs. Although ER is a continuous membrane structure, the subregions on ER are identified and produce different functions. Therefore, it is important that the localisation of STIM1 and Orai1 in subcellular level is a useful information to understand how is the signal transmitted to induce the $Ca^{2+}$ influx via SOCs. Then, the purpose of this thesis is to identify the localisation of STIM1 and Orai1 at the subcellular level in the liver cell and identify the novel associated proteins in related to the activation of SOCs.

## 1.2 Liver and hepatocyte physiology

The liver is the largest organ in human body located at the right upper part of abdominal cavity which is about ~2 to 3 % of adult body weight (Abdel-Misih and Bloomston, 2010). The liver plays an important role in performing different type of metabolisms including glycolysis, detoxification of xenobiotics and secretion of bile acid.

By anatomical appearance, the liver can be divided into right and left lobe by the falciform ligament. The concept of liver segmentation was suggested by various methods. In the 1950s, Hjortsjö used the branching of the bile duct to divide the liver into 6 sectors (Hjortsjo, 1951). Later Healy and Schroy proposed the segmentation of liver based on the distribution of bile ducts and portal vein. According to this system, the liver is divided into left lobe and right lobe with four segments on each lobe (Healey et al., 1953). Couinard segmentation is another system to divide the liver based on the distribution of the portal vein and the hepatic vein. In this segmentation system, the liver is described as eight segments including caudate lobe (segment I), three segments (segment II, III, IV) on left lobe and four segments (segment V, VI, VII and VIII) on the right lobe. (Skandalakis et al., 2004).

The liver contains various cell types to maintain its normal functions. It can categorise liver cells into parenchymal and non-parenchymal cells. Parenchymal cells are mainly composed by the hepatocytes that take part most of the metabolisms. There is about 60% of total liver cells composing by hepatocytes (Tanaka et al., 2011). Hepatocytes are polarized epithelial cell, which have 72 % of the sinusoidal membrane, 15% of lateral membrane and 13% of the canalicular membrane. (Hubbard et al., 1983).

Non-parenchymal cells also called hepatic sinusoidal cells are composed of endothelial cells, Kupffer cells, hepatic stellate cells and Pit cells. Each non-parenchymal cells has their own specific functions. Kupffer cells are liver resident macrophages (Bouwens et al., 1986). The function of Kupffer cells is to remove the different substance from the blood (Baffy, 2009). Pit cells are nature killer in the liver, which shows the cytotoxicity on liver tumour cells (Nakatani et al., 2004). In liver, hepatic stellate cells are used to store vitamin A. In addition, stellate cells show the function of antigen-presenting cells and activate the response of T cell to antigens (Geerts, 2001). Thus, the liver is one of the complex organs in the human body as it contains various cells types to maintain the functions.

Hepatic lobule is the structural unit of the liver. These lobules are arranged in heptagonal shape by plates of hepatocytes (Figure 1.1). In each of the corners at the heptagonal lobule, it contains the structure called portal triad, which is composed of the portal vein, hepatic artery and bile duct. The blood and nutrient supply of the liver are delivered by portal vein and hepatic artery. The sinusoids provided the space for the blood flows from the vessels to central veins are the area between the two plates of hepatocytes. The bile acid is secreted by hepatocytes and the flow of bile acid is from bile canaliculus to the bile duct that is opposite direction to blood flow. The study of fine structure from mouse liver cells showed that the hepatocytes have large round nuclei and the cytoplasm is enriched with mitochondria, smooth endoplasmic reticulum and rough endoplasmic reticulum. The cell volume of hepatocytes is occupied by 18~22% of mitochondria, 13 % of rough ER and 7% smooth ER (Blouin et al., 1977).

(a)

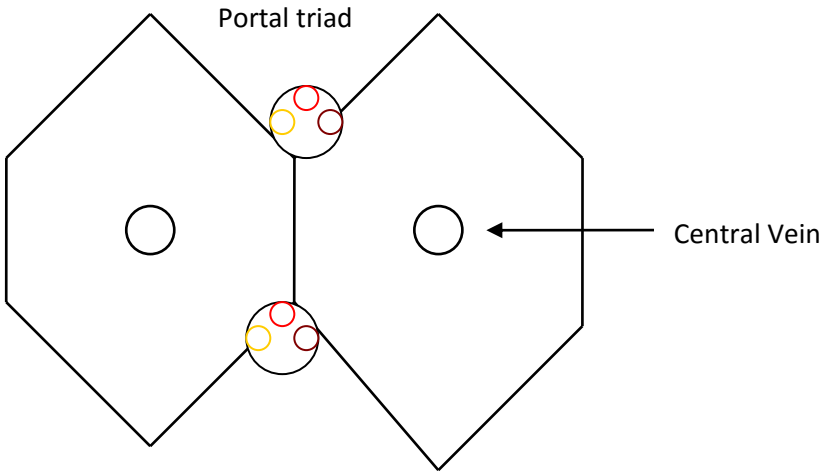


(b)

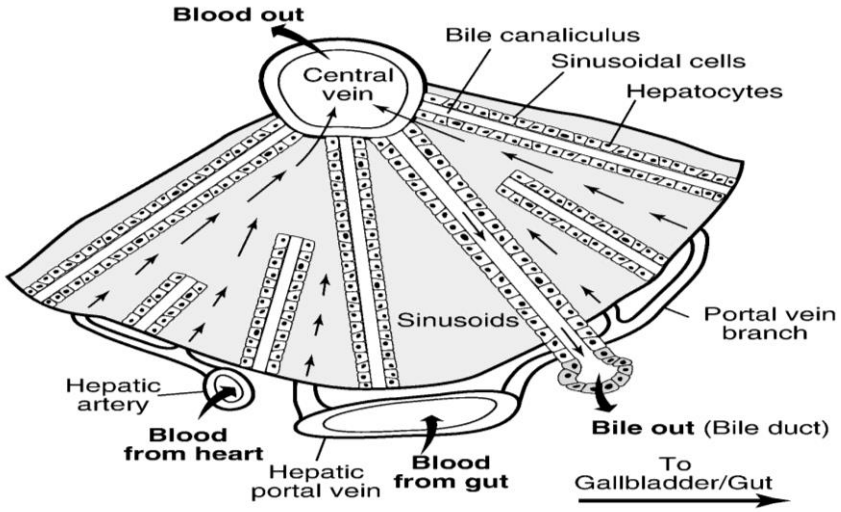


**Fig 1.1 The structure of hepatic lobules (a) and the fine structure of hepatic lobules composing by hepatocytes, portal triad and cental vein (b). (Barritt et al., 2008)**

## 1.3 Role of calcium in hepatocyte as intracellular messenger regulating of hepatocyte function

$Ca^{2+}$ is a universal second messenger that controls and regulates various cellular functions. As liver is the major organ taking part different type of metabolisms to maintain the normal liver functions, the $Ca^{2+}$ signalling in the liver cells needs to be highly organised by spatial and temporal properties in order to maintain the normal metabolism in the liver cells (Thomas et al., 1991, Amaya and Nathanson, 2013). A Large amount of intracellular $Ca^{2+}$ is stored in the endoplasmic reticulum (ER). The homeostasis of $Ca^{2+}$ is maintained by different type of $Ca^{2+}$ channels or $Ca^{2+}$ pumps in ER or on plasma membrane to maintain the liver normal cellular functions (figure1.2). In resting state, the level of [$Ca^{2+}$] at cytosolic space is maintained at about 100 nM~200nM. The amount of cytosolic $Ca^{2+}$ is lower than extracellular and intracellular $Ca^{2+}$ at intra-organellar $Ca^{2+}$ store which is about 1~2mM and 0.5mM, respectively (Meldolesi and Pozzan, 1998). The change of cytosolic [$Ca^{2+}$ ] can be achieved by releasing the intracellular $Ca^{2+}$ from the $Ca^{2+}$ store or influx from the extracellular $Ca^{2+}$ though the plasma membrane.

The link between the production of inositol 1,4,5- trisphosphate ($IP_3$) induced by $Ca^{2+}$-mobilising hormones and the increase of intracellular $Ca^{2+}$ concentration has been showed by Thomas et al since 1984 (Thomas et al., 1984). The initiation of the $Ca^{2+}$ signalling requires the binding of hormones to the receptor on the plasma membrane, then activating the enzyme of phospholipase C (PLC) to produce the molecules of $IP_3$ and diacylglycerol (DAG) by hydrolysis of phosphatidylinositol 4,5 bisphosphate ( $PIP_2$) on plasma membrane(Gary et al., 2004) . Six families of phospholipase C (PLC-β, -γ, -δ, -ε, -ζ and –η) with 13 isozymes have been identified in mammalian cells.

Various form of phospholipase C is activated by different mechanism. For instant, PLC-β is activated by G-protein coupled receptor. PLC –γ is activated by phosphorylation though receptor and tyrosine kinase (Gresset et al., 2012). Thus, the $Ca^{2+}$ signalling is a complex system involved with different molecules to produce its function.

After the formation of $IP_3$, it diffuses through cytoplasm and binds to the receptors on endoplasmic reticulum to induce the release of $Ca^{2+}$ from $Ca^{2+}$ store. $IP_3$ receptor on ER is a major calcium released calcium channel in liver cells (Nunn and Taylor, 1990). Three different isoforms of $IP_3$ receptors have been identified naming type I, type II and type III $IP_3$ receptor. Type I and type II $IP_3$ receptors are mainly expressed in hepatocytes but not type III $IP_3$ receptors (Hirata et al., 2002). In hepatocytes, type I $IP_3$ receptors are distributed evenly through the cytoplasm and type II $IP_3$ receptors are mainly located at the pericanalicular region. The evidence from subcellular fractionation studies suggested that $IP_3$ receptor and the $IP_3$ sensitive $Ca^{2+}$ pool in liver cells are located at a specialized region on ER that is close to the plasma membrane (Guillemette et al., 1988). It suggested that canalicular membrane could be the possible region associated with the specialized ER region as it contains high density of $IP_3$ receptor.

Intracellular $Ca^{2+}$ oscillations are one of the main features in hepatocytes. The trigger zone of $Ca^{2+}$ wave in the liver is at the pericanalicular region and the wave of increased $Ca^{2+}$ is mediated by type II $IP_3$ receptor (Keiji et al., 2002). There is a highly regular oscillations pattern with $2.1m^{-1}$of frequency and over 100 μm/s of speed propagating from the apical region which is enriched with type II $IP_3$ receptors to the basolateral region with the activation of type I $IP_3$ receptor (Nathanson et al., 1994, Hernandez et

al., 2007). In the intact liver, the $Ca^{2+}$ wave originates from hepatocytes near central venules and spreads to the hepatocytes near portal venules. The speed of the $Ca^{2+}$ wave range from 95-156 μm/s (Robb-Gaspers and Thomas, 1995). Therefore, $Ca^{2+}$ signalling in the liver is highly organised and the distribution of different signalling molecules in hepatocytes is important for regulating $Ca^{2+}$ signalling.

## 1.4 Calcium homeostasis in hepatocyte: Endoplasmic Reticulum, Mitochondria and Nucleus

The $[Ca^{2+}]$ of cytoplasm in the resting state is maintained at a low level and is increased when the cells receive a stimulus. $Ca^{2+}$ homeostasis is a dynamic process that involves compartmentalization of $Ca^{2+}$ into different organelles. Mitochondria were first suggested as $Ca^{2+}$ store in animal cells. Evidence showed that mitochondria have a higher capability to buffer the cytosolic $Ca^{2+}$ concentration than the endoplasmic reticulum (Joseph et al., 1983). Thus, it was suggested that mitochondria are the predominant intracellular $Ca^{2+}$ store in liver cells. However, other evidence indicated that endoplasmic reticulum (ER) also acts an important intracellular $Ca^{2+}$ store for regulating cytosolic $Ca^{2+}$ homeostasis. The use of rapid cellular-fractionation technique to measure the content of mitochondria $Ca^{2+}$ revealed that the mobilization of $Ca^{2+}$ in mitochondria is not essential for the increase in the activity of glycogen phosphorylase in the liver cells (Shears and Kirk, 1984). Kimura demonstrated that the administration of phenylephrine to hepatocytes induces the release of $Ca^{2+}$ from mitochondria and ER about 20% and 80%, respectively (Kimura et al., 1982). Therefore, the higher content of $Ca^{2+}$ in ER than in other organelles indicated that ER is the major intracellular $Ca^{2+}$ store.

The $Ca^{2+}$ homeostasis is controlled by the action of $Ca^{2+}$ channels which mediate the influx of $Ca^{2+}$ and $Ca^{2+}$ATPase to mediate the efflux $Ca^{2+}$. The $Ca^{2+}$ ATPase is a specific $Ca^{2+}$ pump that is utilized to mediate the uptake $Ca^{2+}$ from the cytoplasm to the endoplasmic reticulum (Carafoli and Brini, 2000). The image of electron microscopy on the isolated mitochondria from rat hepatocytes showed that those organelles have a close intraconnection. There are about 81% of isolated mitochondria contact with rough ER. (Sanchez-Bueno et al., 1997). The contact of mitochondria and smooth subdomain of the ER become more tightly when the cytosolic $Ca^{2+}$ level increases (Wang et al., 2000). Then, ER and mitochondria would influence with each other for regulating their functions.

Many cellular processes in the nucleus including gene transcription, cell growth and apoptosis are regulated by $Ca^{2+}$ signalling. It has been showed that the addition of ATP results in the increase of [$Ca^{2+}$ ] in the intra-nuclear (Nicotera et al., 1989). Thus, it suggested that $Ca^{2+}$ reuptake system is present at nucleus from liver cells to regulate the cellular function. Nicotra et al also showed that nuclear contain a $Ca^{2+}$ pool that is responsible for the release $Ca^{2+}$ in the response of ATP (Nicotera et al., 1990). Nuclear $IP_3$ receptors are detected on HepG2 cells. The results indicated that the nuclear from HepG2 cells are mainly expressed type II and type II $IP_3$ receptors but no expression of type I $IP_3$ receptor (Leite et al., 2003). Therefore, nuclear has its own mechanism to regulate the $Ca^{2+}$ concentration, which is independent of other cellular compartments.

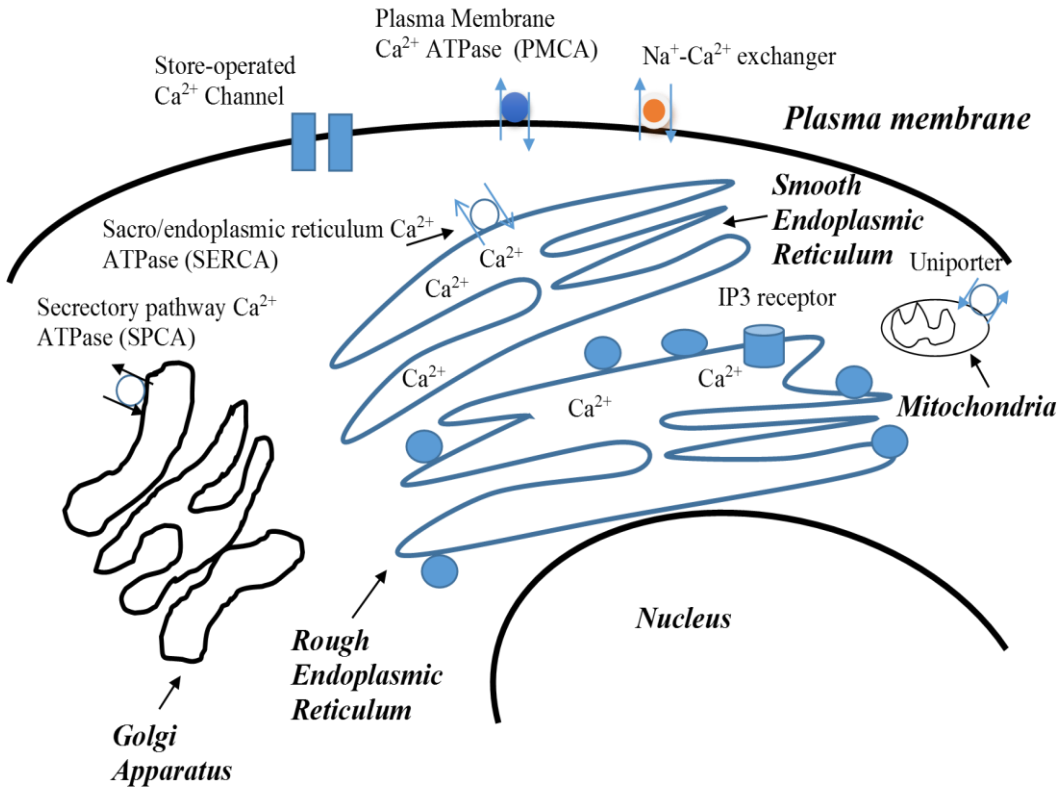


**Figure1.2 Molecular identities in the regulation of Calcium homeostasis in liver cells.**

$Ca^{2+}$ homeostasis in liver cells is regulated by several molecular identities. The cytosol $Ca^{2+}$ increased by the influx of $Ca^{2+}$ from extracellular though $Ca^{2+}$ channel on plasma membrane and the release of $Ca^{2+}$ from ER by $IP_3$ receptor. The excess $Ca^{2+}$ reuptake by sacro/endoplasmic reticulum ATPase (SERCA) to ER and by plasma membrane $Ca^{2+}$ ATPase (PMCA) to extracellular space. Mitochondria utilize uniporter to regulate the $Ca^{2+}$ concentration. Secretory pathway $Ca^{2+}$ ATPase (SPCA) is one of the $Ca^{2+}$ pump located on Golgi Apparatus.

## 1.5 Calcium entry channel in hepatocyte

The influx and efflux of $Ca^{2+}$ ion across the plasma membrane need the assistance of specific ion channels and pumps. In hepatocytes, it has been identified several types of $Ca^{2+}$ -permeable channels including receptor-activated $Ca^{2+}$ channels, store-operated $Ca^{2+}$ channels (SOCs), ligand-gated $Ca^{2+}$ channels , and stretch-activated $Ca^{2+}$ channels. There are no voltage-operated $Ca^{2+}$ channels detected on hepatocytes (Sawanobori et al., 1989).

The $Ca^{2+}$ entry via receptor –operated $Ca^{2+}$ channel (ROCC) is activated by the binding of hormone or agonists on the separated receptor to form second messengers and then activating ROCC (Crofts and Barritt, 1990, Kass et al., 1990). The SOCs are found on the plasma membrane. The activation of SOCs is controlled by the decrease of the $[Ca^{2+}]$ in the $Ca^{2+}$ store. The influx of $Ca^{2+}$ via SOCs is to refill the depleted $Ca^{2+}$ store and maintain the $Ca^{2+}$ oscillation in hepatocytes (Gregory and Barritt, 2003, Gregory et al., 2003). The $Ca^{2+}$ entry via the ligand-gated channel is induced by the binding of the agonist to the domain of the receptor. The stretch-activated $Ca^{2+}$ channel is activated by the mechanical force which is thought to regulate the cell volume (Bear, 1990).

Transient receptor potential (TRP) is non-selective cation channels which are composed of seven sub-families including TRPC (canonical ), TRPV (vanilloid), TRPM (melastatin), TRPML (mucolipin), TRPP (polycysteine), TRPA and TRPN (no mechano receptor potential C) (Ramsey et al., 2006). Evidence showed that TRPs are detected on liver tissue, hepatocytes and liver cell lines. Those results demonstrated that the main TRP channels detected on liver cells are included TRPC, TRPV and TRPM (Rychkov and Barritt, 2007).

## 1.6 Store-operated calcium channels (SOCs)

### 1.6.1 Definition of SOCs

Store-operated $Ca^{2+}$ channels (SOCs), also called capacitative $Ca^{2+}$ entry, was firstly proposed by Putney in 1986 (Putney Jr, 1986). By the definition, the calcium entry via SOCs is controlled by the depletion of calcium store in ER. The observed plasma membrane current induced by calcium store depletion is called $Ca^{2+}$ release-activated $Ca^{2+}$ current ($I_{CRAC}$) which shows the inward rectification current in mast cell and this current is not mediated by voltage and is highly selective to calcium (Hoth and Penner, 1992). However, other evidence showed that there is present another type of current related to store operated which have moderately selectivity to $Ca^{2+}$ called I*soc* (Gusev et al., 2003).

There are several ways to deplete $Ca^{2+}$ store to induce $Ca^{2+}$ operated $Ca^{2+}$ entry (SOCE). The main pathway to deplete $Ca^{2+}$ from the store is the formation of inositol 1,4,5-triphosphate ($IP_3$) by hydrolysis of phosphatidylinositol 4,5-bisphosphate ($PIP_2$) on the plasma membrane after the activation of phospholipase C (PLC) (Putney and Tomita, 2012). In addition to releasing $Ca^{2+}$ from the store by mediating $IP_3$ receptors activation, the $I_{CRAC}$ can also be induced passively by using $Ca^{2+}$ ATPase inhibitors and $Ca^{2+}$ chelators causing the leakage of $Ca^{2+}$ from the $Ca^{2+}$ store. Thapsigargin and methacholine, the inhibitors of SERCA, are a useful pharmacological tool to induce SOCE. The depletion of $Ca^{2+}$ by inhibition of SCERA is similar to $IP_3$-induced $Ca^{2+}$ entry (Takemura et al., 1989). $Ca^{2+}$ chelators such as EDTA and BAPTA are able to induce the $I_{CRAC}$ (Fierro and Parekh, 1999). Hofer et al used TPEN, a membrane-permeant multivalent chelator with moderate affinity to $Ca^{2+}$, to study the correlation

between $I_{CRAC}$ and $Ca^{2+}$ store depletion without interfering the $IP_3$ receptors. The results showed the $I_{CRAC}$ is related to $Ca^{2+}$ store depletion and the onset of the $Ca^{2+}$ entry need about 7s which is slower that other $Ca^{2+}$ channels (Hofer et al., 1998).

Some metal ions are able to influence the activity of $I_{CRAC}$. It has been demonstrated that the divalent ions of $Ba^{2+}$ and $Sr^{2+}$ displayed the dose-dependent inhibitory effect on $I_{CRAC}$ (Hoth and Penner, 1993). In addition to divalent ion, trivalent ions, $Li^{3+}$, also exhibits the inhibitory effect on the activity of SOCs (Mason et al., 1991). The SOCs lose their selectivity of $Ca^{2+}$ and increase $Na^{+}$ permeation when all divalent ions are removed (Braun et al., 2001). The permeation of monovalent ions is decreased by the addition of extracellular $Ca^{2+}$ in voltage- dependent manner (Bakowski and Parekh, 2002).

### 1.6.2 Physiological function of SOC

#### 1.6.2.1 Immune System

$Ca^{2+}$ is an important second messenger for regulating the function of immune cells. Mast cells were the first cells types reporting the presence of $Ca^{2+}$ release-activated $Ca^{2+}$ current ($I_{CRAC}$). Thus, SOCs should play a role in the function of immune system. It has been showed that the release of pro-inflammatory mediators from mast cell is mediated by the increase of $Ca^{2+}$ via SOCs (Chang et al., 2008, Sanchez-Miranda et al., 2010). The activation of neutrophils, one of the white blood cell responsible for innate immune system, requires STIM1 for activating the SOCs. After the deletion of stim1 gene showed less tissue injury in liver on ischemia/reperfusion (the resupply of the blood to liver after ischemia) and impair the host defected to the infection (Zhang et al.,

2014). In addition, the increase of $Ca^{2+}$ in neutrophils cause the phagosomal reactive oxygen species (ROC) production and the ROS is mediated by STIM1-dependent NADPH oxidase activation (Steinckwich et al., 2007, Ye, 2014). Then SOCs have an important role in regulating the function of immunity.

In clinical, the deletion of stim1 gene reduce the function of SOCs and impair the function of T-cells. $Ca^{2+}$ entry via SOCs on both T-cells and B-cells is deficient in patients with severe combined immune deficiency (SCID). It also demonstrated that SCID patients have mutation on Orai1gene. Both of STIM1 and STIM2 are involved in the activation of SOCs in CD8+ T cells and it is an essential step for anti-tumour immunosurveillance (Weidinger et al., 2013). Thus, regulating the function of SOCs could be the new target for tumour treatment

#### 1.6.2.2 Skeletal and Smooth Muscle cells

The function of skeletal and smooth muscles can be influenced by the avtivity of SOCs. When knockdown Orai1 and Orai3 using siRNA method, the activity of SOCs was inhibited and accompanied with the reduction of human myoblast differentiation (Darbellay et al., 2009). Sarcoplasmic reticulum in skeletal muscle showed store operated calcium entry and the activity of SOCs is related to the $Ca^{2+}$ inside the SR (González Narváez and Castillo, 2007). After the $Ca^{2+}$ store depleted, $I_{CRAC}$ was measured in vascular smooth muscle cells (VSMC) and the current was influenced by the knockdown of STIM1 and Orai1 (Potier et al., 2009) so STIM1 is essential for the SOCs activity in smooth muscle. The expression of STIM1 increase in the aortic

smooth muscle from stoke-prone spontaneously hypertensive rat ( SHRSPs) (Giachini et al., 2009).

Although the activation and deactivation of SOCs are normal at wild-type mouse muscle and dystrophy mdx mouse, the threshold of [$Ca^{2+}$] in sarcoplasmic reticulum for SOC activation is higher and the expression of STIM1 and Orai1 in dystrophic mdx mouse are increased. (Edwards et al., 2010). Zhao showed that when activated the SOCs in bladder smooth muscle, the frequency of the contraction was increased but the amplitude of the contraction was reduced (Zhao et al., 2014). These results suggested that SOCs is involved in regulating the excitability of skeletal and smooth muscles.

### 1.6.2.3 Cell cycles and Tumorigenesis

$Ca^{2+}$ signalling also involves in the regulation of cell cycle and the development of cancer. It has been shown that cells proliferation and migration of human hepatocellular carcinoma cells induced by ATP is mediated by the activity of SOCs (Xie et al., 2014). The function of STIM1 in tumorigenesis is controversial. STIM1 is firstly recognised as tumour suppressor gene (Sabbioni et al., 1997). However, evidence showed that STIM1 is overexpressed in the patient with colorectal cancer and it is related to metastasis and tumour size (Wang et al., 2014). The inhibition of STIM1 expression in human glioblastoma cells, causing the cells arrested at the G0/G1 phase and inhibit the cells proliferation (Li et al., 2013). Orai1 also plays a role in cell cycle regulation. The silencing of Orai1 in HEK293 cells induces the cells blocked at G1, S and G2/M phase and the activity of SOCs also reduced (El Boustany et al., 2010). In endothelial cell after the knockdown of STIM1 or Orai1, the cells were arrested at S and G2/M phases,

inhibiting the cells proliferation. (Abdullaev et al., 2008). From those results, it showed that SOCs involve in controlling the proliferation of endothelial cell.

### 1.6.3 Orai1 proteins and their roles to form channel pore

Orai1, also called CRACM1, is a pore- forming subunit of SOCs on plasma membrane. (Vig et al., 2006b). There are another two isoforms of Orai1, called Orai2 (CRACM2) and Orai3 (CRACM3). The evidence showed that Orai1 is a four transmembrane protein (Maruyama et al., 2009). From the study of the crystal study, it displayed that Orai1 is a hexamer structure (Hou et al., 2012). Both C- terminal and N-terminal of Orai1 are involved in the regulation of SOCs activation. The lack of the N terminus proline-rich and arginine-rich domain on Orail reduces the increase of intracellular calcium concentration mediated by SOCs (Takahashi et al., 2007). In other evidence, Muik showed that C-terminal of Orail is important for dynamic coupling and N-terminal of Orai1 is responsible for gating the channel (Muik et al., 2008). Some amino acids at Orai1 have their roles in the ion selectivity of the channels. The negative charge amino acid glutamine at 106 position of first transmembrane domain and 190 position of the third domain at Orai1 are the important amino acids for the function of SOCs. Glutamine at 106 regulates the $Ca^{2+}$ selectivity by binding with $Ca^{2+}$ and glutamine at 190 affect the selectivity of the $Ca^{2+}$ by allosteric changing of the architecture of selectivity filter (Zhou et al., 2010). In addition, aspartate on the loop between first and third domain is another amino acid influence the selectivity (Vig et al., 2006a, McNally et al., 2009). Mutation of valine at the position 109 causes the development of voltage

gating of the channel and coiled-coil domain on STIM1 is the main part for STIM1 binding with Orai1 (Spassova et al., 2008).

The three homologous CRACM proteins display different properties in $Ca^{2+}$ selectivity, $Ca^{2+}$ inactivation and pharmacological profiles (Lis et al., 2007). The formation of heteromer of Orai1 and Orai3 can reduce the $Ca^{2+}$ selectivity of the channel (Schindl et al., 2009). However, when co- expressed of Orai1 and Orai2, these two proteins interact with each other and increase the $I_{CRAC}$ current synergistically (Mercer et al., 2006). Orai1 and Orai2 are more sensitive to the $Ca^{2+}$ dependent potentiation process and the current is less stable in divalent free solution but Orai3 is more resistant to these processes (DeHaven et al., 2007). Mutation of the loop between transmembrane domain II and III reduce the inhibition effect of fast inhibition showing that this loop is main part involving in fast inactivation of SOCs (Srikanth et al., 2010b). Phosphorylation is known to be an important process to regulate the function of Orai1. Serine 27 and Serine 30 at Orai1 N-terminus is the place for the phosphorylation that influence the activity of SOCs (Kawasaki et al., 2010).

### 1.6.4 STIM1 proteins and their roles to activation the channel

STIM1 is belonged to type 1 transmembrane protein which is located at the endoplasmic reticulum. Two types of STIM protein naming STIM1 and STIM2 have been identified. STIM1 protein molecule contains α-sterile motif (SAM) and unpaired EF hand (Dziadek and Johnstone, 2007). Although the high similarity of STIM1 andSTIM2, the structure stability and the aggregation of EF hand domain and SAM domain is different between STIM1 and STIM2 (Zheng et al., 2008). Some of the

domains on STIM1 are important in its function. EF hand forms dimers when the $Ca^{2+}$ store depleted which is the first step of oligomerisation of STIM1 (Stathopulos et al., 2006a). The main function of STIM1 is to act as a $Ca^{2+}$ sensor to detect the change of $Ca^{2+}$ in ER. EF hand domain on STIM1 senses the change of the calcium and induces the conformation change of the STIM1 to form dimmer (Zhang et al., 2005, Stathopulos et al., 2006a, Shi et al., 2010). There is a second EF domain on STIM1 called "hidden" EF domain which is important for stabilizing the canonical EF on the $Ca^{2+}$ binding (Zheng et al., 2008). The other important domain on STIM1 is single α-sterile motif (SAM) which is the vital domain for the interaction between proteins. Several lines of evidence demonstrated that some fragments on STIM1 are important in the regulation of SOCs activity. The amino acid at C terminus from 233-450/474 of STIM1 contains an Orai1 activating small fragment (OASF). This segment can bind to Orai1 and activate the channel. In addition, the extent 30 amino acid after the segment have an inhibitory function to regulate the activity of the channel (Muik et al., 2009). Other evidence also identified the regions on STIM1 are responsible for SOCs activation. The sequence of amino acid on C terminus of STIM1 from 342 to 446 named CRAC activation domain and the sequence from 344-442 named as STIM1/Orai1 Activating region (SOAR) or CRAC activation domain (CDA) is essential sequences for binding with Orai1 and the activation of SOCs (Park et al., 2009, Yuan et al., 2009, Covington et al., 2010). The crystal structure study showed that SOAR is composed of coiled-coil domain2 (CC2) and coiled –coil domain 3 (CC3) which activate Orai1 when clustering. The other region of coiled-coil domain 1 (CC1) inhibits the activity of Orai1 when CC1 binds to CC2 and CC3 (Fahrner et al., 2014). The basic acidic amino acid at the region on STIM1 from 384-386 provide an electrostatic interaction force for the binding of STIM1 and Orai1 to activate SOCs (Calloway et al., 2010). The function of STIM2 is

different from STIM1. STIM2 can function as a regulator to balance the $Ca^{2+}$ level at cytosol and ER (Brandman et al., 2007). The N terminal of STIM2 has an inhibitory action which can reduce the activity of SOCs (Zhou et al., 2009). The function of STIM1 can be influenced by binding to another molecule. Golli-BG21, a negative regulator of T cell activation, binds to C-terminus of STIM1 to inhibit the activity of store-operated $Ca^{2+}$ entry (SOCE) (Walsh et al., 2010)

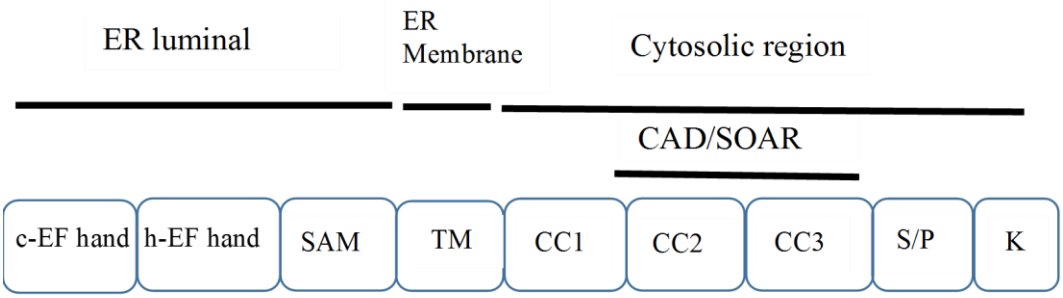


**Figure 1.3 Domain of STIM1 protein.**

STIM1 is a single-pass transmembrane protein that composed of ER luminal region and cytosolic region. The ER luminal region containing canonical EF (c-EF) hand, the $Ca^{2+}$ binding domain and hidden-EF (h-EF), non $Ca^{2+}$ binding domain and α-sterile motif (SAM) which are located at cytoplasmic space. At cytosolic region, CRAC activation domain (CAD)/STIM1 Orai1 activating region (SORA) is the binding site of STIM1 to Orai1 located at the domain of coiled-coil domain 2 (CC2) and coiled-coil 3(CC3). The C- terminal poly-lysine (K) domain associates the PIP2 at the plasma membrane. The transmembrane domain (TM) is the region of STIM1 protein passing though plasma membrane.

### 1.6.5 Mechanism of activation of SOCs

The mechanism of activation of SOCs was a mystery for many years until the discovery of STIM1 and Orai1. The molecular components of SOCs have a great improvement by the large screening on the gene using RNA interference (RNAi) to identify STIM1 and Orai1 as important molecules for SOCs (Roos et al., 2005, Zhang et al., 2006a). After the discovery of STIM1 and Orai1, many studies have been working on understanding the mechanism of SOCs.

#### 1.6.5.1 STIM1 and Orai1 is essential for SOCs activation

The requirement of STIM1 and Orai1 to produce full activity of SOCs was showed by Peinelt and co-worker. They demonstrated that when the cells co-expression of STIM1 and Orai1 together, it can increase the current of I*soc* (Peinelt et al., 2006). The functional unit of SOCs is composed of tetramers of Orai1 and STIM1 dimmer (Penna et al., 2008). The initiation of $Ca^{2+}$ influx via SOCs is triggered by STIM1 sensed the change of [$Ca^{2+}$] after the depletion of $Ca^{2+}$ in ER ( Luik et al., 2006, Spassova et al., 2008). When $Ca^{2+}$ store depleted, STIM1 redistributed to the region of the ER close to the plasma membrane at about 10-15 nm is an essential process for SOCs activation (Luik et al., 2006). During the activation process, STIM1 forms the oligomers and induced the Orai1 to cluster together on the plasma membrane (Luik et al., 2008). It was shown that STIM1 do not involve in other functions. When knockdown STIM1 in the cells, STIM1 do not involve in the refilling process of $Ca^{2+}$ on the ER and the refilling process require SERCA pump and mitochondria (Jousset et al., 2007). Thus, STIM1 has no role in the refilling process of the $Ca^{2+}$ store and only function as a

sensor. After the $Ca^{2+}$ store depleted, Orai1 forms a tetramer to produce functional channel pore (Mignen et al., 2008). The activation of SOCs not only involves the interaction of STIM1 and Orai1 but also other molecules. It has been shown that mitochondria also has a role in regulating the calcium influx via SOCs (Hoth et al., 1997). The disorganization of microtubule cytoskeleton by nocodazole in HEK 293 cell causes the inhibition of SOCE and $I_{CRAC}$ (Smyth et al., 2007). Therefore, the cytoskeleton is another component for the activation of SOCE. In B cells, type II and type III $IP_3$ receptors but not type I $IP_3$ receptors at a specific region on $Ca^{2+}$ store are responsible for the activation of $I_{CRAC}$ (Peinelt et al., 2009). Thus, those results suggested that the activation of SOCs is involved different molecules.

When the $Ca^{2+}$ store depleted, STIM1 cluster to the region called Lipid raft domain (LRD) that is the region on plasma membrane contains high cholesterol (Pani et al., 2008) and the function of LRD is to activate the SOCs activity rather maintain the SOCs activity (Galan et al., 2010). Thus, it suggested that STIM1 might be clustered at the special region to produce its function. After refilling of the $Ca^{2+}$ store, the puncta of STIM1 will be reversed. This rearrangement is dependent on the $Ca^{2+}$ and other molecules(Smyth et al., 2008)

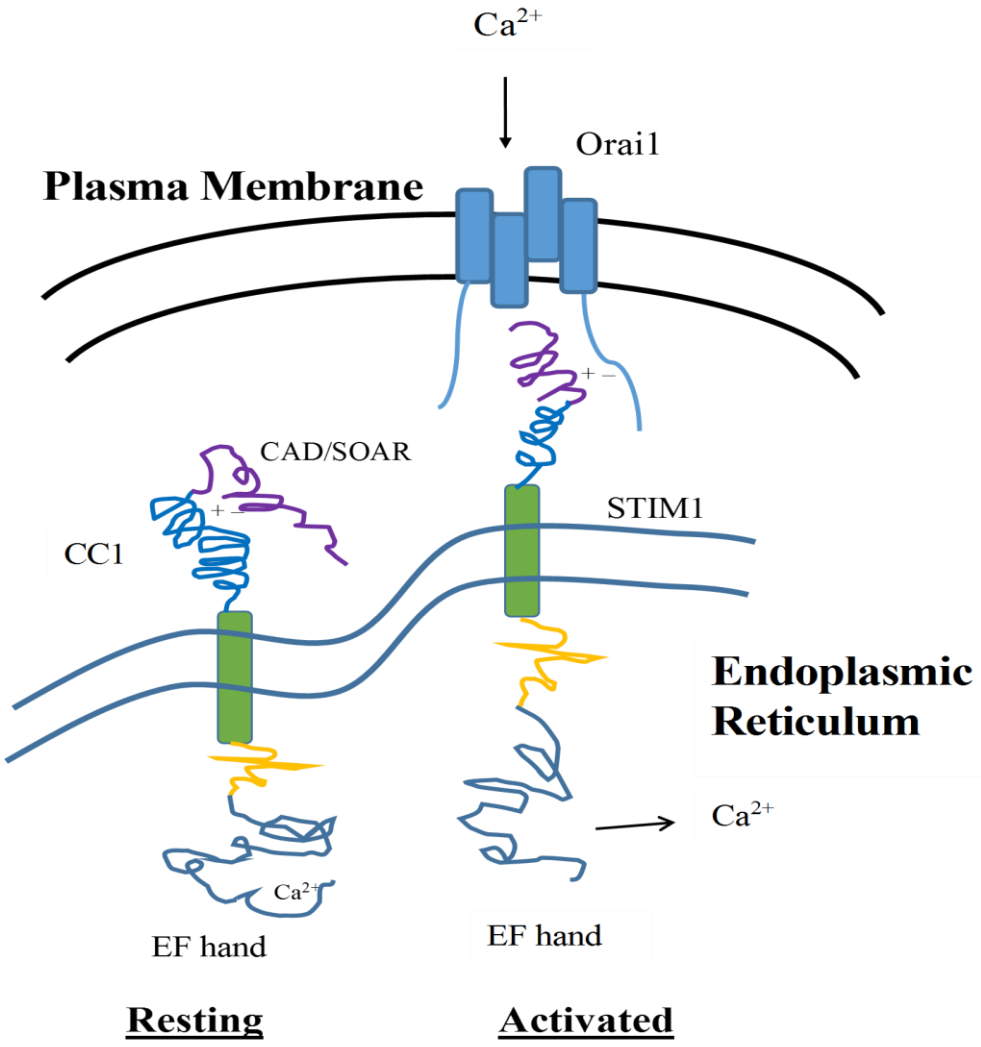


**Figure 1.4 The activation of SOCs by interaction of STIM1 and Orai1.**
At resting state, $Ca^{2+}$ bind with EF hand domain and inhibit the function of STIM1. CDA/SORA interact with CC1 domain blocking the binding of STIM1 to Orai1. When $Ca^{2+}$ store depleted, $Ca^{2+}$ released from the EF hand and cause the exposure of the bind site by the broken of the interaction between of SORA and CC1. The active binding site then interacts with N-terminus of Orai1and induce the influx of $Ca^{2+}$.

1.6.5.2 STIM1 –binding proteins

The additional binding proteins to STIM1 that involved in regulating the activity or other functions of SOCs have been proposed by several experiments (Table 1.1). The idea of STIM1-binding protein was suggested by the results using the molecular bridge formation strategy to visualise the interaction between STIM1 and Orai1. It suggested that the distance between STIM1 and Orai1 is too long to have physical contact with each other. The results indicated that large complex formed with other additional protein should be required for SOCs activation. (Várnai et al., 2007). However, the other results of measuring the distance between STIM1 and Orai1 by using FRET showed that the distance between STIM1 and Orai1 is less than 100 Å which is enough for direct physical contact (Navarro-Borelly et al., 2008).

Some of the proteins have been identified as STIM1 binding protein. CRACR2A, an novel EF hand containing cytosolic protein, binds with STIM1 and Orai1 to form a ternary complex and then regulates the function of SOCs(Srikanth et al., 2010a). The functional components of SOCs are suggested to be composed with other molecules such as SERCA and microtubule end binding protein (EB1) to form a large complex called store-operated $Ca^{2+}$ influx complex (SOCIC) (Vaca, 2010). SOCs also interact with another channel to regulate its function such as TRP. Another channel should be voltage-regulated ion channel. Calcium- activated $K^+$ channel, K(Ca)3.1 channel, suggests to be one of the components providing the driving force for SOCs in the activation (Gao et al., 2010). Thus, SOCs require other protein to maintain or produce its function.

| Protein | Cell type studied | Detection Techniques | Condition | Reference |
|---|---|---|---|---|
| Calumin | HEK 293 | Immunoprecipitation | No $Ca^{2+}$ depletion | (Konno et al., 2012) |
| Calmodulin | *E. Coli* | Nuclear magnetic resonance | On different $Ca^{2+}$ concentration | (Bauer et al., 2008) |
| Calnexin | HeLa cell | Immunoprecipitation | No $Ca^{2+}$ depletion | (Saitoh et al., 2011) |
| Cav1.2 (L-type calcium channel) | HEK293T | Immunoprecipitation | $Ca^{2+}$ depletion | (Park et al., 2010) |
| CRACR2 | HeLa cell | Immunoprecipitation | $Ca^{2+}$depletion | (Srikanth et al., 2010a) |
| EB1(microtubule-plus-end-tracking protein) | HEK293<br>Mast cell | GST pull-down assays<br>Immunofluorescence | No $Ca^{2+}$ depletion<br>$Ca^{2+}$ depletion | (Grigoriev et al., 2008)<br>(Hajkova et al., 2011) |
| Exportin1 | HeLa cell | Immunoprecipitation | No $Ca^{2+}$ depletion | (Saitoh et al., 2011) |
| Golli | HeLa cell | GSt pull- down assays<br>Immunofluorescence | No $Ca^{2+}$ depletion | (Walsh et al., 2010) |
| Junctata | HeLa cell | Immunoprecipitation | $Ca^{2+}$depletion | (Srikanth et al., 2012) |
| SARAF | HEK293-T cells | Immunofluorescence | $Ca^{2+}$depletion | (Palty et al., 2012) |
| TRPC1 | HEK293 | Immunofluorescence | $Ca^{2+}$depletion | (Pani et al., 2009) |
| Transportin1 | HeLa cell<br>HEK293 cell | Immunoprecipitation | No $Ca^{2+}$ depletion | (Saitoh et al., 2011) |
| α-Tubulin | HEK 293<br>Mast cell | Immunofluorescence | $Ca^{2+}$depletion<br>$Ca^{2+}$ depletion | (Smyth et al., 2007)<br>(Hajkova et al., 2011) |

**Table1.1 Summary of STIM1-binding proteins**

| Protein | Cell type studied | Detection Techniques | Condition | Reference |
|---|---|---|---|---|
| P100 | CHO cell | Immunoprecipitation | $Ca^{2+}$ depletion | (Woodward et al., 2010) |
| POST | HEK 293 | Immunoprecipitation | $Ca^{2+}$ depletion | (Krapivinsky et al., 2011) |
| SERCA2 | HEK293T | Immunoprecipitation | $Ca^{2+}$ depletion | (Sampieri et al., 2009b) |
| SERCA3 | Human platelets | Immunoprecipitation | $Ca^{2+}$ depletion | (López et al., 2008) |

**Table 1.1 Table1.1 Summary of STIM1-binding proteins (continuous)**

1.6.5.3 The role of phosphorylation on the activity of SOCs

Several lines of evidence have showed the role of phosphorylation on the activity of SOCs. The inhibition of serine/threonine phosphatase result in the reduction of $Ca^{2+}$ entry induced by the depletion of $Ca^{2+}$ store (Tojyo et al., 1995a). In another study, using staurosporine to inhibit protein kinase C from rat parotid acinar cells caused the enhancement of $Ca^{2+}$ entry via SOCs (Tojyo et al., 1995b). Those results indicated that the processes of phosphorylation and dephosphorylation are involved in the regulation of SOCs activity. Symth demonstrated that STIM1 is phosphorylated during mitosis and also indicated S486 and S668 on C- terminus are the possible site for phosphorylation(Smyth et al., 2009). It has been showed that the SOCs activity is reduced when Orai1 is phosphorylated by protein kinase C β at S27 and S30 on N-terminus (Kawasaki et al., 2010). Thus, phosphorylation on STIM1 and Orai1 is important in the function of the cells.

#### 1.6.5.4 The inhibitory mechanism of SOCs

The activity of the SOCs can be inhibited by fast and slow inhibitory mechanisms. For fast inactivation, the activity of SOCs is deactivated by local increased $Ca^{2+}$ rather than global $Ca^{2+}$ (Zweifach and Lewis, 1995a). The channels can also be inactivated by a slow model which is controlled by the refilling of the calcium store (Zweifach and Lewis, 1995b). Mitochondria also involves in regulating the activation of SOCs (Hoth et al., 1997). The coiled- coil domain 1 (CC1) at C-terminus of STIM1 has an inhibitory function on SOCs. The CC1 acts as a clamp by interacting with coiled-coil domain 3 (CC3) to inhibit the exposure of CAD that binds with Orai1. $Ca^{2+}$ has its own role in regulating the activity of SOCs. Mailli and colleagues showed that the rise of [$Ca^{2+}$ ] at cytosol inhibits the clustering of STIM1 at subplasmalemmal region (Malli et al., 2008).

## 1.7 Subregions of ER and SOCs activation

The endoplasmic reticulum is the main $Ca^{2+}$ store and the change of the $Ca^{2+}$ concentration in the store is critical for the activation of SOCs. Some of the evidence show that only small part of ER rather than the whole ER is necessary for SOC activation. Parekh et. al. showed that the relationship between $IP_3$-induced release $Ca^{2+}$ and the activation of $I_{CRAC}$ exhibited a nonlinear relationship, (Parekh et al., 1997). The kinetic properties of ionomycin on releasing $Ca^{2+}$ from the store and $I_{CRAC}$ activation are different from inositol (2,4,5) triphosphate ((2,4,5)$IP_3$ ), an $IP_3$ receptor activator with minimum $IP_3$ metabolism, and thapsigargin (Huang and Putney, 1998). Those results suggested that a specific distinct $Ca^{2+}$ store is linked to $I_{CRAC}$ activation.

$IP_3$ is degraded rapidly by two enzymes, inositol (1,4,5) P3 5-phosphatase (IP3 5-phosphase) converting $IP_3$ to $IP_2$ and inositol (1,4,5) P3 3-kinases (IP3 3-kinases) converting $IP_3$ to $IP_4$. The maximal concentration of fluorinated inositol 1,4,5 triphosphate (IP3-F) which has low affinity to $IP_3$ 5-phopspatase, activate the submaximal $I_{CRAC}$ and this current can be further increased by adding thapsigargin (Glitsch and Parekh, 2000). This suggested that only part of the $Ca^{2+}$ released from the store is enough to activate the $I_{CRAC}$ and $IP_3$ 5-phoshatase metabolism should involve in the non-linear relationship of the current and $IP_3$. Moreover, the dynamics state of the $Ca^{2+}$ store is another factor involved in regulating the activation. Lower the $Ca^{2+}$ concentration at cytoplasm can induce the activation of $I_{CRAC}$ and not related to the whole $Ca^{2+}$ inside the store (Krause et al., 1999). It implicated that the $Ca^{2+}$ near the subplasmalemmal area activates the $I_{CRAC}$.

$IP_3$ receptor is important for the activity of $I_{CRAC}$. $IP_3$ and its metabolic resistance analogue, L-α-glycerophospho-D-myoinositol-4,5-biophosphate (GPIP2), produce an inhibitory effect on $I_{CRAC}$ when refilling the store and the store contained $IP_3$-s is responsible for activating $I_{CRAC}$ (Broad et al., 1999). At subplasmalemmal region close to the open of Orai1 has high $Ca^{2+}$ concentration which induces the negative feedback inhibition of the SOCs and the inhibitory effect can be regulated by the mitochondria close to this region (Korzeniowski et al., 2009). Moreover, when $Ca^{2+}$ depleted STIM1 forms oligomers and move to the region close to the plasma membrane (Liou et al., 2007). Therefore, the region of ER close to plasma membrane should the area responsible for the activation of SOCs. A specific subcellular structure called Plasma membrane associated membrane (PAM) forms near the plasma membrane when SOCs

is activated (Koziel et al., 2009). Thus, PAM is thought to be a specific region on ER for activating SOCs.

## 1.8 SOCs in Hepatocytes

### 1.8.1 Properties of SOCs in hepatocytes

The nature of the SOCs in hepatocytes is very similar to other cell types. Rychkov et al used patch clamp technique to demonstrate the activity of SOCs in live cells The results indicated that when the liver cells treated with ATP or vasopressin, it produced an inward and high $Ca^{2+}$ selectivity current which is similar to $I_{CRAC}$ (Rychkov et al., 2001). There are some pharmacological agents can regulate the activity of SOCs in liver cells. It was shown that some divalent and trivalent ions inhibit the activity of the SOCs (Rychkov et al., 2005b). The pharmacological agents, gadolinium and SF&K 96365, both are the inhibitors of receptor-activated calcium influx, can inhibit the $Ca^{2+}$ influx induced by vasopressin at hepatocytes (Fernando and Barritt, 1994).

Evidence demonstrated that the increased $Ca^{2+}$ via SOCs is mainly to refill the depleted $Ca^{2+}$ store (Gregory et al., 2003). The activation of SOCs in liver cells is showed to be influenced by some molecules. It was demonstrated that the fast $Ca^{2+}$-dependent inactivation of I*soc* in liver cells is mediated by calmodulin. This process is not related to the activation of SOC (Rychkov et al., 2001, Litjens et al., 2004). Arachidonic acid is another biological inhibitor for regulating the activation of SOCs mediated $Ca^{2+}$ entry in liver cells (Rychkov et al., 2005a). $Ca^{2+}$ oscillations are one of the main features in hepatocytes. Gregory et al. showed that the $Ca^{2+}$ oscillations induced by adrenaline or vasopressin in rat isolated hepatocytes are required the activation of SOCs (Gregory

and Barritt, 2003). Some endogenous substances secreted from the liver like cholestatic bile acid and choleretic bile acids can activate and inhibit SOCs in the liver cells. These two substances can induce the redistribution of STIM1in puncta on ER (Aromataris et al., 2008).

The expression of two major components of SOCs, STIM and Orai have been measured in rat hepatocytes. The results of RT-PCR showed that STIM1 and STIM2 are expressed in a relatively similar amount in hepatocytes. Orai1, Orai2 and Orai3 were also detected in hepatocytes but Orai2 with less expression than Orai1 and Orai3 (Jones et al., 2008). When H4IIE cells transfected with STIM1, the location of STIM1 protein is mainly at endoplasmic reticulum in H4IIE cells (Castro et al., 2009).

### 1.8.2 Activation mechanism of SOCs in hepatocytes

In liver cells, the $Ca^{2+}$ entry via SOCs is mediated by the activation of $IP_3$ receptor to deplete the $Ca^{2+}$ store (Guihard et al., 2000). The knockdown of STIM1 at H4IIE cells causes the reduction of I*soc*. (Litjens et al., 2007). Thus, the activation of SOCs in liver cells requires the involvement of STIM1. When stimulated the STIM1 transfected H4IIE cells by thapsigargin, it results in the redistribution of STIM1 proteins and form the puncta on ER (Castro et al., 2009). These two results suggested SOCs is vital for liver function. The binding of STIM1 to Orai1 should be necessary for the activity of SOCs. The change of the relative expression level of STIM1 in H4IIE cells resulted in reducing of the activity of SOCs after the injection of $IP_3$ to internal solution. It is because the binding of STIM1 to Orai1 is influenced by altering the number of STIM1 expressed (Scrimgeour et al., 2009).

### 1.8.3 Evidence for potential role subregion ER in hepatocytes

The subregion of ER in regulating the function of SOCs in hepatocytes has been shown by several lines of evidence. When $IP_3$ receptors inhibited by the antibody, the calcium release induced by vasopressin and adenophostin A is not in direct proportion at hepatocytes (Gregory et al., 1999). The results implicated that the activation of SOCs only requires small part of the $Ca^{2+}$ in a special region. This special subregion is dominated with type I $IP_3$ receptor (Gregory et al., 2004). By using patch clamp experiment, taurodeoxycholic acid (TDCA), one of the choleretic bile acid, showed that it induced an inwardly-rectifying current in liver cells which are similar to the characteristics of SOCs (Aromataris et al., 2008). In other evidence, Castro demonstrated that TDCA causes the $Ca^{2+}$ influx close to the plasma membrane and redistribute STIM1 on ER but not in the liver cell with ectopically- expressed TRPV1(Castro et al., 2009). Those results suggested the small region of ER is required for the activation of SOCs in liver cells.

## 1.9 Non-alcoholic fatty liver disease and Hepatic Steatosis

Non-alcoholic Fatty Liver Disease (NAFLD) is a common liver disease around the world. Hepatic steatosis is a significant clinical manifestation of NAFLD causing when the liver cells accumulated more than 5% of triglycerides and fatty acid without any consumption of alcohol (Neuschwander-Tetri and Caldwell, 2003). NAFLD can be classified into 4 types: (1) simple steatosis which only observed the hepatocellular steatosis; (2) steatosis with lobular inflammation; (3) the presence of ballooned hepatocytes accompanied with inflammation; and (4) the presence of Mallory's hyaline

or fibrosis (Matteoni et al., 1999). The excess accumulation of lipid at non-adipose cell can induce lipotoxicity (Zámbó et al., 2013). If the condition of hepatic steatosis uncontrolled, the steatosis can associate with the development of insulin resistance (IR) and type 2 diabetes (T2D).

There have two ways to induce the accumulation of fatty acid in the liver cells, which is to increase the activity of lipolysis and the uptake of lipid from the daily fat. It was shown that *De novo* lipogenesis in the liver is one of the main factors to increase lipid accumulation (Postic and Girard, 2008). In addition, the dysfunction of β oxidation of fatty acid in mitochondria also contribute to the induction of lipid accumulation.

### 1.9.1 The Effect of hepatic steatosis on SOCs and protein kinase C

The development of insulin resistance induced by hepatic steatosis is shown to be mediated by the activation of protein kinase C (PKC). It was shown that the isoform of PKCε is activated in diet-induced hepatic steatosis and it is associated with the development of insulin resistance ( Lam et al., 2002, Samuel et al., 2007). In another study, using ethanol-induced steatosis on C57BL/6J mice, the results showed that the development of steatosis causes the formation of diacylglycerol and the activation of PKCε (Phillip Kaiser et al., 2009).

In a recent study, the development of hepatic steatosis can inhibit the activity of SOCs and the inhibition of SOCs is mediated by the activation of protein kinase C (PKC)(Wilson et al., 2014). Thus, protein kinase C is an important signalling molecule involved in inducing hepatic steatosis and insulin resistance.

## 1.10 Evaluation of current knowledge of the distribution and function of STIM1 and Orai1 in hepatocytes

### 1.10.1 The distribution of STIM1 and Orai1

The distribution of STIM1 and Orai1 provides an important information to understand the mechanism of SOCs activation. In most of the studies, using cell lines transfected with STIM1 or Orai1 tagged with GFP or other fluorescent dyes identified the location of STIM1 and Orai1. Those results showed that STIM1 is located evenly at ER and Orai1 at plasma membrane. STIM1 is a $Ca^{2+}$ sensor to detect the change of [$Ca^{2+}$] in ER (Liou et al., 2005) and Orai1 is pore-forming molecules of SOCs on the plasma membrane(Prakriya et al., 2006). The interaction of STIM1 and Orai1 is an essential process for SOCs activation. At resting state when the $Ca^{2+}$ store is full, the EF-hand domain at STIM1 protein binds with $Ca^{2+}$ to inhibit the interaction between STIM1 and Orai1. After the depletion of $Ca^{2+}$ store, it causes the release of $Ca^{2+}$ from the EF-hand and results in the change of the conformation of STIM1 to induce the formation of oligomers (Stathopulos et al., 2006b). These STIM1 oligomers translocate to ER-PM junctions and form the puncta. Then, the binding domains of SORA/CAD on STIM1 oligomers are exposed and bind with Orai1 to induce the $Ca^{2+}$ influx (Muik et al., 2011). In the process of SOCs activation showed by various evidence, it implicated that there should be present a particular region on ER for the binding of STIM1 oligomers with Orai1 to induce $Ca^{2+}$ influx.

The requirement of a small region of the ER rather than the whole ER has been shown by some studies. A lower amount of $Ca^{2+}$ released from the $Ca^{2+}$ store is adequate to induce near-maximal $Ca^{2+}$ inflow via SOCs (Gregory et al., 1999). In other study, using

HII4E cells ectopically expressed with TRPV1 and taurodeoxycholic acid to investigate the small region of ER for SOCs activation. The results indicated that the activation of SOCs only requires the $Ca^{2+}$ released from ER close to the plasma membrane (Castro et al., 2009). Those results suggested that small region of $Ca^{2+}$ from ER is enough to activate SOCs and this region is close to plasma membrane. When $Ca^{2+}$ store depleted, STIM1 is enriched at the region of ER called cortical ER which is the region devoid of ribosomes, juxtaposed to the plasma membrane.

Thus, taken those results together, small region of ER should have special signaling mechanism or proteins to induce the aggregation of STIM1 and the binding between STIM1 and Orai1. Although it is known about the presence of small region on ER related to SOCs activation, the nature and molecular composition of that small region is still unclear. Thus, there is still a lot of works needed to be done to unveil the mystery of that small region of ER.

### 1.10.2 STIM1-binding proteins

It is known that the formation of the STIM1-Orai1 complex at the ER-PM junctions should associate with other proteins to facilitate the activity of SOCs. Numerous binding proteins have been identified by various studies using transfected cell lines. Evidence showed that STIM1 binds with EB1, microtubule plus end tracking protein, to induce microtubules tabulation and assists the movement of STIM1(Grigoriev et al., 2008). SARAF is an ER-resident protein that has an inhibitory effect on SOCs activity (Palty et al., 2012). Other binding proteins like junctata can assist the formation of the STIM1-Orai1 complex(Srikanth et al., 2012). STIM1 also binds with another $Ca^{2+}$

channel to influence SOCs activity. STIM1 binds with TRPC channels to increase the activity of SOCs (Ong et al., 2007a). Thus, the regulation of SOCs not only the STIM1-Orai1 interaction but also requires different type of proteins. However, most of information about STIM1 binding proteins were collected from whole cell lines. There is no enough and clear information about the protein profiling of small region of ER related to SOCs activation so it is essential to identify the different between the small regions to other part of ER.

## 1.11 Aims of the study

The identification of a small region of ER that associates with the activation of SOCs is crucial for understanding the mechanism of SOCs activation. The location of that small ER region should be at the region devoid with ribosome and close to plasma membrane. Although it has been demonstrated the presence of small region of ER the activation of $Ca^{2+}$ influx via SOCs, it is still unclear about the location, the nature and the molecular composition of that small region of ER related to SOCs activation. Therefore, it raises questions that (1) as the region lacked with ribosomes is thought to be the major location of that small region of ER, so is that small ER region mainly located at smooth ER rather than rough ER. (2) Does that small ER region compose with different level of STIM1 and Orai1 to other regions of ER. (3) Do other proteins at that specific small region involve in the regulation of SOCs function? In addition, as far we know, most of the information about the distribution of STIM and Orai1 were obtained by using cell lines transfected with exogenous STIM1 or Orai1 tagged with GFP or other fluorescence dyes. Thus, it would be useful and important to have more information

form animal study. This research should be the first study to use subcellular fractions of whole rat liver tissue to identify the distribution of endogenous STIM1 and Orai1 *in vivo*.

In order to study the specific region of ER with or without ribosome *in vivo*, the technique of subcellular fractionation was used to isolate rough ER and smooth ER to determine the distribution of STIM1 or Orai1 in those organelles by using western blot. Moreover, most of the studies on searching STIM1 binding proteins were used cell lines transfected with STIM1-tagged GFP or other fluorescent dyes from whole cells. Those results only provide the information from whole cell lines *in vitro* rather than the specific region of ER *in vivo*. There is still not enough information from whole tissue cells in vivo and explore the protein profiling of small region of ER. Therefore, the subcellular fractions were also used to study the protein profiling on the specific ER region in order to understand more about the nature of that specific small region *in vivo* and the role of SOCs activation. As most of the information about the mechanism of SOCs activation are from cell lines *in vitro*. The results from this thesis can provide another more useful and helpful information to understand the mechanism of SOCs activation *in vivo*.

The overall aims of the study are as follows:

1. To determine the distribution of STIM1 and Orai1 in subcellular fraction from resting and stimulated rat liver cells
2. To identify the subregion of ER for activating SOCs by depleting $Ca^{2+}$ from the endoplasmic reticulum.
3. To identify potential new associated protein of STIM1 in activating SOCs.
4. To test the role phosphorylation of STIM1 and Orai1 in the steatotic liver cell.

# Chapter II

# Material and methods

# Chapter II Material and methods

## 2.1 Materials

### 2.1.1 Chemicals

Dulbecco's Modified Eagles Medium (DMEM), Sucrose, 4-(2-hydroxyethyl-1-piperazineethanesulfonic acid (HEPEs), ethylene glycol-bis(2-aminoethylether)-*N*,*N*,*N′*,*N′*-tetraacetic acid (EGTA), dithiothreitol, Percoll, phenylmethylsulfonyl fluoride (PMSF), sodium chloride, leupeptin, pepstatin A, benzamidine, aprotinin, trypsin inhibitor, *o*-phenanthroline, phenylephrine, tetramethylethylenediamine (TEMED) , Tween-20, β-glycerolphosphate, glycerol and glucose (GO) assay Kit (GAGO-20), Polyacrylamide, coomassie brilliant blue G-250, Sodium fluoride, Tris and sulphuric acid were purchased from Sigma, St. Louis, MO USA.

Ammonium persulfate, Sodium dodecyl sulphate (SDS), bromophenol blue were purchased from Bio-Rad, Gladesville, New South Wales Australia. protein A/G plus-agarose immunoprecipitation reagent was from Santa Cruz Biotechnology (#SC2003 Dallas, Texas, USA). Acetic acid and methanol were purchased from Merck Millipore, Baysway, Victoria, Australia. Trifluoroacetic acid (TFA) and sodium vanadate were purchased from Ajax Chemical Co. Pty Ltd, Sydney. Skimmed milk is purchased from the local supermarket.

### 2.1.2 Antibodies

The antibodies used in the experiments were monoclonal anti-Stromal interaction molecule 1 (STIM1) antibody (Abcam, # 52458 Cambridge UK), polyclonal anti Orai1

(extracellular) antibody (Alomone Labs, #ACC062 Jerusalem Israel), polyclonal anti calreticulin (Santa Cruz Biotechnology, sc-7431 Dallas, Texas, USA), Monoclonal Anti PMCA ATPase antibody (Affinity Bioreagents, #MA3-914 Goldern Colorado USA) and Monoclonal Anti-SERCA2 antibody (Affinity Bioreagents, #MA3-919 Goldern Colorado USA), anti-Phosphoserine antibody (Abcam, #6639 Cambridge UK), Rabbit polyclonal antibody to peroxiredoxin 4 (65-83): whole serum (Biosensis# R-1593-100 Thebarton South Australia Australia), anti-TRPM2 antibody (Abcam, #63015); normal mouse IgG ( Santa Cruz Biotechnology, #sc-2025 Dallas, Texas, USA) and normal rabbit IgG (Santa Cruz Biotechnology,# sc-2027 Dallas, Texas, USA)

## 2.2 Surgical procedure for isolation of liver tissue

Male Hooded Wistar rats weighing 250-350g were used in the experiment. All the procedures were according to the criteria outlined in the "Australian Code of Practices for the Care and Use of Animals for Scientific Purposes" (National Health and Medical Research Council of Australia) and approved by the Animals Ethics committee from Flinders University of South Australia. The humane care including feeding and cleaning the animal cage was provided by animal care technicians in Flinders medical centre animal facilities. The rats provided *ad libitum* access to normal food and water were housed in feeding room with 12 hours cycle lighting system at Flinders medical centre animal facilities. On the day of the experiment, the rat was taken to the laboratory for conducting liver homogenisation and subcellular fractionation. About 5-10 ml of isoflurane was poured into the plastic chamber with the size of about 40 cm in height and 20 cm in radius covered with a lid and waited for 2 min to let the chamber

full with isoflurane. Then the rat was sedated by putting into the chamber. The sedated rat was taken out from the chamber and anesthetized by injecting ketamine (100mg/kg body weight) and xylazine (8mg/kg body weight) intraperitoneally. After the rat fully sedated and anesthetized, the four limbs of the rat were fixed with the sticky tape on the stage and ready for midline laparotomy. The liver was exposed and the connective tissue around the liver was cleaned. The rat was killed by cutting the heart and drained the blood until the colour of the liver become pale. Then, the liver was taken out and put into iced-cold isolated medium composed of 250mM sucrose, 5mM HEPES/KOH and 1mM EGTA, adjusted the pH to7.4 with 1M potassium hydroxide. The medium was supplied with 1mM dithiothreitol, 0.2mM PMSF, 10µg/ml leupeptin, 10µM pepstatin A, 2 µMbenzamide, 5 µg/ml aprotinin, 50 µg/ml trypsin inhibitor, 1 µg/ml *O*-phenanthroline to inhibit the activity of the protease. The connective tissue remaining on the liver was clean on ice-cold medium before homogenisation.

## 2.3 Surgical procedure for administration of phenylephrine

The effect of phenylephrine is to release the intracellular $Ca^{2+}$ from the store by the formation of inositol triphosphate though the activation of α1-adrenorecptor (Woods et al., 1986, Dasso and Taylor, 1992). Then, phenylephrine was injected to the rats to deplete the $Ca^{2+}$ store in order to activate SOCs. For the phenylephrine- treatment group, the rats were firstly sedated by isoflurane and anesthetised with ketamine/xylazine using the same producers described in section 2.2. Before the removal of the liver, 15µM of phenylephrine in the final blood concentration was injected into the rat though inferior vena cava and circulated for 20 min. Phenylephrine was dissolved in 0.9% sodium chloride and the volume of 1mM stock phenylephrine solution injected is

calculated based on the total blood volume of the rat. The estimation of total rat blood volume is calculated by the value of 7.5ml/100g body weight (Argent et al., 1994). Blood glucose level was measured to determine the effect of phenylephrine. About 500µl of whole blood was taken before the injection of phenylephrine and liver removal. The blood was kept in the tube for 30 min at room temperature to form the blood clot. After 30 min, the whole blood was centrifuged at 13,000g. Serum was collected and kept in -20 ºC until blood glucose assay. In addition, during the 20 minutes of phenylephrine circulation, the physiological response of breathing rate, heart beating and the secretion from the mouth were also monitored. Those parameters were used to determine the effect of phenylephrine. After 20 min circulation of 15µM phenylephrine, the liver was removed out from the rat using the same producers as described at section 2.2.

## 2.4 Preparation of liver subcellular fractions

The producers for the preparation of liver homogenisation and subcellular fractionation were according to the materials and methods described in Prpić, 1984 and Lièvremont, 1994, 1996 (Prpić et al., 1984, Lièvremont et al., 1996, Lièvremont et al., 1994).

The rat liver was first homogenised. The liver homogenate was subjected to subcellular fractionation. The subcellular fractionation was processed into two sections. The first section was to collect microsomal fraction and plasma membrane fraction. The second section was to collect extending subcellular fractions including nuclear, mitochondrial, microsomal and cytosolic fractions.

### 2.4.1 Liver homogenisation

The liver tissue about 12 g from untreated or phenylephrine-treated rats were chopped into small pieces using scissor in ice-cold isolation medium (250 mM sucrose, 1mM EGTA, 5 mM HEPES/KOH, pH 7.4) supplemented with proteolytic inhibitors (1 mM dithiothreitol, 0.2 mM PMSF, 10 µg/ml leupeptin, 10 µM pepstatin, 2 µM benzamidine, 5 µg/ml aprotinin, 50 µg/ml trypsin inhibitor and 1 µg/ml o-phenanthroline). Then the chopped liver tissue was homogenised with 40 ml of Dounce homogeniser (Kont) by using 10 passes of loose-fitting pestle and 3 passes of the tight-fitting pestle. The final volume of liver homogenate was about 170ml. It is about 6% of liver weight to isolation medium. The liver homogenate was ready for subcellular fractionation. All the producers from liver homogenisation and subcellular fractionation were performed on ice in order to avoid the degradation of the protein.

### 2.4.2 Isolation of Nuclear fraction, Mitochondrial fraction, Heavy microsomal fraction, Light microsomal fraction and Cytosol

The 6% of liver weight homogenate (w/v) was then subjected to differential centrifugation using Beckman J2-21centrifuge fitted with JA-20 rotor and Beckman L-70M Ultracentrifuge fitted with 55.2Ti rotor. The temperature in all centrifugation was set to 4 ºC. The crude nucleus fraction was collected from liver homogenate in 50 ml polyallomer tube with screwed cap after the centrifugation at 1,500g for 10 min. The pellets of nuclear fraction were resuspended with 2 ml of wash medium with proteolytic inhibitors and the final volume was about 12 ml. The supernatant from 1500g centrifugation was sedimented in 50 ml polyallomer tube with screwed cap at 8,000g

for 20 min. The pellets obtained are mitochondrial fraction. 6 ml of wash medium was used to resuspend the mitochondrial pellets. The supernatant from 8,000g centrifugation has undergone another centrifugation at 35,000g for 30 min for collecting heavy microsome. The light microsome was obtained from centrifuging of the supernatant of 35,000g at 100,000g for 60 min. Cytosol fractions about 150ml are the supernatant after 100,000g centrifugation. The pellets of heavy and light microsome were resuspended by adding 6 ml of wash medium (250 mM sucrose, 25 mM HEPES/KOH, pH 7.4) containing proteolytic inhibitors. A small pestle was used to help to disperse the pellets.

### 2.4.3 Isolation of plasma membrane fraction

Plasma membrane was prepared by Percoll gradient centrifugation according to producers described from Prpić, 1984 (Prpić et al., 1984). The crude nuclear fraction also containing plasma membrane was further diluted to 6 % (w/v) by adding about 170ml ice-cold isolation medium containing protease inhibitors. The pellets were resuspended by 4 strokes of loose-fitting pestle with Dounce homogeniser. About 22ml of Percoll was added into the suspension with the proportion of 1.4 ml of percoll to 10.4 ml of suspension. The mixture of the suspension and the percoll was undergone centrifugation with Beckman L-70M Ultracentrifuge fitted with 55.2Ti rotor in 37 ml polycarbonate centrifuge tube at 35,000g for 30 min. The white whole top flocculent layer was collected. About 20ml of the top layer was collected and the fraction was washed with incubation medium (250mM sucrose, 50mM Trizma/HCl, pH 8) by adding about 100ml of the incubation medium. It is about 5 volume of collected fraction and then sedimented the plasma membrane fraction with 35,000g for 30 min.

The supernatant was removed and added about 1 ml of incubation medium to resuspend the pellets by trituration for about 10 times.

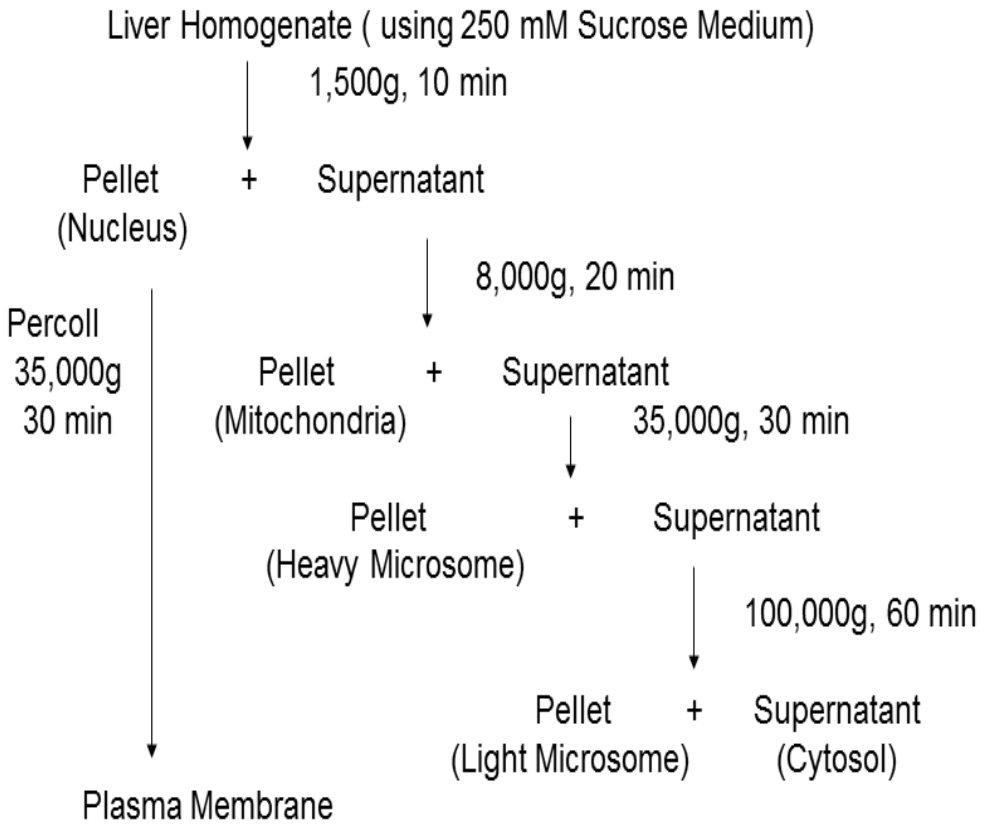


**Figure 2.1. Scheme of Subcellular fractionation on rat liver cells.**

The whole liver homogenate was subjected to differential centrifugation to collect nucleus, mitochondria, heavy microsome, light microsome and cytosol. Percoll gradient centrifugation was employed for preparation of plasma membrane by mixing percoll with nuclear fraction.

## 2.5 Culture of H4IIE cells and the treatment of Amiodarone

H4IIE cells were grown in Dulbecco's Modified Eagles Medium (DMEM) containing 10% foetal bovine serum (FBS) and penicillin/streptomycin in the T75cm$^2$ culture flask. The cells were incubated at 37 °C with 5% $CO_2$ until confluence over 95%. The cells were harvested by adding 1 ml of 1x trypsin-EDTA for 5 min in the incubator. 3 ml of a suspension containing 3x10$^6$ cells was added to 9 ml of culture medium in the culture flask. In the treatment group, 20µM of amiodarone in methanol was added, while in the control group, methanol alone was applied and control group was added methanol as vehicle control. The control and treated cells were incubated for 24 hours in an incubator.

## 2.6 Blood glucose assay

The blood glucose concentration was measured by Glucose (GO) assay kit from Sigma (GAGO-20).

The principle of glucose assay used in the glucose assay kit:

$$\text{D-Glucose} + H_2O + O_2 \xrightarrow[\text{Oxidase}]{\text{Glucose}} \text{D-Gluconic acid} + H_2O_2$$

$$\text{Hydrogen Peroxide} + \text{Reduced o-Dianisidine (colourless)} \xrightarrow{\text{Peroxidase}} \text{Oxidized o-Dianisidine (Brown colour)}$$

$$\text{Oxidized o-Dianisidine (Brown colour)} \xrightarrow{\text{Sulfuric acid}} \text{Oxidized o-Dianisidine (Pink colour)}$$

The Assay Reagent was prepared before the assay by mixing 0.8 ml of o-Dianisidine and 39.2 ml of Glucose oxidase/peroxidase reagent. Four standard glucose solutions ranged from 20, 40, 60 and 80 µg glucose/ml were used to construct the standard curve for the assay. Serum samples collected from 0 and 20 min after the injection were diluted into 1: 50 and 1:100. 1 ml of standard and tested samples were added with 2 ml of assay reagent (o-Dianisidine and glucose oxidase/peroxidase reagent). In blank reagent tube, 1.0 ml of water was mixed with 2.0 ml of Assay Reagent. The addition of reagent to each tube had 30-60 sec intervals and used the pipette to mix the reagents up and down about 10 times. After the mixing of the reagents, the tubes were put into 37 °C water bath for 30 minutes to start the reaction. After 30 minutes, the reaction was stopped by adding 2.0ml of 12N sulfuric acid in 30-60sec intervals for each tube to form stable pink colour product. The absorbance was measured in 3 ml plastic curette at 540 nm by Shimazdzu UV-120-02 spectrophotometer.

## 2.7 Extraction of protein from control and amiodarone-treated H4IIE cells

The protein was extracted from control and amiodarone-treated H4IIE cells. The medium was removed from T75culture flasks and the cells were washed with PBS for 3 times. After the wash, 1 ml of ice-cold lysis buffer containing proteolytic inhibitor and phosphatase inhibitor (150mM NaCl, 50mM Trizma/HCl , 5mM EGTA, 1% Nonidet P-40, 0.25% Sodium deoxycholate , 0.1% sodium dodecyl sulphate (SDS), 0.2mM PMSF, 10 µM pepstatin A, 10 µg/ml leupeptin, 50 mM NaF, 1mM vanadate and 25 mM β-glycerolphosphate) was added directly into the flask for protein extraction. The surface of flask bottom was scraped with a scraper and then collected the lysis buffer by

transfer to 1.5 ml Eppendorf tube. The lysate was put on the ice and waited for 4 minutes to let protein fully dissolve into lysis buffer. The lysate was pipetted up and down for several times until the cell fully dispersed. The cell debris was sedimenting at 15,000g for 5 minutes using Beckman microcentrifuge Microfuge®16 at 4 °C cold room. The supernatants were collected and kept in -80 until further experiment.

## 2.8 Extraction of protein from frozen Zucker rat liver tissue

The frozen Zucker rat liver tissue about 500 mg were kept in -80 ºC freezer until protein extraction. The ratio of ice-cold lysis buffer to liver tissue is 100 µl of lysis buffer to 10 µg of liver tissue weight. It was about 5 ml of lysis buffer added to 500 mg of liver tissue. The lysis buffer containing proteolytic inhibitor and phosphatase inhibitor was composed of were 150mM NaCl, 50mM Trizma/HCl , 5mM EGTA, 1% Nonidet P-40, 0.25% Sodium deoxycholate , 0.1% sodium dodecyl sulphate (SDS), 0.2mM PMSF, 10 µM pepstatin A, 10 µg/ml leupeptin, 50 mM NaF, 1mM vanadate and 25 mM β-glycerolphosphate. The liver tissues were homogenated by Potter-Elvehjem homogenizer. The liver homogenate was put on ice for 30 minutes to let the protein fully dissolve into the lysis buffer. After 30 minutes, the cell debris was centrifuged at 14,000g for 20 minutes at 4 ºC by Beckman J2-21centrifuge fitted with the JA-20 rotor. The supernatant was collected and kept at -80 °C for further experiment.

## 2.9 Protein determinations

The EZQ protein quantitation Kit (Molecular probes the USA), the rapid solid-phase fluorescence protein assay, was used to measure the total protein concentration. The sample protein was spotted on the filter paper. The dye reagents binds to the protein and the protein bound with the dye will emit the fluorescence when excited by laser (Agnew et al., 2004). The intensity of the fluorescence was measured using the protocol provided by the manufacturer. Each subcellular fraction was diluted into 50 and 100 times in 2% sodium deoxycholate to solubilise the protein and waited for 30 min at room temperature. Standard Ovalbumin protein in concentration of 0.02, 0.05, 0.1, 0.2, 0.5, 1.0, 2.0 µg/µl were used to construct the standard curve to estimate the protein concentration in the sample. 1µl of the standard ovalbumin solution and 1µl sample were spotted on the filter paper. The filter paper leaving at room temperature dried by air. After the paper dried, the filter paper was washed with methanol for 5 min to remove the detergent from the sample. The paper was then dried by using Easy Breeze gel drier with low temperature (about 40°C). The proteins on the paper were then stained by 40-50ml of EZQ quantitation reagent (component A) for 30 min at room temperature. After 30 min, the paper was destained 3 times by using destaining buffer (10% methanol, 7% acetic acid and 83% deionized water) for 2 min. The image of the fluorescence spot was obtained by scanning with GE Typhoon 9400 Fluorescence Imager using laser excitation 457nm (Blue1) and emission 610nm. The intensity of the fluorescence on each spot was quantified by ImageQuant software (GE Health) or Carestream MI SE network software (Carestream Health, Inc).

The intensity from the Standard Ovalbumin protein was used to plot a standard curve of intensity against the mass of the protein. The points of the curve were then used to calculate the linear equation. The linear equation obtained from the standard curve was used to calculate the total protein concentration of the samples. The protein concentration of the sample was the average of the values from the 50-fold and 100-fold dilutions.

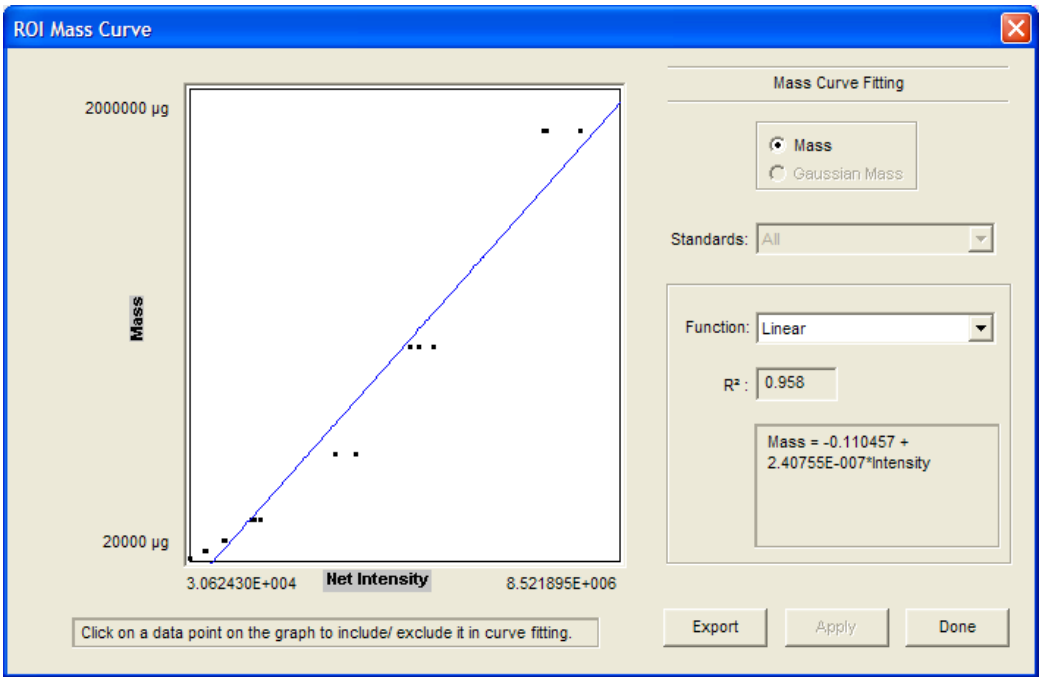


**Figure 2.2 The standard curve of ovalbumin protein obtained from EZQ protein assay by using Carestream MI SE network software**

## 2.10 Western Blot

### 2.10.1 One-dimensional SDS-PAGE

Hoefer miniVE vertical electrophoresis system and Bio-Rad Protean® tetra cell were used in running one-dimensional sodium dodecyl sulfate (SDS)-electrophoresis. Protein in subcellular fractions was resolved by Hoefer miniVE vertical electrophoresis system with self-pour 4%~20% SDS-polyacrylamide gel. The eluted protein from immunoprecipitation of STIM1 was resolved by Bio-Rad Protean® tetra cell with the AnykD TM Resolving precast Gel (Bio-Rad Laboratories). The samples of different subcellular fraction were heated with sample loading buffer (50 mM Tris- HCl, pH 6.6, 2%SDS, 0.1% bromophenol blue, 10% glycerol and 100mM dithiothreitol added freshly) at 87 °C for 10 minutes. The protein amount used for microsomal and plasma membrane western blot experiment was 25 µg per lane for whole liver and light microsome; 15µg per lane for heavy microsome and plasma membrane per lane. In mitochondrial and microsomal subcellular fraction western blot, 30 µg of protein amount per lane was used. After 10 min of heating, 20µl of the sample solution was loaded on 4%~20% SDS-polyacrylamide gel or BioRad AnyKD precast gel and separate the total protein by running at 36mA, 200V. The electrophoresis was stopped when the blue front marker of bromophenol blue was above the bottom of the gel about 1.5~2.0cm.

2.10.2 Semi-dry protein transfer

After the electrophoresis finished, the protein on the gel was transferred to polyvinylidene difluoride (PVDF) membrane by Semi-dry transfer apparatus (Hoefer). The PVDF membrane was cut in the size of 9cm height and 7cm length and also two pieces of BioRad extra thick blot paper in the same size as PVDF membrane. The membrane and the blotting paper were soaked in transfer buffer about 15 min. The PVDF membrane was soaked in methanol for few sec before putting into the transfer buffer. A piece of overhead transparency having a hole in the middle with the same size of the membrane was put over the grid of the semi-dry transfer unit. The steps of assembly the sandwich was put the blotting paper on the hole at the transparency and then PVDF membrane. The gel was placed on the top of the membrane. Another blot paper was finally put on the top of the gel. No air bubbles were allowed to form at the gap of each layer. The lid of the apparatus was placed on the top and applied about 1 kg of weight on the top to improve the contact of the sandwich. The transfer was used 1 mA per $mm^2$ of membrane area for two hours. The PVDF membrane was washed with Tris buffer solution (TBS) for 5 min and then the PVDF membrane was blocked with blocking buffer (5% skim milk in TBS with 0.1% Tween -20) for one hour at room temperature for all western blots except western blot of phosphoserine using 5% or 10 % of bovine serum albumin (BSA) as blocking agents.

2.10.3 Primary antibodies incubation

After blocking, the PVDF membrane was probed with a given primary antibody in sealed plastic bag with 5 ml of blocking buffer containing primary antibody at 4 °C for overnight. The detail of the dilution of different is as in table 2.

2.10.4 Secondary antibodies incubation and visualization of the bands on PVDF membrane

The secondary antibody conjugated with horse radish peroxidase (HRP) was used to visualise the bands on the PVDF membrane. The PVDF was washed three times with TBST (TBS with 0.01%Tween-20) for 10 minutes at room temperature. After the wash, the membrane was incubated with 5 ml of blocking buffer in sealed plastic bag containing with Donkey anti- mouse antibody- HRP for anti-STIM1 and anti-PMCA western blot, Donkey anti-goat-HRP for anti-calreticulin western blot and Donkey anti-rabbit –HRP antibody for Orai1 and Prx4 western blot at room temperature for one hour. All secondary antibodies were diluted in 1:5000 in blocking buffer. After one hour incubation, the PVDF membranes were washed with TBST three times 10 minutes at room temperature before imaging. The image of the band on the PVDF membrane was visualised by FujiFilm LAS4000 Imager. About 4.0 ml of enhanced chemiluminescence detection reagents (SuperSignal® Western Pico substrate, Thermo Scientific) containing 2.0 ml of luminol enhancer solution and 2.0 ml stable peroxide solution was added on the PVDF membrane and reacted for 6 minutes before imaging. The settings of the imaging are the same in each experiment. The resolution of the image is set to standard that has the pixels of 1536x1024 and the exposure time is 10 minutes. All the imaging in the different experiment is kept at the same resolution and

exposure time in order to compare the quantitative results between different experiments.

2.10.5 Quantitation of the bands on westerns

The band intensity was quantified by using MultiGauge software. Briefly, the rectangle was drawn on one of the band of interest that cover enough of the band and use that rectangle as standard to cover other interested bands. Moreover, the same size of the rectangle was also used to place above the band of interest in order to measure the background value. The two values were obtained for quantification of western blot results, the band intensity and background of the membrane. The value of the intensity of the band was subtracted by the background. Then the intensity value after the background subtraction was normalised by the amount of protein that loaded onto the SDS-PAGE.

The total units of the protein of each specific protein in each subcellular fraction were calculated by the equation as follows:

**Total amount of specific protein= Intensity after normalised (unit/mg protein) x protein concentration in the subcellular fraction (mg/ml) x Total volume of the subcellular fraction (ml).**

For TRPM2 western blot on mitochondria and microsomal fractions, the intensity of the total protein on PVDF was measured by using BioRad Gel Doc EZ Imager. The measured intensity of total protein was used to normalise the intensity of the band of interest.

| Primary Antibody and animals raise | Dilution in Primary Antibody | Company for primary antibody | Secondary Antibody and dilution |
|---|---|---|---|
| Goat Polyclonal Anti Calreticulin | 1:2500 | Santa Cruz Biotechnology, sc-7431 | Donkey Anti Goat-HRP 1:5000 |
| Mouse Monoclonal Anti PMCA | 1:2000 | Affrinity Bioregant, #MA3-914 | Donkey Anti Mouse-HRP 1:5000 |
| Monoclonal Anti-STIM1 | 1:2000 | Abcam, # 52458 | Donkey Anti Mouse-HRP 1:5000 |
| Rabbit Polyclonal Anti-Orai1 | 1:500 | Alomone Labs, #ACC062 | Donkey Anti Rabbit-HRP 1:5000 |
| Rabbit Polyclonal Anti-Peroxiderine 4 | 1:1000 | Biosensis, # R-1593-100 | Donkey Anti Rabbit-HRP 1:5000 |
| Sheep Polyclonal TRPM2 | 1:500 | Abcam, #ab63015 | Donkey Anti-Sheep-HRP 1:5000 |
| Mouse Anti-phosphoserine | 1:500 | Abcam, # 6639 | Donkey Anti Mouse-HRP 1:5000 |

**Table 2.1 Antibodies used in western blot on subcellular fraction**

## 2.11 Immunoprecipitation

The procedures of immunoprecipitation in this section are modified from the methods described previously at Litjens et al (Litjens et al., 2007)

### 2.11.1 Immunoprecipitation of STIM1 protein from heavy microsome to search for STIM1 binding protein

500 ml of lysis buffer (150mM NaCl, 50mM Trizma/HCl , 5mM EGTA, 1% Nonidet P-40, 0.25% Sodium deoxycholate , 0.1% sodium dodecyl sulphate supplied with proteolytic inhibitors, 0.2mM PMSF, 10 µM pepstatin A, 10 µg/ml leupeptin) was used to dissolved the protein in heavy microsome. The final protein concentration is 5mg/ml. The lysis buffer containing heavy microsome was then incubated with 1 µg anti-STIM1 antibody at 4°C overnight. In order to avoid the loss of weakly bound STIM1 binding proteins, no preclear step was done on the lysate from heavy microsome.

After overnight incubation, 20µl of Protein A/G plus agarose was added to the mixture and incubated for another 4 hours at 4°C. After the 4 hours incubation, the Protein A/G plus agarose was collected by centrifugation at 15,000g for 10 minutes at 4°C by Beckman microcentrifuge Microfuge®16. The Protein A/G plus agarose collected was washed with lysis buffer for 3 times. 40µl of 1Xsample loading buffer with dithiothreitol freshly was added to the immunoprecipitate/Protein A/G plus agarose and heat at 87°C for 10 min to elute the protein from Protein A/G plus agarose. The eluted protein from Protein A/G plus agarose was separated by centrifugation at 15,000 g for 1 min and 20µl of the supernatant was loaded into the Any kD TM Resolving Gel (Bio-Rad Laboratories) to run the electrophoresis. The producers used were described in section 2.10. The resolved protein on the gel was then transferred to PVDF membrane

by semi-dry transfer. The PVDF membrane was washed with TBS buffer for 5 min and then blocked with 5% skimmed milk in TBS with 0.1% Tween -20 for one hour at room temperature. After blocking, the PVDF membrane was incubated with anti-STIM1 antibody, anti-Orai1 antibody or anti-SERCA2 antibody in TBST for overnight at 4 °C and secondary antibody with HRP for 1 hour room temperature. The bands on the PVDF membrane was visualized by reacting enhanced chemiluminescence detection reagents (SuperSignal® Western Pico substrate, Thermo Scientific) and detected by FujiFilm LAS4000 Imager.

### 2.11.2 Immunoprecipitation of STIM1, Orai1 and phosphorylated protein from steatotic liver cells for detecting phosphorylation

The liver lysate from Zucker rat and lipid-loaded H4IIE cell were diluted to 5mg/ml of total protein into 500µl of lysis buffer (150mM NaCl, 50mM Trizma/HCl , 5mM EGTA, 1% Nonidet P-40, 0.25% Sodium deoxycholate , 0.1% sodium dodecyl sulphate supplied with proteolytic inhibitors, 0.2mM PMSF, 10 µM pepstatin A, 10 µg/ml leupeptin and phosphatase inhibitors , 50 mM NaF, 1mM vanadate and 25 mM β-glycerolphosphate). The Zucker rat liver lysate was precleared by incubating with Protein A/G plus agarose at 4 °C for 1 hour. The precleared lysate was then centrifuged at 15,000g for 10 min by Beckman microcentrifuge Microfuge®16 and collected the supernatant to conduct immunoprecipitation. The Zucker rat liver lysate and lipid-loaded H4IIE cells lysate were then incubated with 1 µg anti-STIM1, 1 µg anti-Orai1 or anti-phosphoserine antibody (1:1000 dilution) at 4°C overnight.

Then 20µl of Protein A/G plus agarose was added to the mixture and incubated for another 4 hours at 4°C. After the incubation, the Protein A/G plus agarose was

collected by centrifugation at 15,000g for 10 minutes at 4°C by Beckman microcentrifuge Microfuge®16. The Protein A/G plus agarose collected was then washed with lysis buffer for 3 times. 40µl of 1x sample loading buffer with freshly added dithiothreitol was added to the immunoprecipitate/Protein A/G plus agarose and heat at 87°C for 10 min to elute the protein from Protein A/G plus agarose. The eluted protein from Protein A/G plus agarose was separated by centrifugation at 15,000 g for 1 min and 20µl of the supernatant was loaded into the Any kD TM Resolving Gel (Bio-Rad Laboratories) to run the electrophoresis. The producers were same as section 2.10 described. The resolved protein on the gel was then transferred to PVDF membrane by semi-dry transfer. The PVDF membrane was washed with TBS buffer for 5 min. For western blot of STIM1 or Orai1, 5% skimmed milk in TBS with 0.1% Tween -20 was used as blocking buffer and the buffer was incubated with the PVDF for one hour at room temperature. For western blot of phosphoserine, the blocking agent was used 5% of bovine serum albumin (BSA) and incubated the PVDF with the blocking buffer for one hour at room temperate. After blocking, the PVDF membrane was incubated with anti-STIM1 antibody, anti-Orai1 antibody or anti-phosphoserine antibody for overnight at 4 °C and secondary antibody with HRP for 1 hour room temperature. The visualisation of the bands is described as the procedures in section 2.10.4. The bands on the membrane were visualised by reacting enhanced chemiluminescence detection reagents (SuperSignal® Western Pico substrate, Thermo Scientific) and detected by FujiFilm LAS4000 Imager.

## 2.12 Identification of protein by LC/MS

### 2.12.1. Immunoprecipitation of STIM1 from heavy microsome and Trypsin digestion

Mass spectrometry was used to identify STIM1 binding protein by analysis of protein, which co-elute when STIM1 is immunoprecipitated from the microsomal fraction. After the immunoprecipitation of STIM1 protein from heavy microsome fraction, the immunoprecipitates/protein A/G Plus agarose was washed with PBS and removed the supernatants after centrifuging at 15,000g for 10 minutes. Then, the protein was eluted from the protein A/G plus agarose by adding 3 volume of 0.1% trifluoroacetic acid (TFA) to immunoprecipitates/Protein A/G plus agarose for three times with 2 minutes at 4 °C. The supernatants were collected after centrifugation at 15,000g for 10 minutes. The collected supernatants were then concentrated using a Centrivep concentrator (Labconco). The pH was adjusted by 100mM ammonium bicarbonate to about 8 before adding trypsin. The pH was tested by using pH paper. 20µl of 100mM ammonium bicarbonate containing 5ng/ µl of trypsin was added to the concentrated protein extract and incubated at 37°C overnight.

### 2.12.2 Detection of digested peptide by LC-MS/MS

The peptide resulting from the protein digestion described above were analysed by Thermo Orbitrap XL high resolution mass spectrometer connected with nanospray. The sample was applied to a 300 mm id×5 mm C18 PepMap 100 precolumn (Dionex, Sunnyvale, CA) and then separated the peptide on a 75 mm×150 mm C18 5 µm 100 Å column (Nikkyo Technos, Tokyo, Japan) using a Dionex Ultimate 3000HPLC with a

mobile phase of acetonitrile (ACN) gradient from 2% to 45% in 55 minutes in 0.1% formic acid at a flow rate of 200 nL/min followed by 77% ACN for 9 minutes. The mass spectrometry was operated in positive ion mode. Fourier transform mass spectrometry (FTMS) m/z 300-3000 at 60, 000 resolution was performed on the precursor ions followed by ion trap mass spectrometry (ITMS). Analysis of the top 6 multiply charged ions. Charged state rejection was employed. The ions were rejected when the charged state was 1.

### 2.12.3 Identification of protein by searching Database

The spectra were searched with version 1.2 using the SEQUEST algorithm against the rat International Protein Index (IPI) database version 3.74 composed of a total 39,708 protein entries. The search parameters were: (1) up to two missed cleavage for trypsin as protease; (2) the mass tolerance of the identification was 10 ppm for precursor ions and 0.8 Da for product ions and variable modifications of carbamidomethylation, oxidation of methionines and phosphorylation of serine, threonines and tyrosines. The filter used in the acceptance of the spectra is as follows: (1) cross-correlation (Xcorr) of matches is 1.5, 2.0 and 2.5 for charge 1,2 and 3 peptide, respectively. (2) more than 2 different peptides are matched.

# Chapter III

# The Distribution of STIM1 and Orai1 in Subcellular Fractions

# Chapter III The Distribution of STIM1 and Orai1 in Subcellular fractions

## 3.1 Introduction

The subcellular localisation of specific molecules is an important information for determining how the signal pathways regulate the functions of the cells. The rise of [$Ca^{2+}$] in cytoplasmic space mediated by SOCs is one of the major $Ca^{2+}$ channels to regulate the cellular function in non-excitable cells (Parekh and Putney, 2005). STIM1 and Orai1 are two essential components required for the activation of SOCs. It has been showed that the depletion of $Ca^{2+}$ store induces the movement of STIM1 to the region on the ER close to plasma membrane and form oligomers (Liou et al., 2007). These oligomers of STIM1 then activate Orai1 to induce the $Ca^{2+}$ influx. In the liver cell, STIM1 is distributed evenly on ER and form puncta after the depletion of $Ca^{2+}$ store (Aromataris et al., 2008, Berna-Erro et al., 2012). Orai1 is showed to be expressed on plasma membrane at human submandibular gland cells line (HSG cells) (Ong et al., 2007a) and can be detected the expression in rat liver cells (Guzman et al., 2014). Thus, STIM1 and Orai1 are two vital molecules to the function of liver cells.

The small region of ER has been suggested responsible for the activation of SOCs in liver cells (Castro et al., 2009), but the detail information of the location, the nature and the molecular compositions of that small ER region is still not well understood. Then, it is essential to understand the location, the nature and the molecular compositions of that small region of ER. Moreover, there is still no clear information about the distribution of endogenous STIM1 and Orai1 at the

subcellular level *in vivo*. As far we know, most of the results in studying the distribution of STIM1 and Orai1 were from over-expressed tagged cell lines (Wu et al., 2006, Fukushima et al., 2012). It is known that STIM1 is enriched at cortical ER after $Ca^{2+}$ store depletion (Orci et al., 2009). Thus, it would assume that the small region of ER for SOCs activation might be located at ER deprived with ribosome. Then, the aim of this chapter is to identify the intracellular distribution of endogenous STIM1 and Orai1 at the rough ER and smooth ER in rat liver cells as smooth ER is thought to be the main location of that small region.

In order to achieve the goal of detecting the intracellular distribution of STIM1 and Orai1 at rough and smooth ER, the subcellular fractionation technique was employed by using differential and gradient centrifugation to collect subcellular fractions of rough and smooth ER according to their density (Lee et al., 1969). Two methods of subcellular fractionation were employed. In the first, called microsomal and plasma membrane subcellular fractionation, the liver homogenate was subjected to differential centrifugation to yield heavy microsome, light microsome and nuclear fraction was subjected to percoll gradient centrifugation to yield plasma membrane. In the second, called mitochondrial and microsomal subcellular fractionation, the liver homogenate was subjected to differential centrifugation to yield nuclear fraction, mitochondrial fraction, heavy microsomal fraction, light microsomal fraction and cytosolic fractions. The heavy microsome with higher density collected from the subcellular fractionation is derived from rough ER as it attached with ribosome. Light microsome is derived from smooth ER with lower density (Dallner and Ernster, 1968).

After the subcellular fractions had been collected, the distribution of endogenous STIM1 and Orai1 among those subcellular fractions were detected by using quantitative western blotting method. Firstly, the subcellular fractions collected from the rat liver were tested by the western blot of calreticulin, the marker protein of ER, and plasma membrane $Ca^{2+}$ ATPase (PMCA), plasma membrane marker protein in order to confirm the subcellular fractions collected are from ER and plasma membrane. After the subcellular fractions confirmed by the western blot of calreticulin and PMCA, the distribution of STIM1 and Orai1 was then tested.

In order to quantify the western blot results, the intensity of the bands from the western blot was validated by establishing the correlation between the amounts of protein to the band intensity from western blot by using different antibodies in the experiments. In addition, the effect of $Ca^{2+}$ store depletion on the distribution of STIM1 and Orai1 was also explored. I collected the subcellular fraction from the rat after the injection of phenylephrine to activate the SOCs.

## 3.2 Results

### 3.2.1 Identification and quantification of western blot of calreticulin (ER marker) and Plasma membrane $Ca2^{+}$ ATPase (PMCA) (plasma membrane marker) on subcellular fractions from rat liver cells

#### 3.2.1.1 Identification of calreticulin and PMCA on microsomal and plasma membrane fraction by Western blot

The amount of total proteins on each subcellular fraction was firstly measured in order to assist the quantification of the distribution of STIM1 and Orai1. From Table 3.1, heavy microsome contains higher amount of total proteins than other fractions. It contains about 5.5% in untreated liver. Light microsome has about 3.2% of total protein and plasma membrane only contains 0.01% of total protein.

| Subcellular Fraction | Amount of Calreticulin in Liver Homogenate or Subcellular fractions (%) | Amount of PMCA in Liver Homogenate or Subcellular fractions (%) | Total protein in Liver Homogenate or Subcellular fractions (%) |
|---|---|---|---|
| | untreated (n=5) | Untreated (n=5) | untreated |
| Whole Liver Homogenates | 100 | 100 | 100 |
| Heavy Microsome | 19.0% | 20.8% | 5.5% |
| Light Microsome | 3.2% | 4.3% | 3.2% |
| Plasma membrane | 0.02% | 0.58% | 0.01% |
| Sum of the subcellular fraction % | 22.3% | 25.7% | 8.4% |

**Table 3.1 The Distribution of total protein, calreticulin and PMCA in microsomal and plasma membrane fraction.**

Subcellular fractions of whole liver, heavy microsome, light microsome and plasma membrane obtained from differential centrifugation from untreated rat livers were subjected to western blot. The bands were detected by immunodetection and the intensity of the bands was measured on each subcellular fraction. The data expressed as % of whole liver homogenate. N is represented as the number of subcellular fractionation done.

The identities of the subcellular fractions were examined by specific marker protein to the organelles using western blot method. Calreticulin the $Ca^{2+}$ binding protein resided at ER and plasma membrane $Ca^{2+}$ ATPase (PMCA) were selected as endoplasmic reticulum (ER) marker protein and plasma membrane marker protein, respectively (Smith and Koch, 1989, Kessler et al., 1990).

Figure 3.1a was the western blot of calreticulin on heavy and light microsome by loading with different protein amount ranging from 10µg to 60µg. The subcellular fraction of heavy microsome and light microsome only displayed a strong band at the size of 55 kDa, which is the size of calreticulin (Smith and Koch, 1989, Garcia-Arcos et al., 2010).

The result of western blot of PMCA loading the proteins ranging from 7.5µg to 25µg indicated that only plasma membrane fraction showed two strong bands only at 140 kDa and 180 kDa (Figure 3.2 a). The band of 140 kDa is the expected size of PMCA (Kessler et al., 1990). For the band of 180 kDa, other evidence demonstrated that the PMCA antibody would detect this slightly high molecular weight band on western blot (Hilfiker et al., 1994). However the nature of the higher molecular weight band is still not clear, it was suggested that this higher molecular weight band would be an aggregation of PMCA (de Talamoni et al., 1993). There were no significant bands detected at both heavy and light microsomes.

### 3.2.1.2 Quantification of the bands intensity from western blot of calreticulin and PMCA on microsomal and plasma membrane fraction

After obtaining the image from the western blot, the intensity of the bands from western blot was then measured and quantified. In order to quantify the intensity of the bands, the quantification method is needed to be validated. It was done by establishing the correlation of the intensity to the protein amount from different antibodies.

The intensity of the band was measured and the values were subtracted by the background. The values of the intensity were used to plot the graph again the amount of the protein. In Figure 3.1b, it was the results of correlation between the intensity from calreticulin western blot and amount of protein. The results displayed that the immunosignal from calreticulin western blot produced a linear relationship to the protein amount between 10 µg and 60µg. $R^2$ is the statistic measure to show the correlation between two factors. The value of $R^2$ is ranging from 0 to1. When the value of $R^2$ close to 1, that means it has a good linear relationship between two factors. From the result, the $R^2$ is about 0.93 in both heavy microsome and light microsome.

The graph of the correlation between band intensity from PMCA and protein amount was showed at figure 3.2b. As mentioned before, there has 2 bands showed on PMCA western blot so I used the sum of the intensity from these two bands to construct the correlation between the band intensity and protein amount. In Figure 3.2b, it showed that the band intensity from PMCA western blot had a linear correlation to protein amount. The $R^2$ of the curve from immunosignal of PMCA to protein amount is 0.99.

(3.1a)

(i) Heavy Microsome

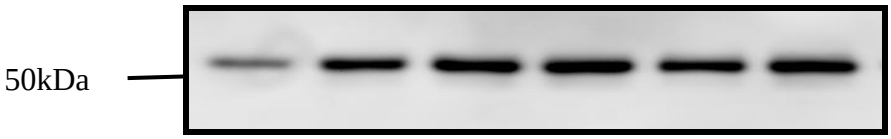


(ii) Light Microsome

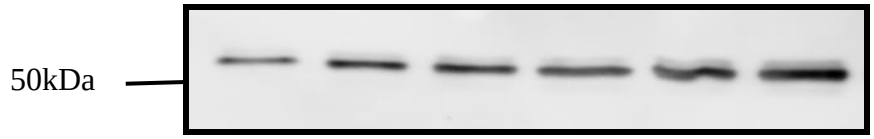


10μg 20μg 30μg 40μg 50μg 60μg

(3.1b)

(i) Heavy microsome

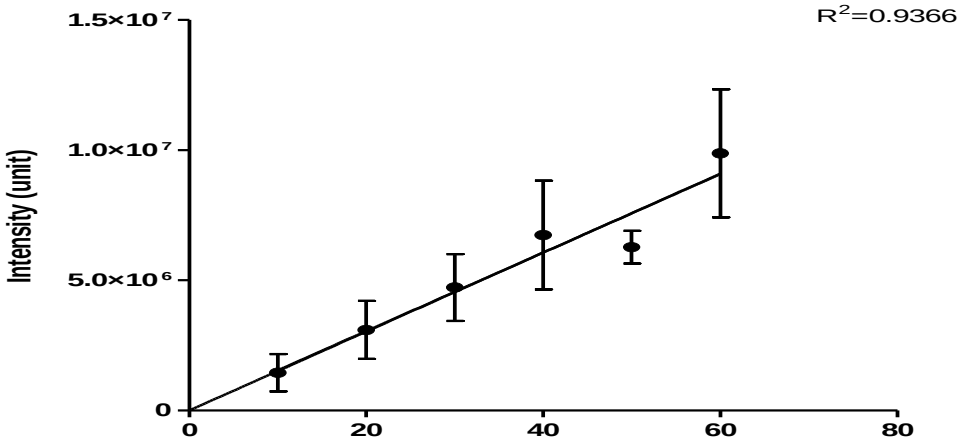

(ii) Light Microsome

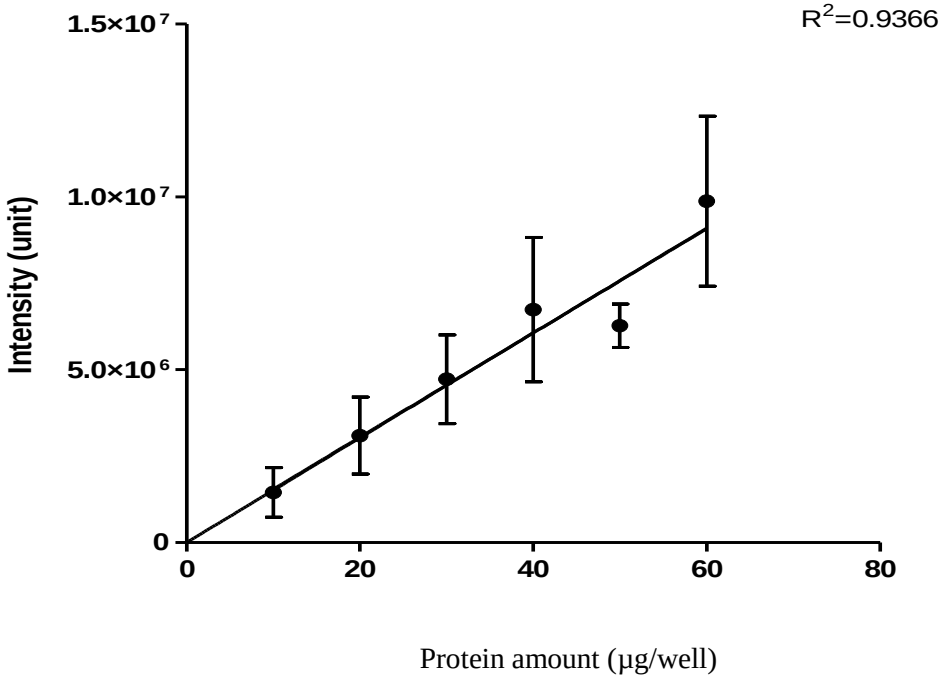


**Figure 3.1 Detection and Quantification of band intensity on calreticulin western blot on heavy and light microsomes.**

**(a)**Western blot of calreticulin on (i) heavy microsome and light microsome (ii) by loading with the protein amount ranging from 10 µg to 60 µg onto the SDS-PAGE. The results shown are representative of those obtained from one out of four experiments which give similar results (N=4). **(b)** Quantitation of band intensity from western blot of calreticulin in heavy microsome (i) and light microsome (ii). The band intensity from western blot against the function of protein amount was plotted to show the correlation. The results were expressed as mean ± SEM.

**(a)**

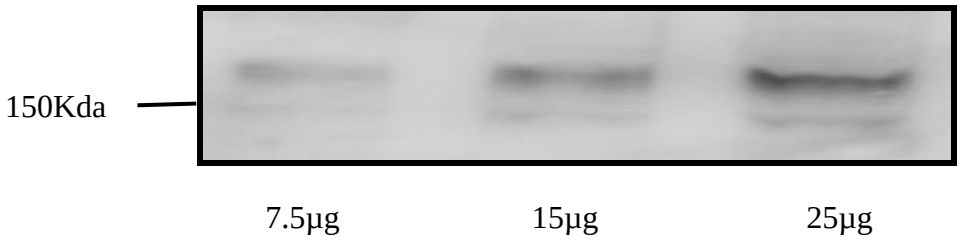


**(b)**

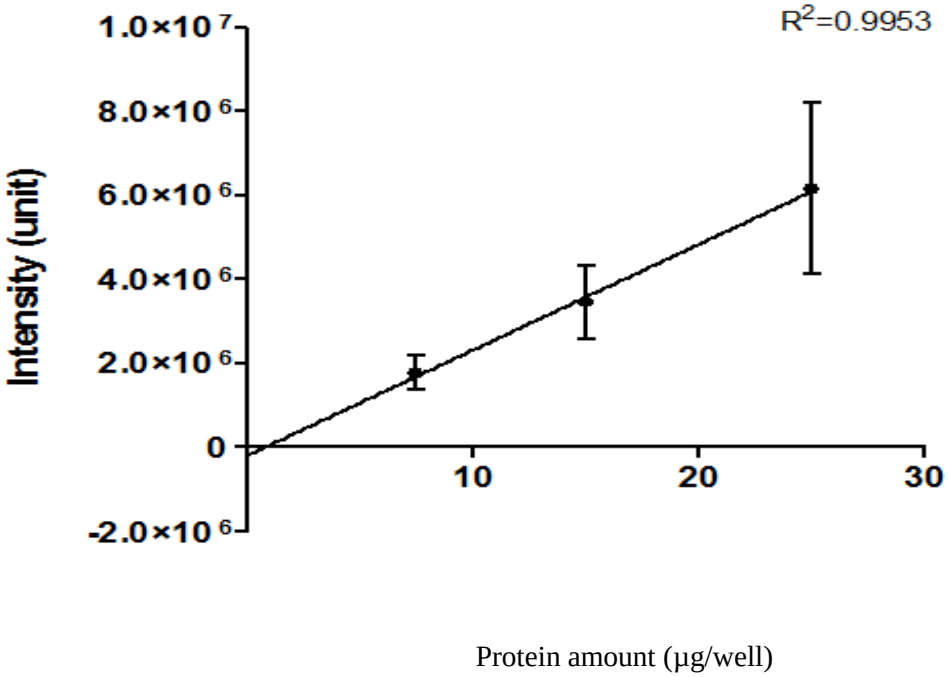


**Figure 3.2 Detection and Quantification of the band intensity on PMCA western blot on plasma membrane fraction obtained from the microsomal and plasma membrane subcellular fractionation.**

**(a)**Western blot of PMCA on plasma membrane by loading with the protein amount ranging from 7.5µg to 25 µg onto the SDS-PAGE. The results shown are representative of those obtained from one out of four experiments which give similar results (N=4). **(b)** Quantitation of band intensity from western blot of PMCA on plasma membrane. The intensity of the band against the function of protein amount was plotted to show the correlation. The results were expressed as mean ± SEM.

### 3.2.1.3 Detection and quantification of bands intensity corresponding to calreticulin and PMCA in western blot on microsomal and plasma membrane fraction

The bands intensity from western blot of calreticulin and PMCA on microsomal fraction and plasma membrane fraction were measured and quantified after the establishment of the correlation between bands intensity and protein amount. The values of the intensity obtained from the western blot were subtracted by the background and the values were normalised by dividing the intensity units with the amount of protein loaded on the SDS-PAGE. The values were expressed as arbitrary intensity per milligram of protein on each subcellular fraction after the normalisation.

Figure 3.3a was the western blot of calreticulin (i) and PMCA (ii) on microsomal and plasma membrane fractions. The western blot of calreticulin showed a band on 55 kDa on microsomal and plasma membrane fraction. Although calreticulin is an ER resident protein, evidence has indicated that calreticulin has its function on the cell surface (Gardai et al., 2005). Thus, it is not surprisingly that calreticulin antibody can also detect calreticulin on plasma membrane fraction in our experiment. In PMCA western blot, only plasma membrane fraction showed two strong bands at 140 kDa and 180 kDa. There were no significant bands observed on both heavy and light microsomes.

After quantifying the intensity of the bands from western blot, the results showed that the heavy microsome has higher enrichment of calreticulin than in light microsome and plasma membrane. The enrichment of calreticulin in heavy microsome is 2.5-fold and 3.4-fold more than light microsomes and plasma membrane, respectively (figure 3.3 b, i). Heavy microsome and light microsome contain a higher amount of total PMCA. It is about 23.0% and 3.2% of total calreticulin in heavy microsome and light microsome, respectively. Plasma membrane only has 0.02% of total calreticulin (Table 3.1). As

plasma membrane has a lower amount of total proteins, thus the plasma membrane fraction contains a relative lower amount of total PMCA protein. However, when the data express as units per mg of protein, the data showed that plasma membrane has a higher portion of PMCA to total proteins on plasma membrane fraction. Thus, PMCA is mainly enriched in plasma membrane fraction. Microsomal fraction contains small portion of PMCA as showed on fig 3.3 b, ii.

(a)

(i) Calreticulin


(ii) PMCA


**HM LM PM WL**

(b) (i) Calreticulin (ii) PMCA

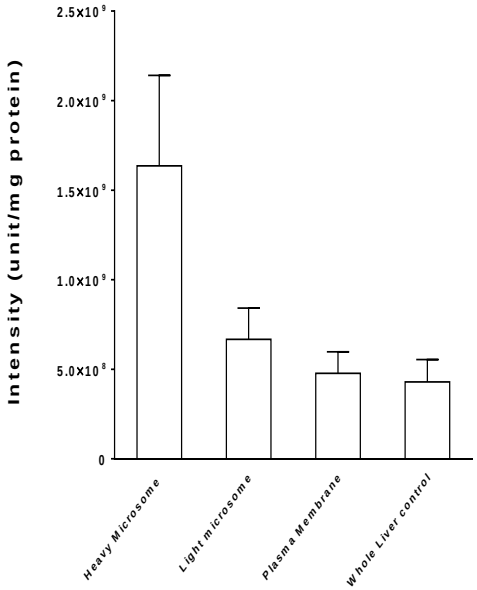


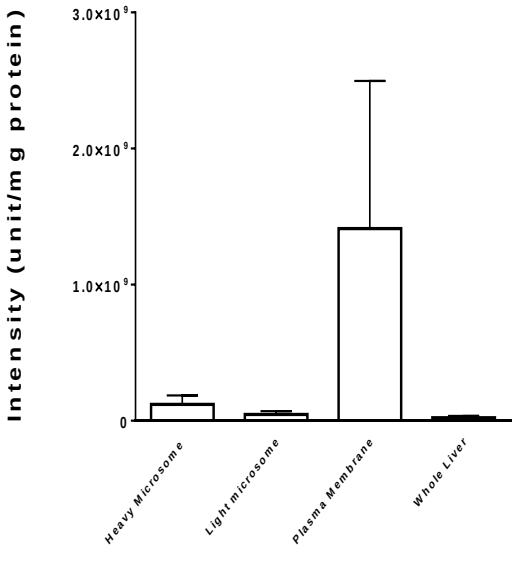

**Figure 3.3 Distribution of calreticulin (ER marker) and PMCA (PM marker) proteins in whole liver homogenate, microsomal fractions and plasma membrane fractions obtained from the microsomal and plasma membrane subcellular fractionation of rat liver.**

**(a)** Western blot of calreticulin (i) and PMCA (ii) on whole liver (WL), heavy microsome (HM), light microsome (LM) and plasma membrane (PM). The results shown are representative of those obtained from one out of five experiments which give similar results (N=5). **(b)** Quantitation of western blot of calreticulin (i) and PMCA (ii) on microsomal fractions and plasma membrane. The intensity was normalised by mg of protein loaded on the SDS-PAGE (unit/mg protein) and the data were expressed as mean± SEM.

### 3.2.1.4 Detection and quantification of bands intensity corresponding to calreticulin in western blot on mitochondrial and microsomal subcellular fractionation

From the previous section, the results showed that the recovery of calreticulin from microsomal and plasma membrane fraction is only 22.3%. It has about 77.7% of calreticulin was not detected by the western blot of calreticulin on microsomal and plasma membrane fractions. In order to determine the distribution of calreticulin in more detail, I performed other experiment using differential centrifugation on rat liver to collect more fractions including nuclear fraction, mitochondrial fraction, heavy microsome, light microsome and cytosolic fractions. Then the distribution of calreticulin on those subcellular fractions was detected by using western blot.

Figure 3.4a shows a representative western blot of calreticulin on mitochondrial and microsomal subcellular fractions including the nucleus, mitochondria and cytosol. The results show that bands were detected on nucleus, mitochondria, heavy microsome and light microsome. The cytosolic fraction has less portion of calreticulin in the fraction compared with other fractions.

Apart from measuring and quantifying the distribution of calreticulin on microsomal and plasma membrane fractions, the distribution of calreticulin on mitochondrial and microsomal fractions was also measured and quantified. Mitochondria, heavy microsome and light microsome are three subcellular fractions contained a higher portion of calreticulin. Heavy microsome has about 68% of total calreticulin. 30% and 15 % of calreticulin were found in mitochondria and light microsome, respectively (Table 3.2). Mitochondria has 1.3-fold of calreticulin more than light microsome.

(a)

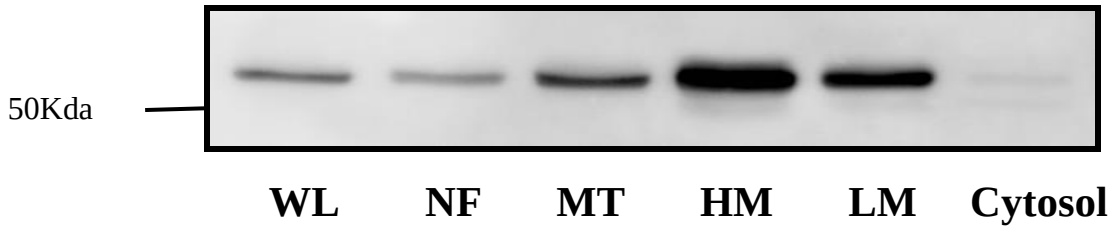
50Kda
WL
NF
MT
HM
LM
Cytosol

(b)

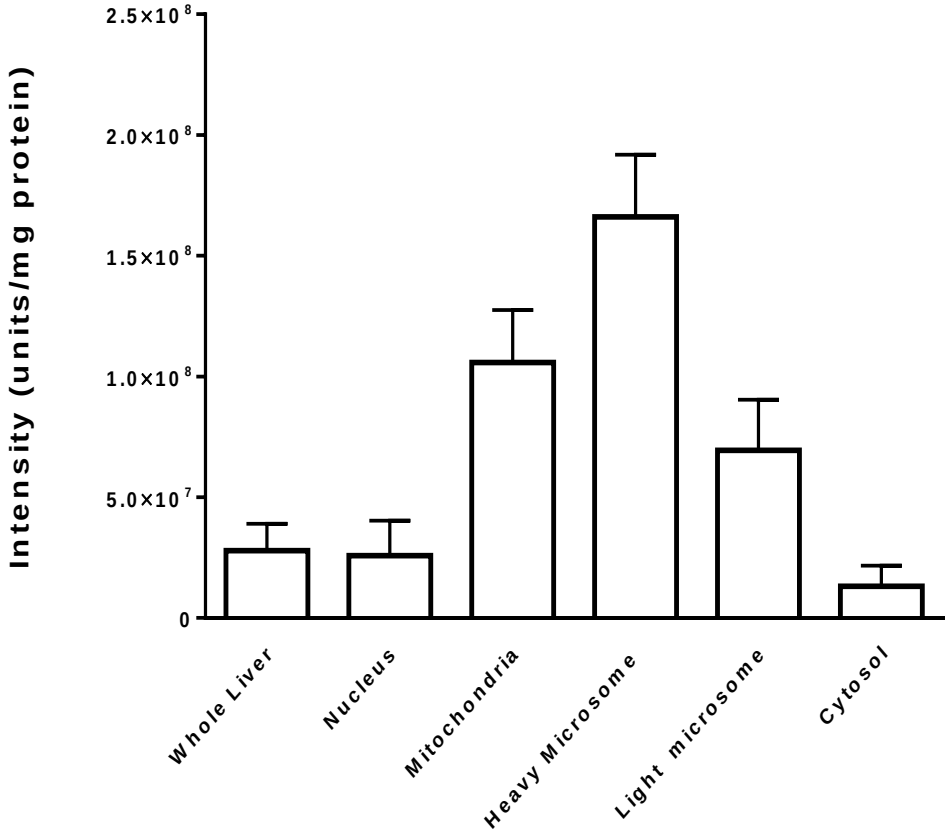
Intensity (units/mg protein)
2.5×10 8
2.0×10 8
1.5×10 8
1.0×10 8
5.0×10 7
0
Whole Liver
Nucleus
Mitochondria
Heavy Microsome
Light microsome
Cytosol

**Figure 3.4 Distribution and quantification of western blot of calreticulin on mitochondria and microsomal fractions from rat liver.**

**(a)** Western blot of calreticulin on whole liver (WL), nuclear fraction (NF), mitochondria (MT), heavy microsome (HM), light microsome (LM) and cytosol from control rat liver. The results shown are representative of those obtained from one out of six experiments which give similar results (N=6). **(b)** Quantitation of western blot of calreticulin on extending subcellular fractions. The intensity was normalised by mg of protein loaded on the SDS-PAGE (unit/mg protein) and the data were expressed as mean± SEM.

| Subcellular Fraction | Amount of Calreticulin (n=6) | | Amount of STIM1 (n=4) | | Amount of Orai1 (n=2) | | Total protein | |
|---|---|---|---|---|---|---|---|---|
| | Arbitrary Intensity per fraction | Fraction of Homogenate (%) | Arbitrary Intensity per fraction | Fraction of Homogenate (%) | Arbitrary Intensity per fraction | Fraction of Homogenate (%) | Arbitrary Intensity per fraction | Fraction of Homogenate (%) |
| Whole Liver Homogenates | $3.7x10^{11}$ $\pm1.3x10^{11}$ | 100 | 5.0 ±5.3 | 100 | $137x10^{10}$ $\pm84x10^{10}$ | 100 | 13213.7 ±1249.8 | 100 |
| Nucleus | $0.4x10^{11}$ $\pm0.07x10^{11}$ | 12 | -0.08 ±0.05 | -2 | $7x10^{10}$ $\pm6x10^{10}$ | 10 | 1898.8 ±114.8 | 15 |
| Mitochondria | $0.9x10^{11}$ $\pm0.09x10^{11}$ | 30 | -0. 2 ±0.2 | -4 | $0.7x10^{10}$ $\pm0.1x10^{10}$ | 3 | 755.2 ±59.8 | 6 |
| Heavy Microsome | $2.9x10^{11}$ $\pm1.7x10^{11}$ | 69 | 4.0 ±1.4 | 80 | $3.5x10^{10}$ $\pm0.3x10^{10}$ | 12 | 706.4 ±75.7 | 5 |
| Light Microsome | $0.9x10^{11}$ $\pm0.6x10^{11}$ | 15 | 1.7 ±1.4 | 34 | $2.9x10^{10}$ $\pm0.4x10^{10}$ | 5 | 376.0 ±32.2 | 3 |
| Cytosol | $1.0x10^{11}$ $\pm0.5\ x10^{11}$ | 21 | 1.0 ±0.5 | 20 | $48.0x10^{10}$ $\pm22.6\ x10^{10}$ | 32 | 5310.8 ±555.6 | 40 |
| Sum of the subcellular fraction % | | 147 | | 128 | | 62 | | 69 |

**Table 3.2 The Distribution of total protein, calreticulin, STIM1, Orai1 on mitochondrial and microsomal fractions.**

Subcellular fractions of whole liver, nucleus, mitochondria, heavy microsome, light microsome and cytosol obtained by differential centrifugation from untreated and phenylephrine-treated rat liver were subjected to western blot. The bands were detected by immunodetection and the intensity of the bands was measured on each subcellular fraction. The data were expressed as an arbitrary unit of intensity and % per fraction to whole liver homogenate. N is represented as the number of subcellular fractionation done.

### 3.2.2 Distribution and quantification of western blot of STIM1 and Orai1 in subcellular fractions from rat liver western blot

From the previous section, I have identified the heavy and light microsome are from ER, and plasma membrane fraction is enriched with the plasma membrane. Then, I used these subcellular fractions to study the distribution of STIM1 and Orai1

#### 3.2.2.1 Distribution of STIM1 in microsomal fraction and plasma membrane subcellular fractions determined by western blot from rat liver

Figure 3.5a was the results of STIM1 western blot on heavy microsome (i) and light microsome (ii) loading with different protein amount ranging from 10 µg of protein to 60 µg of protein. The results demonstrated that STIM1 antibody can detect the bands at about 77kDa which is the size of STIM1 proteins (Manji et al., 2000).

After obtaining the western blot of STIM1 from microsomal fractions, the correlation between the intensity of the bands from western blot of STIM1 on heavy and light microsome and protein amount was established. The intensity of bands from STIM1 antibody has a good linear relationship to the amount of protein ranging from 10 µg to 60 µg on heavy microsome and 20µg to 60 µg on light microsome. The bands intensity from STIM1 western blot in heavy and light microsome below the protein amounts of 10 µg for heavy microsome and 20µg for light microsome are not in a linear relationship.

The distribution of STIM1 was then detected and measured in order to identify the localisation of STIM1 on the subcellular fraction of heavy microsome, light microsome and plasma membrane. The western blot of STIM1 showed that STIM1 protein is

mainly presented at heavy microsome and light microsomes. No evident band was observed at plasma membrane fraction (figure 3.6a). Heavy microsome has a higher portion of STIM1 than in light microsome. Heavy microsome has 2.5-fold of STIM1 more than in light microsome (figure 3.6b). 85% of total STIM1 is found at heavy microsome and 15.2% of STIM1 is at light microsome (Table 3.3).

| Subcellular Fraction | STIM1 | | | | Orai1 | | | |
|---|---|---|---|---|---|---|---|---|
| | Untreated (n=6) | | Phenylepherine-treated (n=5) | | Untreated (n=4) | | Phenylepherine-treated (n=4) | |
| | Arbitrary Intensity per fraction | Fraction of Homogenate (%) | Arbitrary Intensity per fraction | Fraction of Homogenate (%) | Arbitrary Intensity per fraction | Fraction of Homogenate (%) | Arbitrary Intensity per fraction | Fraction of Homogenate (%) |
| Whole Liver Homogenates | -3.6 ±19 | 100 | 17 ±47 | 100 | 9.0 ±2.9 | 100 | 83 ±36 | 100 |
| Heavy Microsome | 39 ±17 | 85 | 50.1 ±29 | 76 | 3.9 ±0.8 | 44 | 39 ±0.8 | 45 |
| Light Microsome | 5.6 ±2.0 | 12.5 | 16.1 ±3.2 | 24 | 2.4 ±2.6 | 27 | 3.9 ±0.8 | 27 |
| Plasma membrane | 0.04 ±0.04 | 0.09 | 0.002 ±0.01 | 0.003 | 0.03 ±0.002 | 0.03 | 0.07 ±0.04 | 0.09 |
| Sum of the subcellular fraction % | | 101 | | 100 | | 71 | | 72 |

**Table 3.3 The Distribution of STIM1 and Orai1 in microsomal and plasma membrane fraction.**

Subcellular fractions of whole liver, heavy microsome, light microsome and plasma membrane obtained from differential centrifugation from control and phenylephrine-treated rat liver were subjected to western blot. The bands were detected by immunodetection and the intensity of the bands was measured on each subcellular fraction. The data expressed as an arbitrary unit of intensity of the band from western blot and % per fraction to whole liver homogenate. N is represented as the number of subcellular fractionation done.

(3.5a)

(i) Heavy microsome

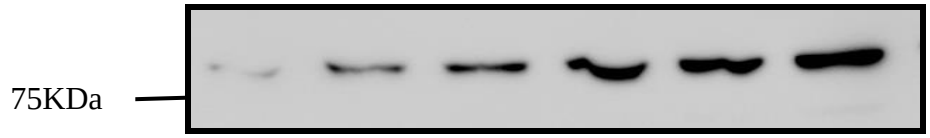


(ii) Light Microsome

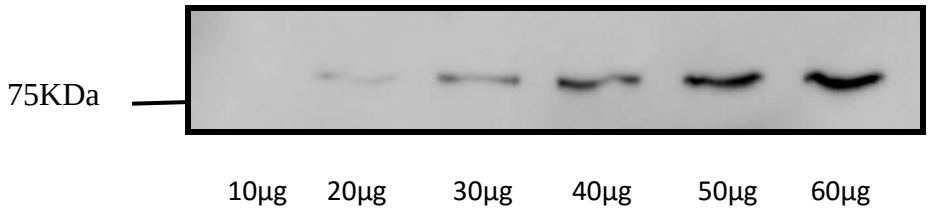


(3.5b)

(i) Heavy microsome

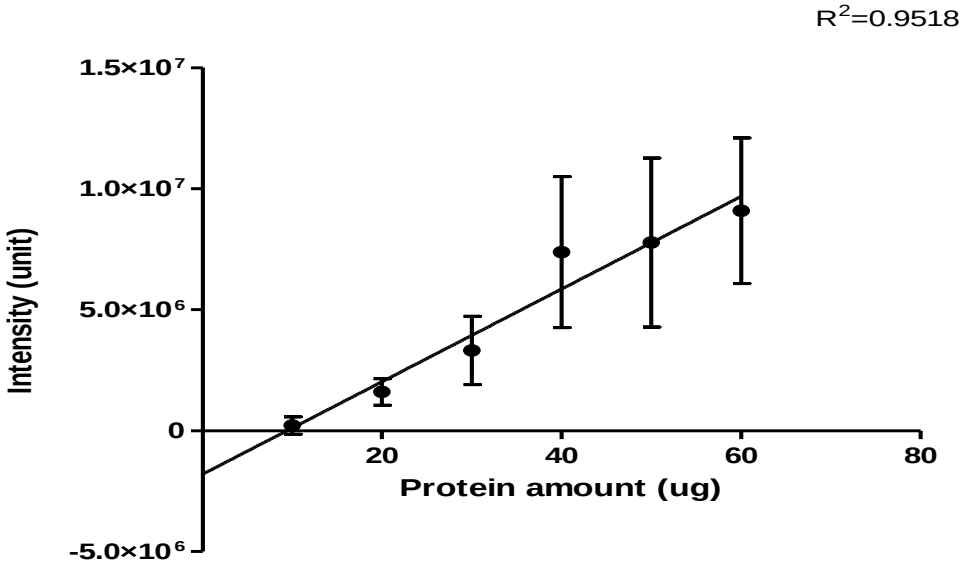

(ii) Light Microsome

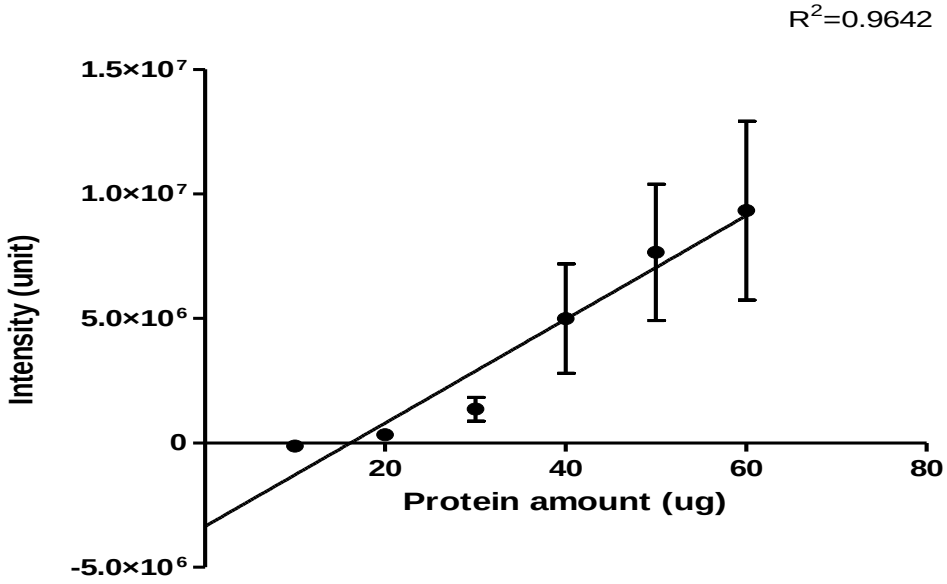


**Figure 3.5 Detection and quantification of band intensity on STIM1 in western blot in the heavy and light microsomal fractions obtained from the microsomal and plasma membrane subcellular fractionation.**

**(a)**Western blot of STIM1 on heavy microsome (i) and light microsome (ii) by loading with the protein amount ranging from 10 µg to 60 µg onto the SDS-PAGE. The results shown are representative of those obtained from one out of five experiments which give similar results (N=5). **(b)** Quantitation of the band intensity from western blot of STIM1 on heavy microsome (i) and light microsome (ii). The intensity of the band against the function of protein amount was plotted to show the correlation. The results were expressed as mean ± SEM.

(a)

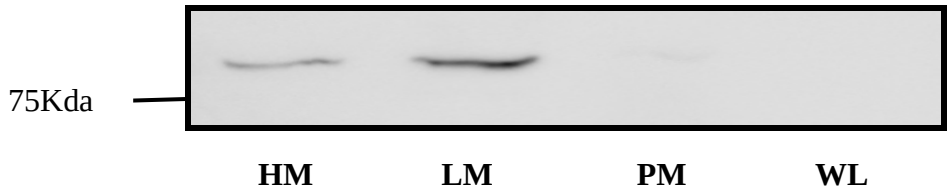


(b)

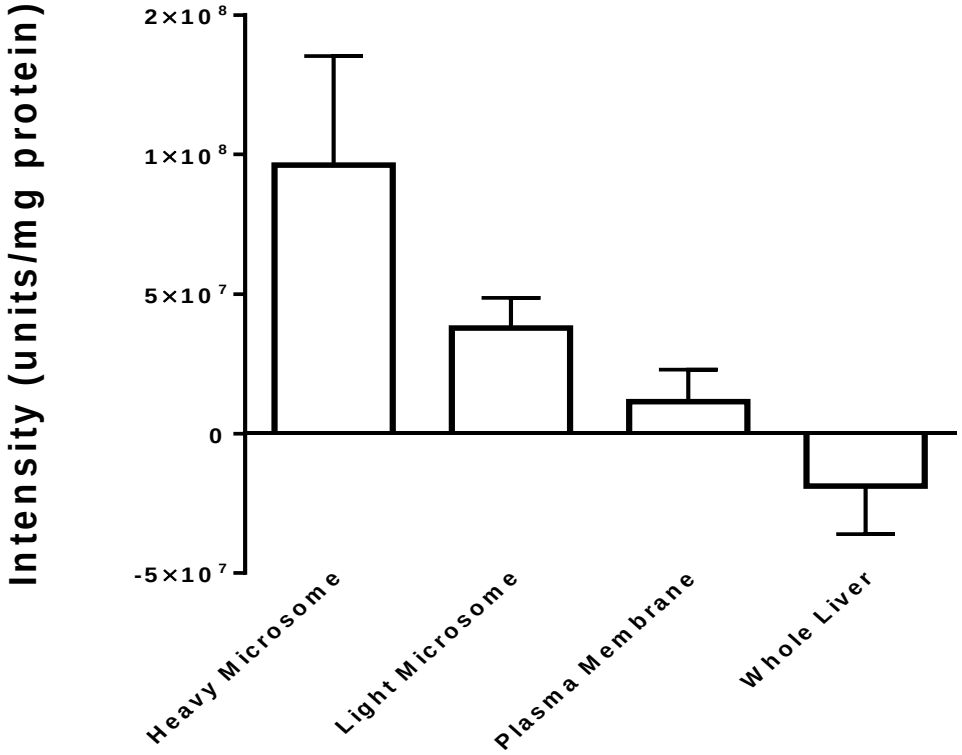


**Figure 3.6 Distribution and quantification of band intensity on STIM1 in western blot on microsomal fractions and plasma membrane fraction from rat liver.**

**(a)** Western blot of STIM1 on whole liver (WL), heavy microsome (HM), light microsome (LM) and plasma membrane (PM). The results shown are representative of those obtained from one out of six experiments which give similar results (N=6). **(b)** Quantitation of western blot of STIM1 on microsomal fractions and plasma membrane. The intensity was normalised by mg of protein loaded on the SDS-PAGE (unit/mg protein)and the data were expressed as mean± SEM.

### 3.2.2.2 Distribution of Orai1 on microsomal fraction and plasma membrane by western blot from untreated rat liver

The distribution of Orai1 was also tested on the microsomal and plasma membrane fraction. Similar to other antibodies, the linear correlation of bands intensity from western blot of Orai1 to protein amount was also established before testing the Orai1 distribution on subcellular fractions by western blot. In figure 3.7 a, the Orai1antibody was able to detect the Orai1 protein on plasma membrane fraction from 7.5µg to 25 µg of total protein. The immunosignal displayed a linear relationship from 7.5µg to 25 µg of total protein, but it obtained negative values below 7.5µg of total protein. The $R^2$ of the curve is 0.99.

The western blot of Orai1 on microsomal and plasma membrane fractions showed that bands at about 45kDa which is the size of glycosylated Orai1 (Guzman et al., 2014) were detected by Orai1 antibody. Orai1 is mainly detected at heavy and light microsome but not plasma membrane fraction (Figure 3.8 a). Light microsome has a higher portion of Orai1 than heavy microsome and plasma membrane. The enrichment of Orai1 in light microsome is 2.5-fold and 34-fold more than heavy microsome and plasma membrane (Figure 3.8b). 44% and 27% of total Orai1 are in heavy and light microsome from control rat liver, respectively (Table 3.3).

(a)

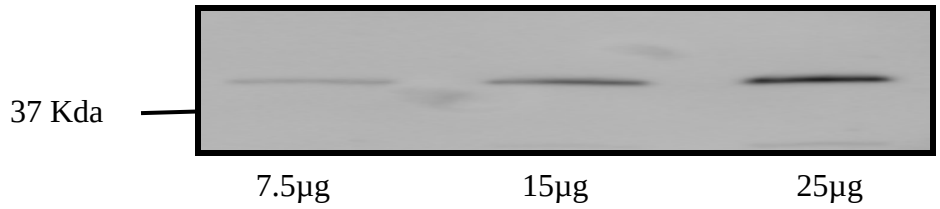


(b)

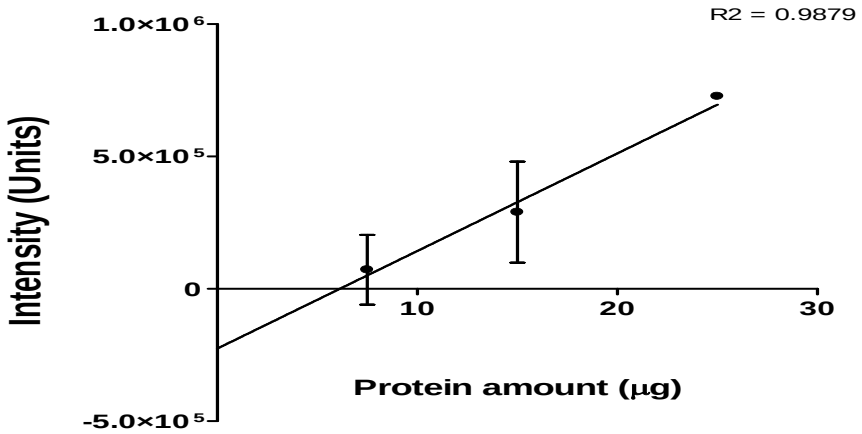


**Figure 3.7 Detection and quantification of Orai1 protein in western blot on plasma membrane fractions obtained from microsomal and plasma membrane subcellular fractionation from rat liver.**

**(a)**Western blot of Oai1 on plasma membrane by loading the protein amount ranging from 7.5 µg to 25 µg. The results shown are representative of those obtained from one out of two experiments which give similar results (N=2). **(b)** Quantitation of the intensity of the band from western blot of PMCA on the plasma membrane. The intensity of band against the function of protein amount was plotted to show the correlation. The results were expressed as mean ± SEM.

(a)

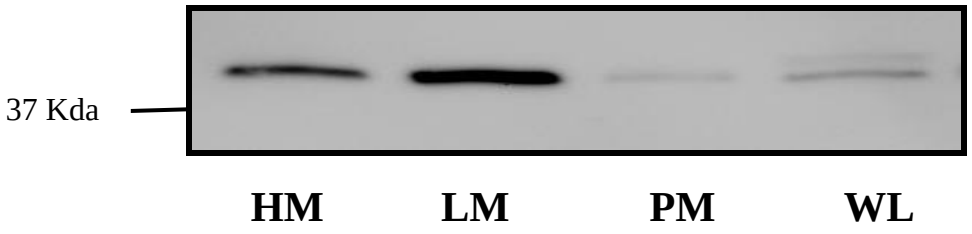


(b)

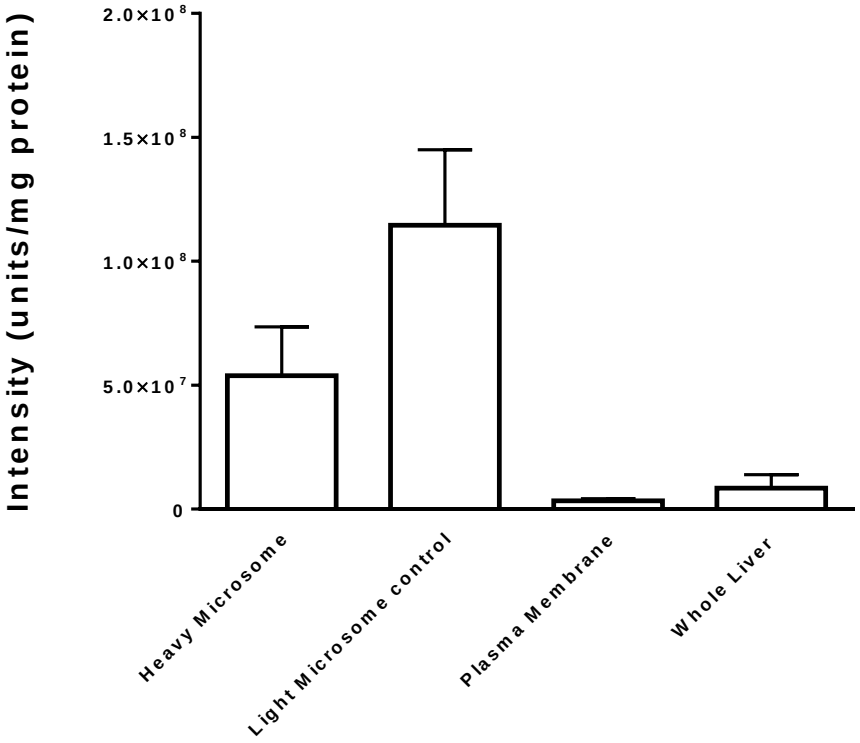


**Figure 3.8 Distribution and Quantitation of Orai1 in western blot on microsomal fractions and plasma membrane fraction from rat liver.**

**(a)** Western blot of Orai1 on whole liver (WL), heavy microsome (HM), light microsome (LM) and plasma membrane (PM). The results shown are representative of those obtained from one out of four experiments which give similar results (N=4). **(b)** Quantitation of western blot of Orai1 on microsomal fractions and plasma membrane. The intensity was normalised by mg of protein loaded on the SDS-PAGE (unit/mg protein) and the data were expressed as mean± SEM

3.2.2.3 Distribution and Quantification of Orai1 in mitochondrial and microsomal fractions from rat liver

As the unexpected results of Orai1 on microsomal and plasma membrane, thus, I tried to examine the distribution of Orai1 on subcellular fractions from untreated rat liver. The result showed that there are only two bands presented at all subcellular fractions from untreated rat liver except cytosol. These two bands are represented glycosylated Orail for 45kDa and unglycosylated Orai1 for 33kDa (Figure 3.10 a)(Gwack et al., 2007, Guzman et al., 2014). Cytosol had a higher amount of Orai1. It contains about 32% of Orai1. 12% and 4% of Orai1 was found at heavy microsome and light microsome, respectively (Table 3.2). Nuclear and mitochondrial fractions have less Orai1 protein. There are about 10% for nucleus and 3% for mitochondria (Table3.2)

(a)

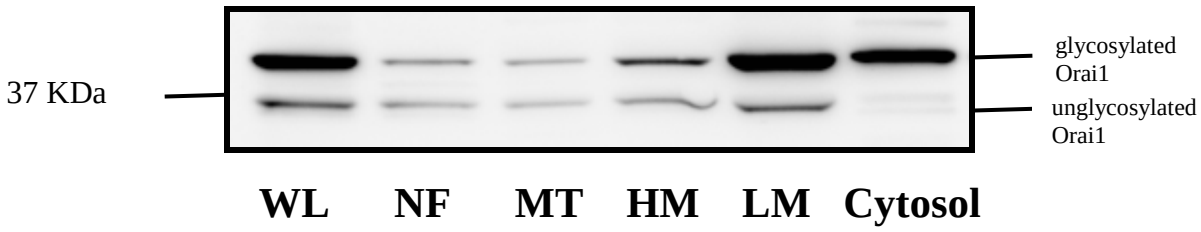


(b)

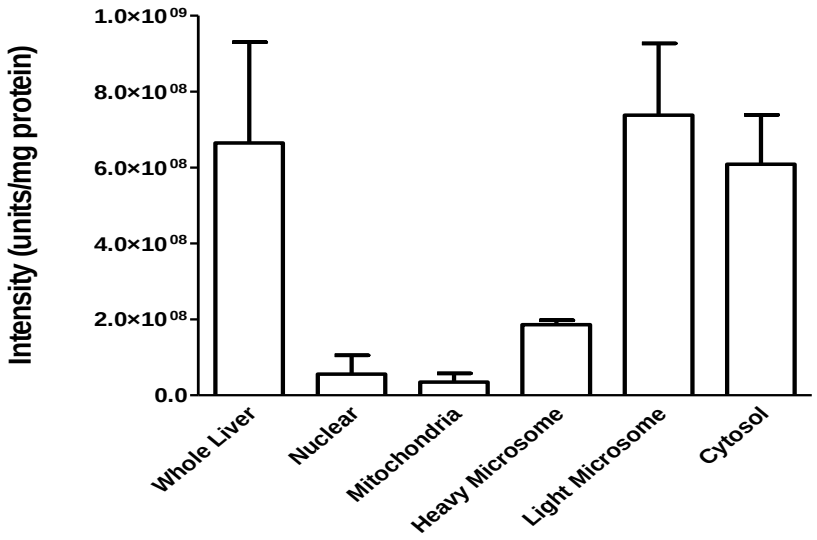


**Figure 3.10 Distribution of western blot of Orai1 on mitochondria and microsomal fractions from control rat liver.**

**(a)** Western blot of Orai1 on whole liver (WL), nuclear fraction (NF), mitochondria (MT), heavy microsome (HM), light microsome (LM) and cytosol from control rat liver. The results shown are representative of those obtained from one out of two experiments which give similar results (N=2). **(b)** Quantitation of western blot of Orai1 on extending subcellular fractions. The intensity was normalised by mg of protein loaded on the SDS-PAGE (unit/mg protein) and the data were expressed as mean± SEM.

### 3.2.3 The Distribution of TRPM2 on mitochondria and microsomal fractions from rat liver

Orai1 is pore-forming molecule of SOCs. It has been showed Orai1 is mainly found at plasma membrane. However, the results from this chapter indicated that Orai1 is mainly located at ER and less in plasma membrane. Therefore, in order to explore more about why most Orai1 located at ER, then we tested the subcellular distribution on another known plasma membrane protein to determine the trafficking system for plasma membrane protein is working properly. The evidence showed that TRPM2 channels are located on the plasma membrane (Mei et al., 2006, Zhang et al., 2006b). It has been showed that the present of nonselective cation current on hepatocytes is mediated TRPM2 channels (Kheradpezhouh et al., 2014). Thus, I decided to identify the subcellular distribution of TRPM2 to test the plasma membrane protein is expressed properly in hepatocytes.

The result of TRPM2 western blot on mitochondria and microsome fractions showed that there is a band at 140kDa which is the size of TRPM2 (Kheradpezhouh et al., 2014) found mainly at mitochondrial and nuclear fraction. No TRPM2 protein is detected at heavy microsome, light microsome and cytosol (Figure 3.11). As it has been showed that TRPM2 produced its function on the plasma membrane in hepatocytes (Kheradpezhouh et al., 2014). Then, it can conclude that the TRPM2 protein transport to plasma membrane after protein synthesis, so the transport system for plasma membrane is working properly in liver cells from our experiment

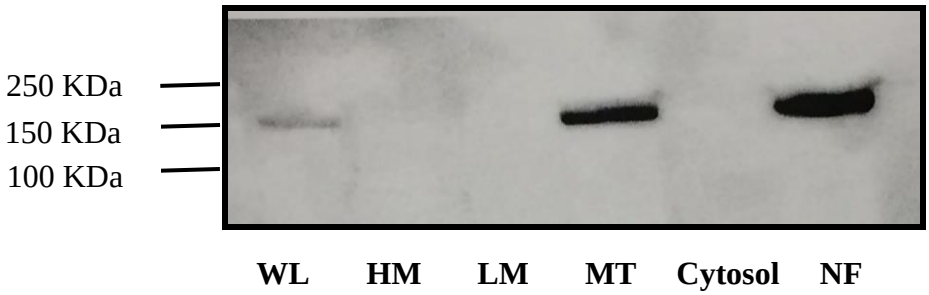
250 KDa
150 KDa
100 KDa
WL
HM
LM
MT
Cytosol
NF

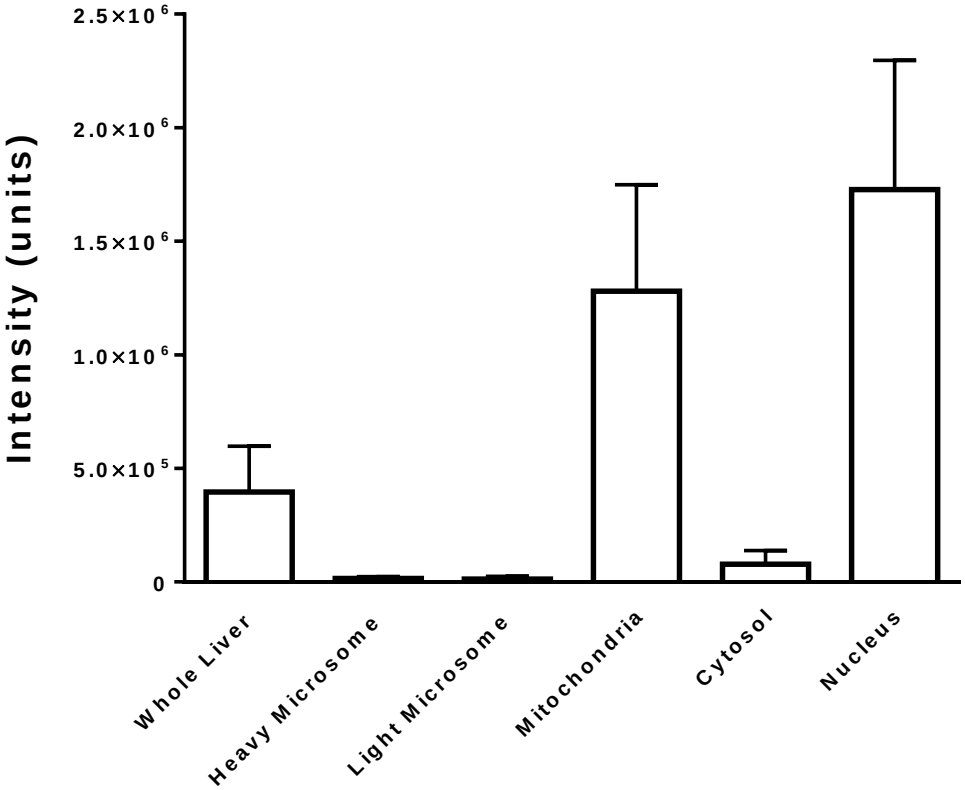
Intensity (units)
2.5×10⁶
2.0×10⁶
1.5×10⁶
1.0×10⁶
5.0×10⁵
0
Whole Liver
Heavy Microsome
Light Microsome
Mitochondria
Cytosol
Nucleus

**Figure 3.11 Distribution and quantification of TRPM2 in western blot on mitochondria and microsomal fractions from rat liver.**

**(a)** Western blot of Orai1 on whole liver (WL), nuclear fraction (NF), mitochondria (Mit), heavy microsome (HM), light microsome (LM) and cytosol (cyto) from rat liver. The results shown are representative of those obtained from one out of three experiments which give similar results (N=3). **(b)** Quantitation of western blot of TRPM2 on extending subcellular fractions. The intensity was normalised by a total protein on PVDF membrane and the data were expressed as mean± SEM.

### 3.2.4 The effect phenylephrine on the distribution of STIM1 and Orai1 in liver subcellular fractions

It has been showed that hormone like vasopressin or epinephrine could induce the release of $Ca^{2+}$ from ER and activate SOCs in liver cells (Gregory and Barritt, 2003). In other evidence, it indicated that during the activation of SOCs STIM1 form puncta and move the region of ER closed to the plasma membrane. Therefore, it might suggest that specific subregion should present on ER for STIM1 to form puncta and induce the activation of SOCs. Thus, in order to investigate and understand more about the redistribution of STIM1 and Orai1 on the subcellular level when SOCs are activated. The subcellular fractions of heavy microsome, light microsome and plasma membrane were collected after the administration of phenylephrine.

#### 3.2.4.1 Effect of phenylephrine administration on blood glucose

To achieve the goal of $Ca^{2+}$ depletion, phenylephrine was injected into the rat to activate $\alpha_1$-adrenorecptor and deplete the $Ca^{2+}$ from ER in the liver. One of the effect of phenylephrine on the liver can activate the process of glycogenolysis and increase the blood glucose level. Thus, the glucose level in the blood was used to determine the effect of the phenylephrine after the injection. The basal blood glucose level from the rats was 19 mol/L and rose up to 29 mol/L after the injection of phenylephrine (Figure 3.12). The basal blood glucose level in our experiment is higher than normal level (6 mmol/L) as isoflurane, ketamine and

xylazine used in anesthesia can also increase the glucose level (Saha et al., 2005). There is no statistical difference in blood glucose between 0 min and 20 min.

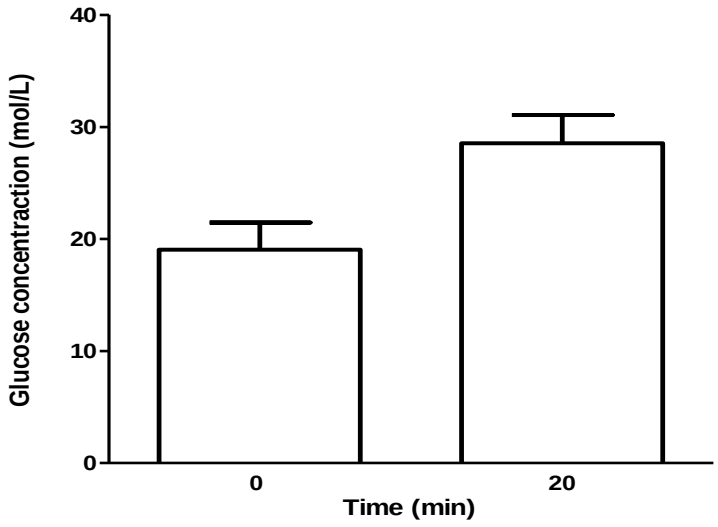


**Figure 3.12 The rat blood glucose assay.**
Blood collected at 0 min and 20 min after the injection of phenylephrine. Serum was isolated from a whole blood sample and used for measured the glucose level. N=3**,** no of the rat was taken blood for assay the blood glucose.

3.2.4.2 Effect of phenylephrine administration on the distribution of STIM1 and Orai1 in microsomal and plasma membrane fractions

In Figure 3.13a, this was the western blot of STIM1 and Orai1 in microsomal and plasma membrane fractions collected after the administration of phenylephrine. The results of western blot of STIM1 and Orai1 on phenylephrine-treated group showed the same results as subcellular fraction samples from the untreated group (Figure 6 and 8). It is no significant change of the distribution of STIM1 and Orai1 on microsomal and plasma membrane fractions on the untreated and phenylephrine-treated group (Figure 3.13b).

(a)

(i) STIM1


(ii) Orai1


**HM LM PM WL**

(b)

(i) STIM1

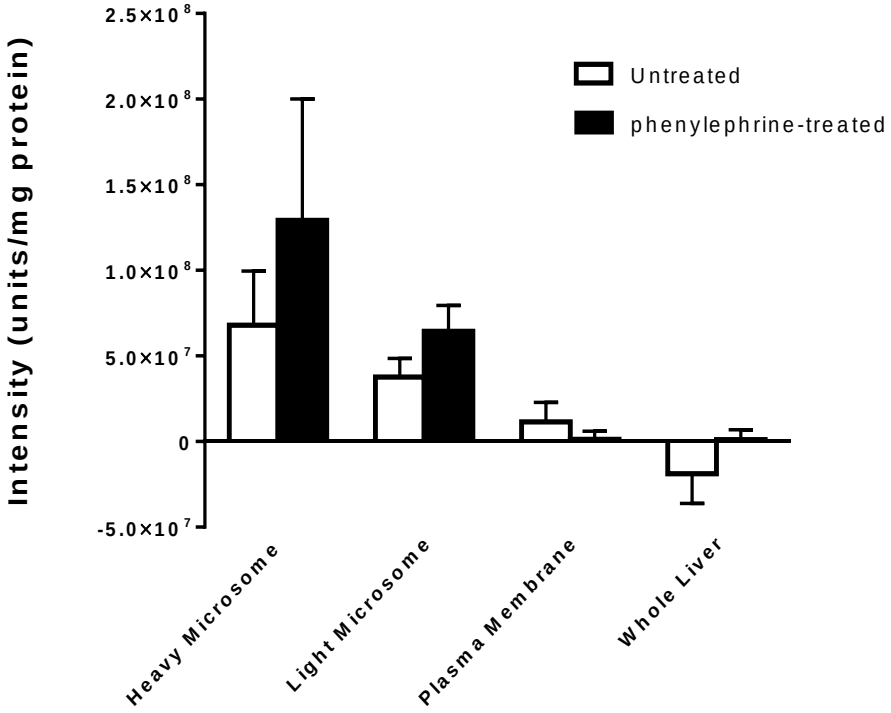

(ii) Orai1

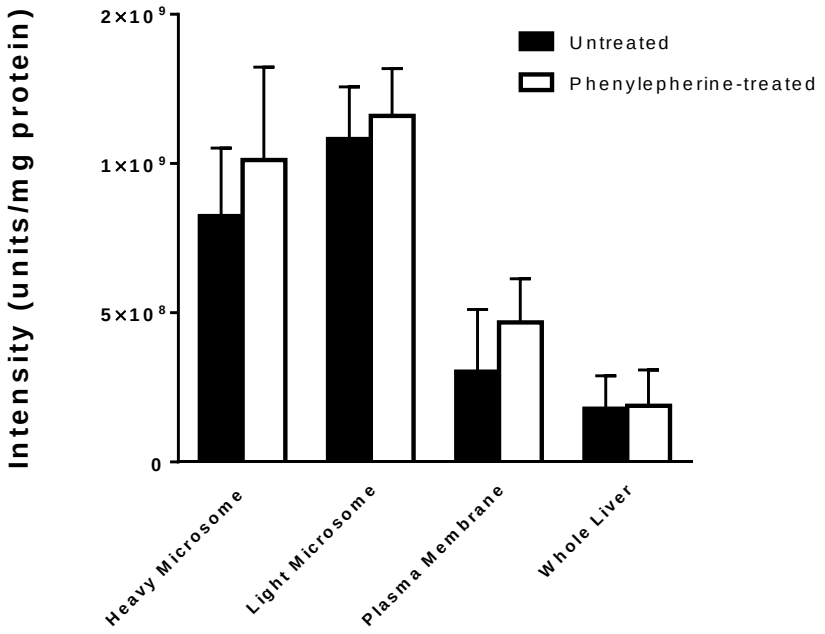


**Figure 3.13 Distribution and Quantification of STIM1 and Orai1 in western blot on microsomal fractions and plasma membrane fraction from untreated and phenylephrine-treated rat liver.**

**(a)** Western blot of STIM1 and Orai1 on whole liver (WL), heavy microsome (HM), light microsome (LM) and plasma membrane (PM) from phenylephrine-treated rat liver. After the injection of phenylephrine and circulated for 20 min, the liver was removed. The results shown are representative of those obtained from one out of five-four experiments which give similar results. **(b)** Quantitation of western blot of STIM1 and Orai1 on microsomal fractions and plasma membrane. The intensity was normalised by mg of protein loaded on the SDS-PAGE (unit/mg protein) and the data were expressed as mean± SEM. (N=4)

### 3.2.4.3 The distribution of STIM1 on mitochondria and microsomal fractions from untreated liver and phenylephrine-treated liver

In order to understand more about the distribution of STIM1, the other subcellular fractionation was performed to collect more subcellular fractions including the nucleus, mitochondria and cytosol. Then those subcellular fractions also used to investigate the distribution of STIM1 and Orai1 in mitochondrial and microsomal subcellular fractions.

STIM1 antibody could not detect significant bands at the size of 77 kDa on the subcellular fractions of the nucleus, mitochondria and cytosol. STIM1 was mainly found at heavy and light microsomes (figure 3.14). There was no change of the STIM1 found on the western blot from the phenylephrine-treated subcellular fractions. STIM1 was still located at heavy and light microsomes from phenylephrine-treated subcellular fractions (figure 3.13). Heavy and light microsomes had a higher portion of STIM1 to other fractions and there was no significant difference of STIM1 expression on control and phenylephrine-treated subcellular fractions.

(a)

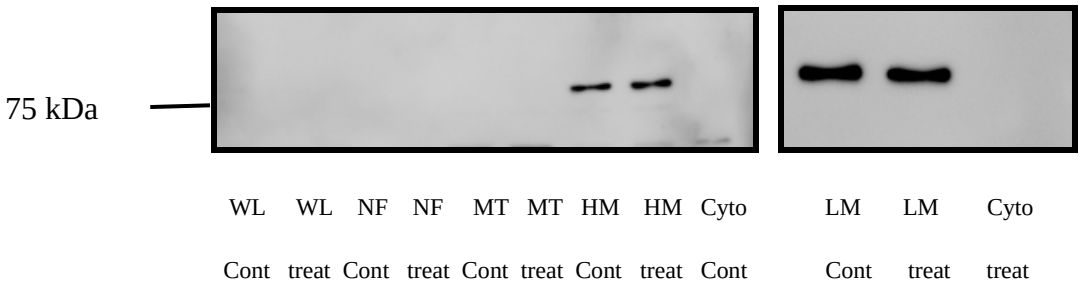
75 kDa
WL Cont
WL treat
NF Cont
NF treat
MT Cont
MT treat
HM Cont
HM treat
Cyto Cont
LM Cont
LM treat
Cyto treat

(b)

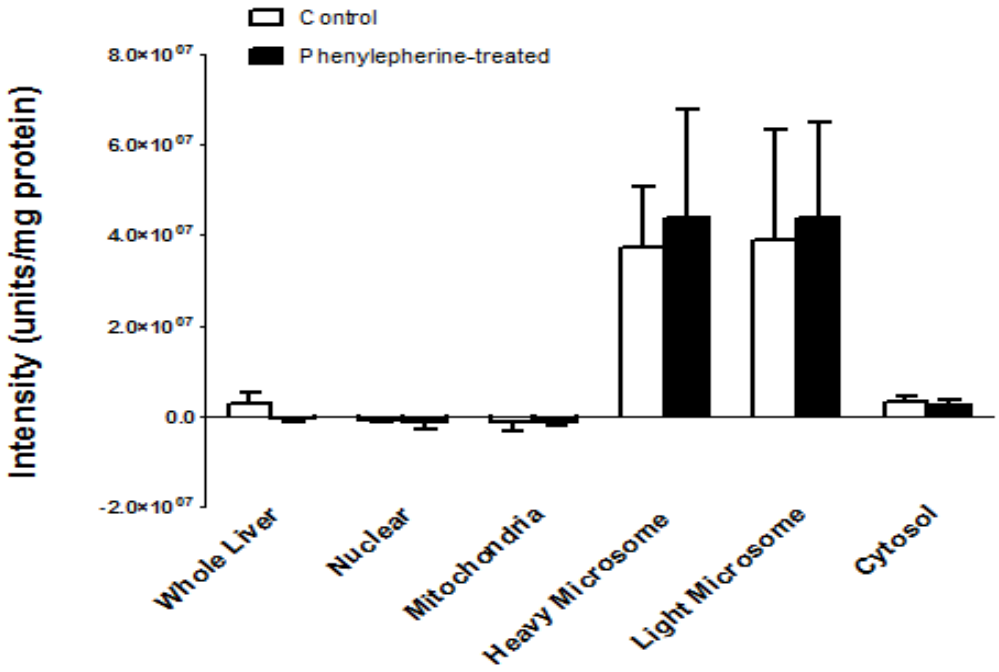
Control
Phenylepherine-treated
Intensity (units/mg protein)
8.0×10^07
6.0×10^07
4.0×10^07
2.0×10^07
0.0
-2.0×10^07
Whole Liver
Nuclear
Mitochondria
Heavy Microsome
Light Microsome
Cytosol

**Figure 3.14 Distribution and Quantitation of STIM1 in western blot on mitochondria and microsomal fractions from untreated and phenylephrine-treated rat liver.**

**(a)** Western blot of calreticulin on whole liver (WL), nuclear fraction (NF), mitochondria (MT), heavy microsome (HM), light microsome (LM) and cytosol (cyto) from control (cont) and phenylephrine-treated(treat) rat liver. After the injection of phenylephrine and circulated for 20 min, the liver was removed. The results shown are representative of those obtained from one out of four experiments which give similar results (N=4). **(b)** Quantitation of western blot of calreticulin on extending subcellular fractions. The intensity was normalised by mg of protein loaded on the SDS-PAGE (unit/mg protein) and the data were expressed as mean± SEM.

## 3.3 Discussion

STIM1 and Orai1 are the two important molecules for SOCs function. It has been proposed that small region of ER is important for controlling the $Ca^{2+}$ entry mediated SOCs in liver cells (Gregory et al., 1999, Castro et al., 2009). The evidence demonstrated that the depletion of $Ca^{2+}$ store induces the aggregation of STIM1 to form puncta on the ER. The aggregate then translocates to the subcompartment of ER near plasma membrane (Xu et al., 2006, Baba et al., 2006). Thus, the hypothesis is that the vital region of ER for the SOCs function should be located on the ER underneath plasma membrane. As for this reason, the subcellular fractions from ER and plasma membrane are the two main organelles used in the experiments to explore the distribution of STIM1 and Orai1.

### 3.3.1 Characterisation of Subcellular fractions from rat liver cells

The subcellular fractions collected from differential and gradient centrifugation were needed to be confirmed its identity by using specific organelle marker proteins.

In the experiments, two marker proteins were selected to determine the subcellular fraction identity that we collected from correct fractions. Calreticulin was chosen as ER marker to identify the microsomal fractions derived from ER and $Mg^{2+}$-$Ca^{2+}$ -plasma membrane $Ca^{2+}$ ATPase (PMCA) was selected as plasma membrane marker protein.

The methods of the subcellular fractionation were employed in this chapter. The first series of subcellular fractionation called microsomal and plasma membrane fractions were to collect heavy microsome, light microsome and plasma membrane fraction. The second series of subcellular fractionation called mitochondrial and microsomal fractions was to collect the subcellular fractions including nucleus, mitochondria, heavy microsome, light microsome and cytosol fractions. The fraction collected from Percoll gradient centrifugation on nuclear fraction was enriched with PMCA and not observed at microsomal fractions so that the fraction collected from percoll gradient centrifugation is plasma membrane fraction. Mitochondria, heavy microsome and light microsome are the three main subcellular fractions enriched with ER marker, calreticulin. Therefore, heavy microsome and light microsome should be the fractions derived from endoplasmic reticulum. As the density of rough ER is heavier than smooth ER, so heavy microsome pelleted at 35,000g RCF (the relative centrifugal force that is the ratio of centrifugal force to gravity) is derived from rough ER and light microsome collected after 100,000g RCF is derived from smooth ER. Although, a certain amount of calreticulin was detected at mitochondria, it may be the contamination of ER because mitochondria have a very close contact with ER especially at the region of smooth ER so it is possible that mitochondria co-sedimented with ER during subcellular fractionation (Wang et al., 2000). The contamination of mitochondria on microsomal fraction during the subcellular fractionation can be solved by using mitochondria marker to determine the purity of the subcellular fractions.

In addition, Sarco/endoplasmic reticulum $Ca^{2+}$ ATPase (SERCA) is another commonly used ER marker in subcellular fractionation (Nagata et al., 2007). Thus, SERCA was also tried to use as ER marker in the subcellular fractionation experiments. However, the results of western blot of SERCA on microsomal fractions and plasma membrane fraction showed the bands on 75kDa which is not the expected size of SERCA at about 110kDa. Therefore, we cannot determine the bands detected is SERCA (data not shown). Each subcellular fraction contains different amount of total proteins. ER contains about 9% of total protein and plasma membrane has about 0.02% of total protein.

### 3.3.2 The Distribution of STIM1 on subcellular fraction from rat liver cells

The function of STIM1 is to sense the change of $[Ca^{2+}]$ in ER and transmit the signal to Orai1 to induce the $Ca^{2+}$ influx. In liver cells, the $Ca^{2+}$ released only need a small region on the ER and the activation of SOCs induce the redistribution of STIM1 to form a puncta (Castro et al., 2009). As ER can be divided into rough ER and smooth ER based on its morphology. Then we thought that smooth ER would contain more STIM1 than rough ER as smooth ER. The technique of subcellular fractionation was used to collect rough ER, smooth ER and plasma membrane fraction in order to study the specific sub-region of ER that is important for SOCs function.

In the results, heavy microsome (derived from rough ER) and light microsome (derived from smooth ER) are two main subcellular fractions detected with

significant amount of STIM1 by western blot. It is not same as the assumption that STIM1 should mainly locate at smooth ER. In mitochondrial and microsomal subcellular fractions, STIM1 cannot be detected on nucleus, mitochondria and cytosol so the movement of STIM1 is only confined on ER and STIM1 do not move across to different organelles to get closer to plasma membrane in order to activate Orai1.

### 3.3.3 The Distribution of Orai1 on subcellular fraction from rat liver cells

After we identified the distribution of STIM1 in subcellular level, I then tried to identify the distribution of Orai1 using the same method detecting the distribution of STIM1. The results in this chapter showed that Orai1 was enriched at heavy microsome and light microsome. Less amount of Orai1 was presented at the plasma membrane. Some evidence used HEK 293 transfected with Orai1 to detect the location of Orai1, showing that Orai1 is expressed on the cell surface (Prakriya et al., 2006). When the expression of Orai1 on the cell membrane reduced, the $I_{CRAC}$ current was dropped on the transfected cells (Soboloff et al., 2006, Vig et al., 2006b). Those results provide evidence that Orai1 is located on plasma membrane to produce its function. In liver cells, the result from patch clamp experiment showed that the liver cells present enough SOCs on plasma membrane to produce the current induced by $Ca^{2+}$ influx (Rychkov et al., 2001). Those results suggested that the plasma membrane of liver cells should express enough Orai1 to form SOCs to maintain its normal function. Thus, it is an

interesting evidence that why a large amount of Orai1 on ER rather than plasma membrane from our results.

Then I also identified the distribution of Orai1 on mitochondrial and microsomal fractions including nucleus, mitochondria and cytosol to determine the distribution of Orai1 on other organelles. Interestingly, cytosol contains over 30% of total Orai1 and microsomal fractions had 17% of total Orai1. Thus, these results showed that Orai1 is not only located at ER but also transport to another region of the cells. It should contain some other signal pathways to control the transportation of Orai1.

The result of the distribution of TRPM2, the known plasma membrane protein, on mitochondria and microsomal fractions showed that no TRPM2 protein was detected at heavy and light microsome. The western blot of PMCA only showed that PMCA is enriched at plasma membrane fraction, not at heavy and light microsome. Thus, those results suggested that TRPM2 and PMCA, both are plasma membrane protein, do not retain at ER and are trafficked to plasma membrane after synthesis. As the pattern of Orai1 western blot is different from TRPM2 or PMCA western blot, it could suggest that some other mechanisms are involved in regulating the transport of Orai1 to the plasma membrane and the retention of Orai1 in ER. Evidence showed that Orai1 is presented at secretory granules (Dickson et al., 2012) so it implicated that Orai1 may mediate the secretory pathway to transport to other regions of the cells

### 3.3.4 Effect of phenylephrine on subcellular distribution of STIM1 and Orai1from Rat liver Cells

The results of STIM1 distribution from treated and untreated- rat liver subcellular fractions showed that there was no different on the distribution STIM1 in the microsomal fraction and plasma membrane fraction between these two groups. Moreover, it is also no significant change on the distribution of STIM1 on the nucleus, mitochondria and cytosol after the injection of phenylephrine. It is also no difference observed on the distribution of Orai1in the microsomal fractions and plasma membrane fraction from treated and untreated rat liver.

Although there are not difference observed between the phenylephrine-treated and untreated group, it is still possible that the distribution of STIM1 and Orai1 is different between treated and untreated subcellular fractions. Firstly, the method of subcellular fractionation cannot obtain a high purity of subcellular fractions; it is easy to get contamination from other fractions during centrifugation, so the results could be influenced by the present of other subcellular fractions. Secondly, it may be the movement of STIM1 or Orai1 is only in a small region that is not easily to be isolated and detected.

In summary, STIM1 is mainly located at rough ER and smooth ER but rough ER contains most of the STIM1 than smooth ER. The larger amount of STIM1 in heavy microsome than in light microsome suggested that STIM1 may have another non-store-operated $Ca^{2+}$ entry (SOCE) function. Orai1, the pore-forming molecule of SOCs, which is thought to be located on plasma membrane protein was mainly found at microsomal fractions and cytosol not plasma membrane from our experiments. The possible explanation of why a large amount of Orai1 at

microsomal fraction may need to be trafficking to the right position or reshape of the ER to redistribute Orai1 so it needs more evidence to confirm the Orai1 trafficking in the liver cells.

# Chapter IV

# Investigation of STIM1 binding partners in the heavy microsome fraction

# Chapter IV Investigation of STIM1 binding partner in the heavy microsome fraction

## 4.1 Introduction

In chapter 3, I have demonstrated that in liver subcellular fractions STIM1 and Orai1 proteins are mainly located at heavy and light microsome which are derived from the rough ER and the smooth ER, respectively. STIM1 and Orai1 in the heavy microsome were found to be greater than in light microsome. Substantially lower levels of STIM1 and Orai1 were found in plasma membrane fraction. These observations raise the question of why there are so much STIM and Orai1 in the ER, whether the proteins have a function in the ER, and what these functions might be. A number of possibilities were discussed in the Discussion of the previous chapter.

It has been shown by the result of immunoprecipitation that the activation of SOCs requires direct coupling of STIM1 and Orai1 to induce the $Ca^{2+}$ influx (Navarro-Borelly et al., 2008). However, Varnai et al indicated that the distance between STIM1 and Orai1`is too long to produce the direct contact and require additional proteins to form a large complex at ER-PM junction to activate the $Ca^{2+}$entry (Várnai et al., 2007). Thus, additional binding protein should be involved in the function of STIM1 and Orai1.

Numerous proteins have been identified as STIM1 binding partners from different studies. Calmodulin and CRACR2A, the $Ca^{2+}$ binding protein, are showed to be an STIM1 binding proteins which can inhibit the activity or influence the stability of the protein complex (Mullins et al., 2009, Srikanth et al., 2010a). The

cytoskeleton proteins such as EB 1 associate with STIM1 to form the ER-PM junction and the microtubules protrusions but those functions are not related to the regulation of the $Ca^{2+}$ entry (Grigoriev et al., 2008, Hajkova et al., 2011). STIM1 binds to TRPC channels and L-types voltage-gated $Ca^{2+}$ channel and regulate those channels function (Lee et al., 2010, Park et al., 2010).

SERCA is $Ca^{2+}$ pump located on ER to regulate the $Ca^{2+}$ concentration in cytosol by reuptake the $Ca^{2+}$ from cytosol back to ER (MacLennan et al., 1997, Burk et al., 1989). It has been showed that STIM1 proteins associate with SERCA to regulate the refilling process on $Ca^{2+}$ store (Jousset et al., 2007) . Other evidence showed that the isoform of SERCA2a is one of the membranes to form the protein complex with STIM1 and Orai1 (Sampieri et al., 2009b). Those evidence suggested that SERCA is STIM1 binding protein and located on ER to produce its function.

Taken together, the results of Chapter 3 and literatures summarised above suggest that additional proteins in the ER may interact with STIM1 and/or Orai1 to activate or regulate SOCE, or to serve other intracellular functions, which are not related to SOCE. Thus, the overall aim in this Chapter was to identify proteins in the heavy microsomal fraction (rough ER) which bind to STIM1. This has been done by using immunoprecipitation, LC/MS, and western blot. As mentioned before, SERCA is showed to be one of the known STIM1 binding proteins located on ER, so I firstly tested the interaction of STIM1 and SERCA on both heavy and light microsomes using immunoprecipitation and western blotting to identify is there any difference of known STIM1 binding protein on ER between HM and LM. The specific aims were to (1) determine the conditions which could

successfully immunoprecipitate STIM1 from microsomal fractions. (2) test whether STIM interacts with SERCA using immunoprecipitation and western blot on microsomal fractions, (3) detect other new STIM1 binding proteins using immunoprecipitation and LC/MS on microsomal fractions (4) confirm the interaction between STIM1 and the new STIM1 binding proteins using immunoprecipitation and western blotting.

The use of heavy microsome as a starting material for searching STIM1 binding proteins because heavy microsomal fraction contains large amount of STIM1,so it could have higher opportunity to get the success of the immunoprecipitation of STIM1. As far we know, whole cells protein extract from the over-expressed transfected cells were commonly used materials to search the new STIM1 binding proteins. Those results only can provide the information about the protein profiling of STIM1 binding protein from whole cell lysis but not on specific region of ER. Moreover, it is still no clear and detail information on the protein profiling at specific region of ER because most of the information was obtained from over-expressed cell line experiments.

Immunoprecipitation (IP) is a commonly use technique to study the protein-protein interaction. The method of IP is to use specific antibody to pull down the target protein-protein complex by forming an immune complex and then analysing the immunoprecipitate by western blot or mass spectrometry to identify the binding protein (Kaboord and Perr, 2008).

However, the common problems of IP are to obtain a suitable condition which have good solubilisation of protein, preserve the intact protein-protein interaction

and reduce the unspecific protein bound to the protein A/G agarose. In order to get the best results, optimization of the stringency of lysis buffer is critical for IP (Yang et al., 2009). The stringency of lysis buffer is dependent on the use of detergents and salt concentration (Conlon et al., 2012). Strong and weak lysis buffer were used to test the immunoprecipitation of STIM1 in these two lysis buffers, and then used either lysis buffer to search for the potential STIM1 binding proteins from the heavy or light microsome. In immunoprecipitation experiment, choosing proper control in the experiment is critical to determine the unspecific binding of the undesired proteins. When setting up the immunoprecipitation experiment for my studied, the method from Litjens et al was chosen and used because they studied STIM1 interaction with PLC-γ using immunoprecipitation. In the method, PBS was used as negative control to determine the unspecific binding. (Litjens et al., 2007). This method is easy and quick for me to set up the experiments. However, the nonspecific binding of non-immunised IgG from the same species of animal is still needed to be considered and more suitable being as negative control (Bonifacino et al., 2001). Thus, I also used non-immunised normal IgG from the same species animal as negative control to determine the influence of the non-immunised IgG. The results showed no significant different between PBS and normal IgG control.

## 4.2 Results

### 4.2.1 Immunoprecipitation of STIM1 from Heavy microsome (HM) and Light microsome (LM) under strong dissociation condition

The STIM1 antibody used in this chapter for conducting immunoprecipitation is the same STIM1 antibody used in western blot experiment for quantification of STIM1 in subcellular fractions. In order to confirm the ability of the STIM1 antibody used in our experiment can pull down STIM1 protein from microsomal fractions, the antibody was firstly validated by STIM1 western blot on eluted protein from the immunoprecipitate after the immunoprecipitation of STIM1. Radioimmunoprecipitation assay buffer (RIPA), a harsher denaturing lysis buffer containing sodium dodecyl sulphate, sodium deoxycholate and nonidet P-40, is commonly used buffer in extracting protein and performing immunoprecipitation experiment as it has lower background noise (Johansen and Svensson, 1998, Yang et al., 2009, Kan et al., 2013). Then I firstly tried to use RIPA in our immunoprecipitation experiment. PBS was used as negative control in the immunoprecipitation.

In figure 4.1a and b, it was the result of western blot of STIM1 on heavy and light microsomes after immunoprecipitation of STIM1 in using RIPA buffer to solubilise the proteins. From the result, the input lysate from both heavy and light microsomal fractions displayed the bands at about 77 kDa that is the size of STIM1. In STIM1 immunoprecipitation group of heavy and light microsomes, the results indicated that the STIM1 antibody can detect the bands on the immunoprecipitate from heavy and light microsomes at the size of 77 KDa which

is the same size as the group of input lysate of heavy and light microsomes. In PBS negative control groups, no bands were detected on from heavy and light microsomes when the protein extract incubated with PBS instead of STIM1 antibody.

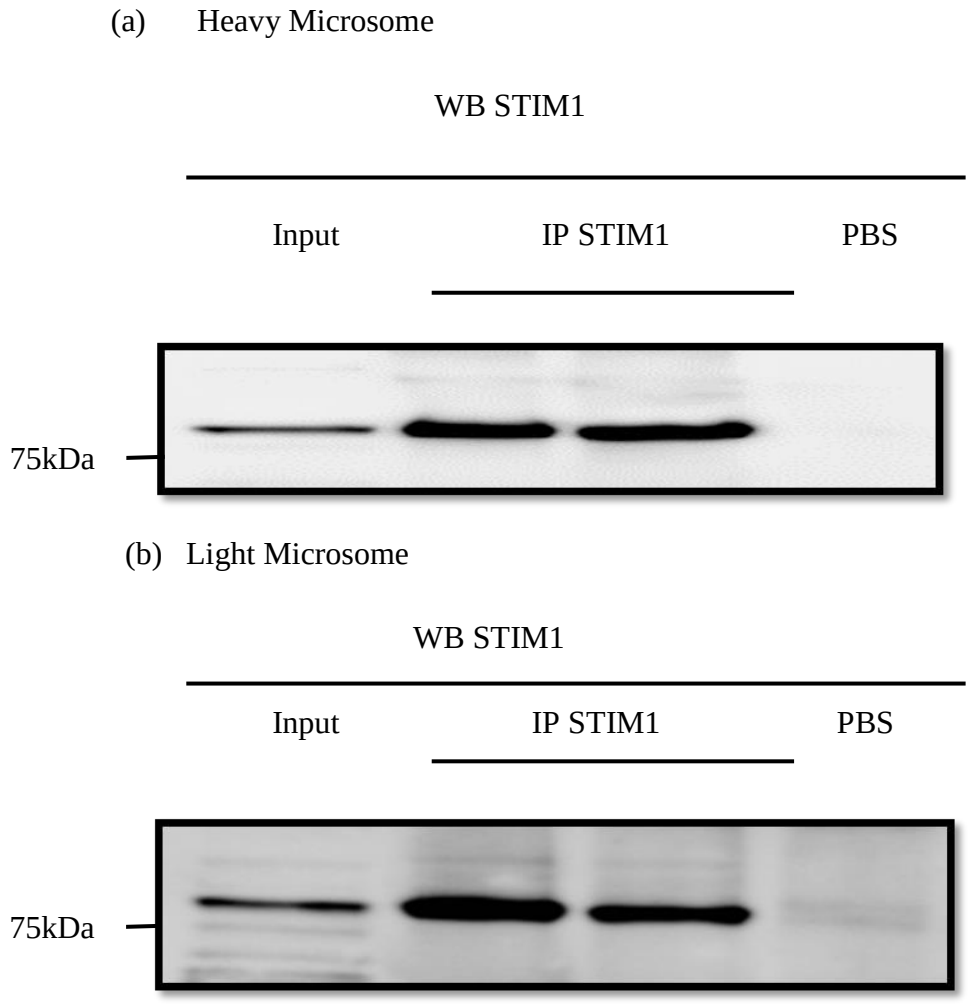


**Figure 4.1 Evidence that STIM1 is immunoprecipitated from heavy and light microsomes in strong stringency lysis buffer.**

STIM1 is immunoprecipitated from (a) heavy and (b) light microsome by anti-STIM1 antibody in RIPA buffer containing sodium dodecyl sulphate (SDS), sodium deoxycholate and nonidet P-40. The eluted proteins from protein A/G plus agarose were detected with same anti-STIM1 antibody by western blot. The results on heavy microsome shown are representative of those obtained from one out of three experiments which give similar results (N=3). The bands detected at 77 kDa is STIM1. The lysate incubated with PBS was acted as negative control of immunoprecipitation.

### 4.2.2 Immunoprecipitation of STIM1 from heavy microsome (HM) under weak dissociation condition

As mentioned in the previous section, the composition of detergents in lysis buffer is critical for maintaining the intact of protein-protein interaction. Therefore, in this section I was using another formula of lysis buffer with weak protein-protein dissociation power to conduct STIM1 immunoprecipitation on heavy microsome. The composition of weak dissociating lysis buffer contains 1% Nonidet P-40 to dissolve the protein from heavy microsome (Pozo-Guisado et al., 2010, Elion, 2001).

In figure 4.2, it was the result of STIM1 western blot from heavy microsome after immunoprecipitation of STIM1 by using the same STIM1 antibody in weak dissociating lysis buffer. The immunoblot of STIM1 showed that band at the size of 77 kDa from the group of STIM1 immunoprecipitation was detected. The band from the immunoprecipitation group was also observed band at about 77 kDa which is similar to the input heavy microsome lysate. In this experiment, normal mouse IgG was used as negative control instead of PBS in order to determine the isotype of IgG from normal mouse does not bind unspecifically to the protein A/G. There was no band was observed at the mouse IgG control group by using weak dissociating lysis buffer.

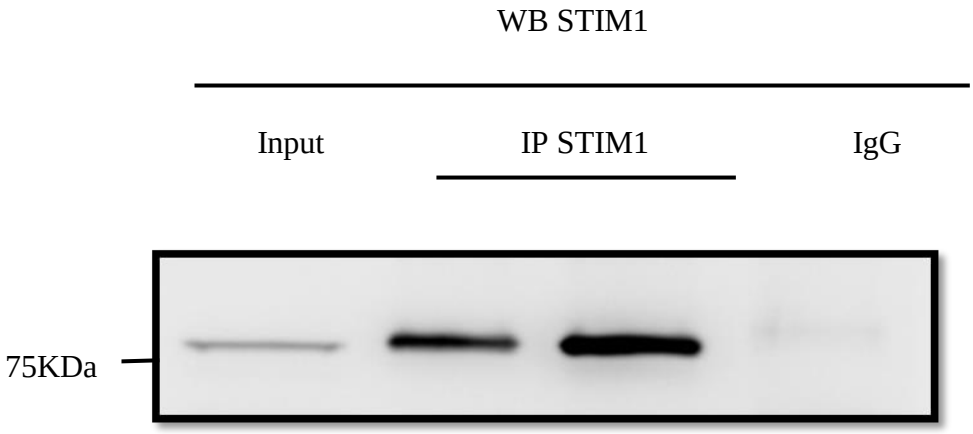


**Figure 4.2 Evidence that STIM1 is immunoprecipitated from heavy microsome with weak stringency lysis buffer.**

STIM1 is immunoprecipitated from heavy microsome in 1% nonidet P-40 by anti STIM1 antibody and detected with same anti-STIM1 antibody by western blot. The bands detected at 77 kDa is STIM1. The lysate incubated with IgG is acted as negative control.

### 4.2.3 Test for co-immunoprecipitation of SERCA with STIM1

After the confirmation of STIM1 antibody can immunoprecipitate STIM1 protein from heavy and light microsome fractions. Evidence showed that SERCA is suggested as an STIM1 binding protein and SERCA is mainly located on ER (Sampieri et al., 2009a). Thus, the interaction of STIM1 and SERCA at the heavy and light microsome fractions were detected and this results could help to determine is there any different between STIM1 in heavy and light microsome binding to SERCA. STIM1 protein was pulled down from the lysate of microsomal fractions in RIPA buffer. The proteins were eluted from the protein A/G agarose and tested the interaction of STIM1 and SERCA by SERCA western blot.

In Figure 4.3 a and b, the results showed that there were no bands detected on STIM1 immunoprecipitation group from both heavy microsome and light microsome. Thus, no interaction STIM1 and SERCA on microsomal fractions were detected by western blot. In the input lysate of heavy microsome and light microsome, SERCA can detect the bands at 75kDa. PBS was used as negative control of immunoprecipitation showed there was not no any band observed on both heavy and light microsomes samples.

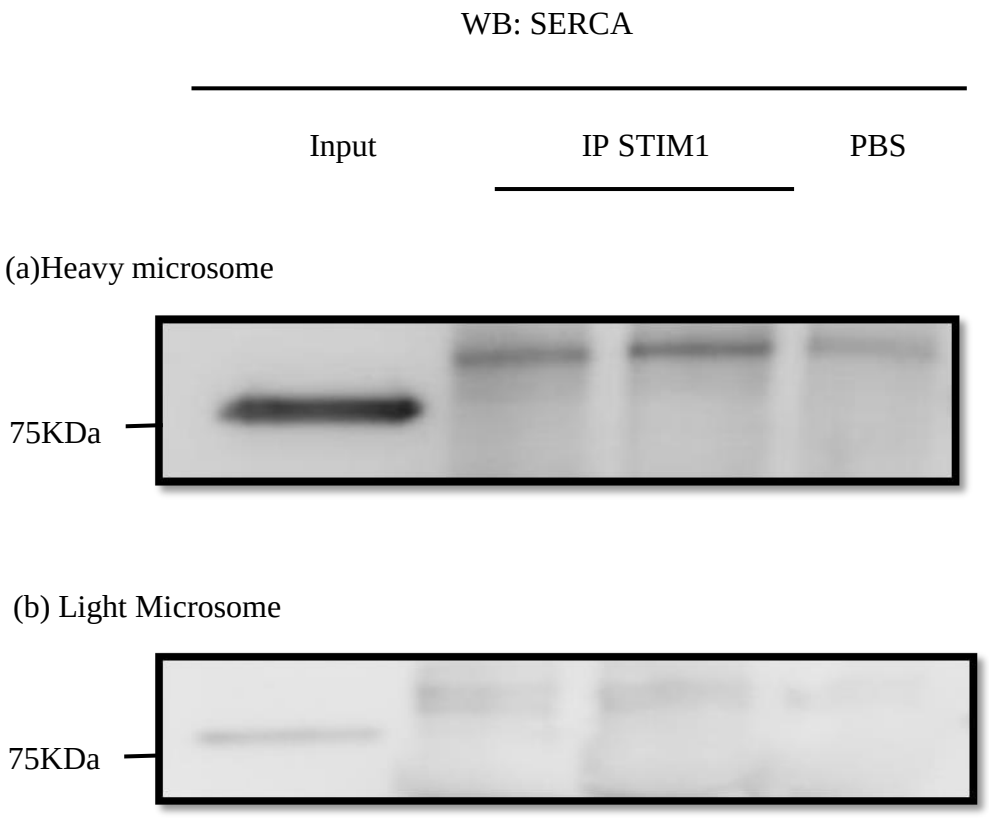


**Figure 4.3 Western blot of SERCA on microsomal fractions after immunoprecipitation of STIM1 protein.**

STIM1 protein was immunopreipitated from (a) heavy and (b) light microsomes with RIPA lysis buffer containing SDS, sodium deoxycholate and nondiet P-40. The eluted protein from protein A/G plus agarose were then tested western blot with SERCA antibody. The results on heavy microsome shown are representative of those obtained from one out of two experiments which give similar results (N=2). The lysate incubated with PBS is acted as negative control of immunoprecipitation.

### 4.2.4 Detection of STIM1 binding partner by Liquid Chromatography-Mass Spectrometry (LC/MS)

LC/MS is one of useful tool to identify the unknown proteins. In this section, LC/MS was used to search the new STIM1 binding proteins that located in heavy microsome after the immunoprecipitation of STIM1. The approaches of searching STIM1 binding proteins were immunoprecipitated STIM1 from heavy microsome. Those proteins bound to protein A/G plus agarose after immunoprecipitation of STIM1 from heavy microsome were then eluted by adding trifluoroacetic acid to lower the pH value and analysis the peptides by LC/MS after trypsin digestion. The peptides were identified by searching on the database.

In study protein-protein interaction, it is important to distinguish between the true and false STIM1 binding proteins from the LC/MS result. The contaminants and unspecific binding protein could be appeared on the data causing the false positive result. In our study, the conventional strategy was used to identify the unspecific protein binding on the bead. In this strategy, STIM1 immunoprecipitation was conducted at the same time with mock immunoprecipitation that only present the bead in the reaction. The purpose of the mock immunoprecipitation is to identify the unspecific binding of the bead (Markham et al., 2007). Therefore, the experiments were divided into two groups. One group was STIM1 immunoprecipitation group and another group was bead control. The bead control is the lysate incubated with protein A/G plus agarose and PBS.

In table4.1, it is the list of the proteins detected by LC/MS after immunoprecipitation of STIM1 in heavy microsome. The proteins that present in

both immunoprecipitation group and control bead group are recognised as unspecific binding of the agarose or contaminants, then the proteins would be removed form the list of potential STIM1 binding protein. The proteins showed on table 4.1 was the protein after the elimination of the proteins that are presented at both immunoprecipitation group and bead control group.

After the elimination of the proteins, 14 proteins were identified and listed on the table 4.1. The proteins on the table were arranged in according to the score that was obtained from database searching. The higher score means the predicted peptide more likely match with the peptide from the database (Eng et al., 1994) The protein with the higher score is on the top and lower score protein is at the bottom.

STIM1 was one of the proteins identified from the sample by LC/MS. This can be one of the indicators to show the success of STIM1 immunoprecipitation and the detection of protein by LC/MS. Some of the other proteins found were cytoskeleton protein included Keratin, type I cytoskeletal 42, Actin-related protein 3 and ProteinKrt16. Another proteins identified were classified as nuclear protein including histoneH2B. Keratin is recognised as contaminants from the skin tissue (Hodge et al., 2013). Some evidence showed that nuclear-binding protein is unspecific binding protein to the agarose (Trinkle-Mulcahy et al., 2008). As for these reasons, cytoskeleton –related protein and nuclear-binding protein are not included as potential new STIM1-binding from our experiment. After removal of the contaminants and unspecific binding protein, Peroxiderine 4 (Prx4) is the only protein that do not belong to any catalogue as mentioned above and suggest Prx4 is a potential new STIM1-binding protein.

| **Accession number** | **Coverage (%)** | **No. of Peptides** | **Score** | **Protein Name** |
|---|---|---|---|---|
| P84903 | 25.55 | 15 | 79.86 | Stromal interaction molecular 1(STIM1) |
| D4ABS3 | 36.96 | 5 | 58.74 | HistoneH2B |
| P20762 | 14.29 | 4 | 44.99 | Ig gamma-2C chain C region |
| Q9Z0V5 | 21.98 | 5 | 31.65 | Peroxiredoxin-4 |
| Q5BJT0 | 11.44 | 4 | 18.02 | Arginine and glutamate protein 1 |
| Q6IFU7 | 11.06 | 4 | 15.47 | Keratin, type I cytoskeletal 42 |
| Q6IFU9 | 9.72 | 3 | 13.81 | ProteinKrt16 |
| Q6AXS5-2 | 6.89 | 2 | 10.19 | Isoform 2 of plasminogen activator inhibitor 1 RNA-binding protein |
| F1M7H9 | 7.58 | 2 | 9.75 | Protein Luc712 (Fragment) |
| B2RZB7 | 20.17 | 2 | 7.53 | Protein Snrpd1 |
| P02600-2 | 16.00 | 2 | 5.91 | Isoform MLC3 Myosin light chain 1/3, skeleton muscle isoform |
| F1LRK8 | 4.56 | 2 | 5.08 | Actin-related protein 3 |
| D4A1G4 | 30.00 | 2 | 4.86 | Cytochrome b5 |
| B5DES0 | 16.10 | 2 | 4.20 | Protein Snrpd2 |

**Table 4.1 Protein detected by LC/MS in immunoprecipitate of heavy microsome using anti-STIM1 antibody.**

STIM1 protein was immunoprecipitated from heavy microsome. The proteins bound on protein A/G plus agarose was eluted by adding 0.1% trifluoroacetic acid and were digested by trypsin into peptides. Those peptides were analysed by LC/MS. The spectra obtained were searched with IPI database to identify the peptides. Coverage is the percentage of unique peptide identified by mass spectrum covered the protein sequence. The value from the number of peptide is the number of peptide match with the protein sequence. Two individual heavy microsme samples were used to search for STIM1 binding protein (N=2)

### 4.2.5 The distribution of peroxiredoxin 4 (Prx4) on subcellular fraction from rat liver

From the results of LC/MS, peroxiredoxin 4 (Prx4) is identified as a potential new STIM1 binding protein that only confined in the region of rough ER. Further experiments were conducted to confirm the interaction between STIM1 and Prx4. In order to investigate the potential interaction between STIM1 and Prx4 further, the western blots of Prx4 on mitochondria and microsomal subcellular fractions was firstly conducted to confirm the presence of Prx4 in the liver and heavy microsome. The interaction between STIM1 and Prx4 was tested by immunoprecipitating STIM1 from heavy microsome and western blot with Prx4.

Figure 4.4 a is the result of western blot of Prx4 on mitochondria and microsomal subcellular fractions from rat liver. The results showed that whole liver sample showed the strong band at 25 kDa and faint band at 50 kDa. Evidence indicated that 25 kDa is monomer of Prx4 and 50 kDa is dimer of Prx4 (Tavender and Bulleid, 2010). Heavy microsome, light microsome, mitochondria and nuclear fraction showed bands at 25 kDa. The bands at 50 kDa were also observed at heavy microsome, light microsome, mitochondria and nuclear fraction, but the band intensity from those fractions were weaker than 25 kDa expect nucleus has similar intensity from 25 kDa and 50 kDa. Light microsome present weaker band at 25kDa than heavy microsome and mitochondria. The cytosolic fraction only showed 50kDa band and there was no band observed at 25 kDa. After quantifying the intensity of the band from the Prx4 western blot, it showed that heavy microsome contains most of the Prx 4 protein.

(a)

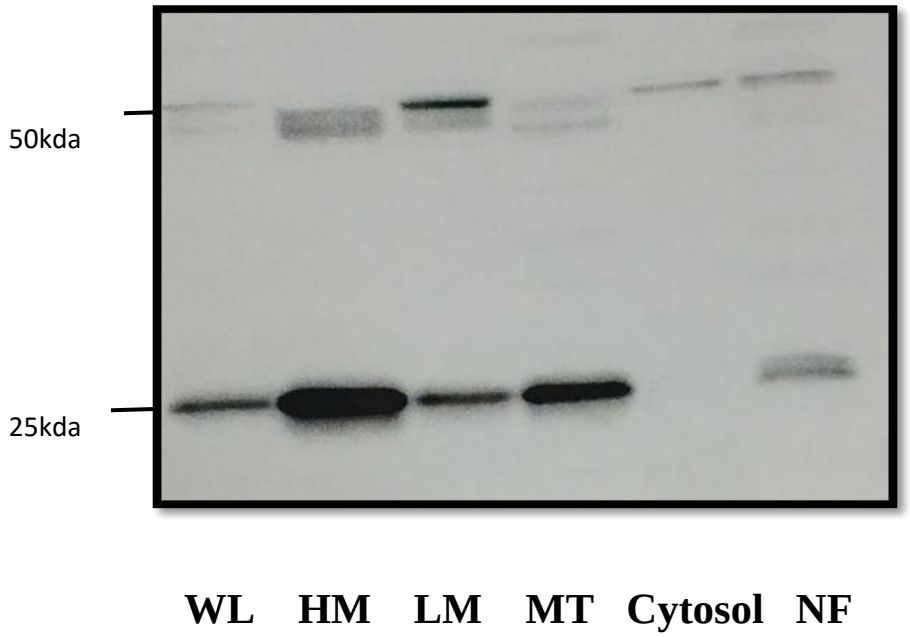
50kda
25kda
WL
HM
LM
MT
Cytosol
NF

(b)

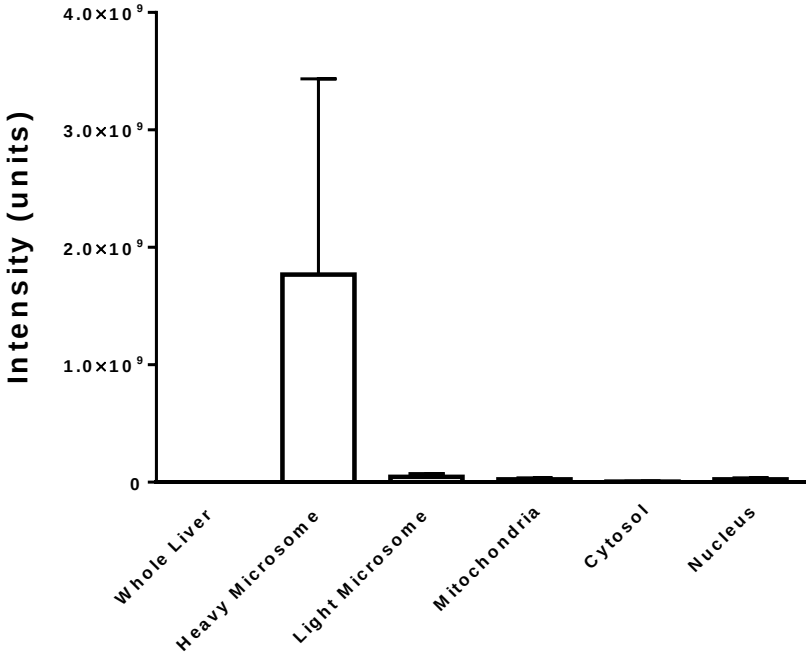
Intensity (units)
4.0×10⁹
3.0×10⁹
2.0×10⁹
1.0×10⁹
0
Whole Liver
Heavy Microsome
Light Microsome
Mitochondria
Cytosol
Nucleus

**Figure 4.5 Detection and Quantitation of western blot of peroxiredoxin 4 ( Prx4) on mitochondria and microsomal fraction from untreated rat liver.**

**(a)** Western blot of Prx4 on whole liver (WL), nuclear fraction (NF), mitochondria (MT), heavy microsome (HM), light microsome (LM) and cytosol from untreated rat liver. The results shown are representative of those obtained from one out of three experiments which give similar results (N=3). **(b)** Quantitation of western blot of Prx4 on mitochondria and microsomal fraction. The intensity was normalised by total protein on the PVDF membrane after transfer and the data were expressed as mean± SEM.

### 4.2.6 Test of interaction of STIM1 and Prx4 by immunoprecipitation and western blot

From the result of LC/MS in the previous section, Prx4 was considered as a new STIM1 binding protein that is associated with STIM1 in heavy microsome. The idea of Prx4 as new STIM1 binding protein was then further tested by western blot of Prx4 on the eluted protein after STIM1 immunoprecipitation on heavy microsome.

In figure 4.4, it showed the immunoblot of Prx4 on the eluted protein from the protein A/G plus agarose after STIM1 immunoprecipitation from heavy microsome. RIPA lysis buffer was used to perform the immunoprecipitation of STIM1. The input of the heavy microsome lysate displayed two band at the size about 50kDa and 25 kDa, respectively. The band of 25 kDa is the monomeric form of Prx4 and 50 kDa is dimeric form of Prx4 (Tavender et al., 2010). When the STIM1 protein pulled down from heavy microsome, the immunoblot also showed these two bands at the size of 50 kDa and 25 kDa which is similar to the input sample. In the experiment, normal mouse IgG was used as negative control for the STIM1 immunoprecipitation by incubating the mouse IgG with heavy microsome lysate instead of STIM1 antibody. The results showed that there were two faint band showed on the immunoblot at the size about 25 kDa and 50 kDa, which may be the unspecific binding.

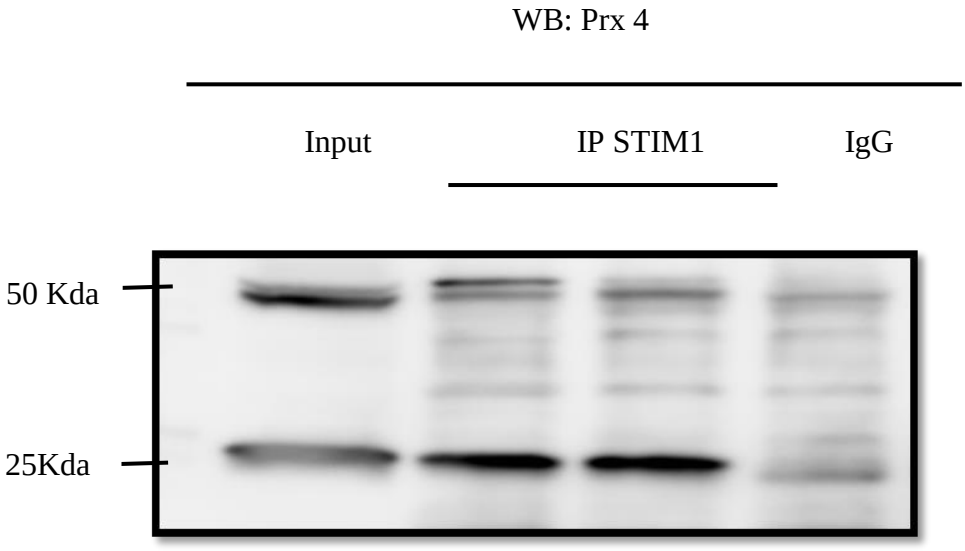


**Figure 4.6 Western blot of peroxiredoxin 4 (Prx4) on heavy microsome after immunoprecipitation of STIM1 with RIPA lysis buffer.**

STIM1 was immunoprecipitated from heavy microsome in RIPA lysis buffer buffer containing sodium dodecyl sulphate (SDS), sodium deoxycholate and nonident P-40. The eluted proteins were tested with western blot of peroxiredoxin 4. The results shown are representative of those obtained from one out of three experiments which give similar results (N=3). The size of monomer and dimer of Prx4 are 25kDa and 50 kDa, respectively. The lysate incubated with mouse IgG is acted as negative control.

## 4.3 Discussion

In this chapter, I was trying to identify new STIM1 binding proteins at specific region on ER rather than whole cells. The strategy of the experiments is that STIM1 protein at heavy microsome was isolated by immunoprecipitation. Then, the novel STIM1 binding proteins were then detected by LC/MS and western blot. In order to achieve the goal, I firstly tested the ability of STIM1 antibody in immunoprecipitating STIM1 from heavy microsome following by searching the new STIM1 binding protein using LC/MS and western blot.

### 4.3.1 Confirmation of STIM1 antibody in immunoprecipitating STIM1 protein from heavy microsome

Immunoprecipitation is a common method used in studying the protein-protein interaction. The ability and specificity of the antibody in pulling down the target protein is critical for the experiment. Therefore, the STIM1 antibody used in the experiment need to be tested firstly to demonstrate that the STIM1 antibody can precipitate STIM1 protein from the microsomal fractions.

The stringency of lysis buffer used in immunoprecipitation is important for detecting the protein-protein interaction. In experiments, two different stringency lysis buffer were used in conducting immunoprecipitation. The first one is RIPA lysis buffer that has strong dissociation power containing ionic detergents SDS, sodium deoxycholate and non-ionic detergent nonidet P40. The second lysis buffer is weak ionic strength lysis buffer containing 1% nonidet P-40 that is non-ionic detergent (Harlow and Lane, 2006). The results of immunoprecipitation

from both different lysis buffer suggested that the STIM1 antibody can pull down the STIM1 protein from the microsomal fractions. STIM1 protein can also be detected by LC/MS after the immunoprecipitation of STIM1. It is another evidence to prove the ability of STIM1 antibody in immunoprecipitation of STIM1 protein from microsomal fractions. From both of the results, the STIM1 antibody is good to be used in immunoprecipitation on heavy microsome from rat liver cells samples to search for the new STIM1 binding proteins.

### 4.3.2 Peroxiredoxin 4 is novel STIM1 binding protein

After the removal of contaminants and unspecific binding from the list of protein candidates, Prx4 should be one of the STIM1 binding protein that is only confined at the region of ER. In order to determine whether Prx4 is also located at other subcellular functions, the distribution of Prx4 on other subcellular fractions was detected by western blot. The results of Prx4 western blot indicated that Prx4 is mainly located at heavy microsome, light microsome and mitochondria. Less Prx4 is found at nucleus and cytosol. Therefore, Px4 is mainly located at the region of ER to produce its function, not another region.

Interestingly, some other reported STIM1 binding proteins such as actin or microtubule plus end-binding EB1 did not detect by our LC/MS experiments. There are several possible explanations of why other reported STIM1 binding protein cannot be detected. Firstly, different STIM1 binding proteins have its specific function. Some STIM1 binding proteins are related to the formation of ER-PM junction or translocation of STIM1, then it could be possible that the

binding proteins are dissociated from STIM1 or relocate to another part of subcellular fractions during subcellular fractionation. Secondly, the heavy microsome collected is from untreated rat liver so Orai1 or other reported STIM1 binding protein may not be bind to STIM1 when SOCs is inactivated. No interaction of STIM1 and SERCA was detected from our experiment. It is possible that the condition of immunoprecipitation is still not suitable for detecting the interaction of STIM1 and SERCA. Although STIM1 can be pulled from heavy microsome under RIPA and 1% nonidet P 40 lysis buffer, it is still not sure the interaction still keeping intact under the condition using in the experiments. Thus, it is needed to optimize the condition by using different concentration of detergents. In addition, it is ideal to perform an experiment in three replicate at least. If time is allowed, it is good that increase the number to at least three replicate.

Peroxiredoxin 4 (Prx4) is an ER-resident thio peroxidase which is belonged to typical 2-cys Prx family containing active cysteine resident to detoxify hydrogen peroxide in ER (Tavender et al., 2008). The crystal structure analysis showed that Prx4 is a decamer ring structure composing of five dimers (Cao et al., 2011). The oligomers of the Prx4 structure are linked by disulfide bond. When Prx4 fully reduced, it forms monomeric Prx4 with the size of 25 kDa. The band at about 25kDa on western blot of Prx4 should be the monomeric of Prx4 (Tavender et al., 2010, Wang et al., 2012). Due to the present of DTT in running of SDS-PAGE, the disulfide bond of Prx4 should be reduced, so reduced monomeric Prx4 with 25 kDa and dimeric Prx4 with 50 kDa were detected in the results of

immunoprecipitation and western blot. As most of Prx4 was reduced to monomeric Prx4, the band of monomeric Prx4 is stronger than dimeric Prx4.

In conclusion, the result in this chapter provides additional information about the protein profiling on a specific region on ER that related to the protein interaction of STIM1. Among the protein identified by western blot and LC/MS, Prx4 is identified as novel STIM1 binding protein that may be interact with STIM1 in rough ER region.

# Chapter V

# The role of phosphorylation of STIM1 and Orai1 in Steatotic liver cells

# Chapter V The role of phosphorylation of STIM1 and Orai1 in Steatotic liver cells

## 5.1 Introduction

In Chapter 3 and 4, I have successfully quantified STIM1 and Orai1 proteins in the subcellular fractions of rat liver. STIM1 protein can be pulled down from immunoprecipitation by using anti-STIM1 antibody. Then, I used these methods to search for STIM binding proteins using Liquid chromatography-mass spectrometry (LC/MS) and identified peroxiredoxin 4 (Prx4) as one of the potential STIM1 binding protein. The result was further confirmed using western blot. At the same time, other researchers in our laboratory demonstrated the $Ca^{2+}$ influx via store-operated $Ca^{2+}$ channel was reduced at lipid-loaded H4IIE cells and leptin genetically modified obese Zucker rat liver cells, and the $Ca^{2+}$ entry was reversed by the pretreatment of the protein kinase C (PKC) inhibitors (Wilson et al., 2014). Several approaches provided evidence that the inhibition of SOCE is mediated by PKC (Galiano et al., 2004, Sundivakkam et al., 2013). It has been showed that the kinase of ERK1/2 and PKC can phosphorylate STIM1-serine77, serine-608, serine-621 and Orai1 on serine-27, serine-30 (Pozo-Guisado et al., 2013, Kawasaki et al., 2010). Regarding physiological function, the phosphorylation of STIM1 mediates the regulation of spindle formation and involves the change of morphology of ER during cell mitosis (Smyth et al., 2009). Therefore, the activity of SOCs is regulated by the phosphorylation and STIM1 or Orai1 could be the main targets for the phosphorylation.

The overall aim of the experiments described in this chapter was to determine whether STIM1 and/or Orai1 are phosphorylated in steatotic liver cells. To address this question, I used two different hepatic steatosis cells and animals models to explore the role of phosphorylation of STIM1 and Orai1 in the development of hepatic steatosis *in vitro* and *in vivo* level. Amiodarone- induced lipid accumulation in cells is a useful cells-based model to study steatosis *in vitro* (Donato et al., 2009). Zucker obese rats that have mutation in leptin receptor inducing the development of steatosis is a useful animal model to study obesity-related diseases *in vivo* (Forcheron et al., 2009). Thus, in our experiments H4IIE cell, a rat hepatoma cells line, treated with amiodarone to induce lipid accumulation and liver cells from Zucker rat were employed as models to test the role of phosphorylation in the development of steatosis in liver cells.

The development of antibody that bind specifically to phosphorylated protein is becoming a common and useful tool for studying protein phosphorylation (Mandell, 2003). As phosphorylation of STIM1 and Orai1 occurs on serine amino acid, then I used anti-phosphoserine antibody to detect the phosphorylation on STIM1 and Orai1. Then the strategy for detecting the phosphorylation was to immunoprecipitate STIM1 or Orai1 protein from steatotic liver lysate and the phosphorylation of STIM1 or Orai1 are detected by either western blot with anti-phosphoserine antibody or LC/MS. Thus, the specific aims of the research in this chapter are (i) to find out the conditions which can isolate STIM1 or Orai1 protein from extracts of steatotic liver cells by immunoprecipitation using anti-STIM1 antibody and anti-Oai1 antibody, (ii) to test the presence of phosphorylated STIM1 or Orai1 using anti-phosphoserine antibody. According to the information

from Abcam, the chosen anti-phosphoserine antibody in our experiments was prepared by injecting carrier proteins conjugated with phosphoserine into the mouse to induce the production of the phosphoserine antibodies. Thus, the phosphoserine antibody used can potentially detect most of the phosphorylation site on serine on at protein.

## 5.2 Results

### 5.2.1 Test the ability of STIM1 antibody in immunoprecipitating STIM1 protein from steatotic liver

In order to detect the phosphorylation on STIM1, the capability of anti-STIM1 antibody in imunoprecipitating STIM1 protein from steatotic liver was firstly tested by western blot. The success of the STIM1 immunoprecipitation on steatotic liver lysate is shown by pulling down STIM1 protein in liver lysate using STIM1 antibody, and then detect the presence of STIM1 protein in the immunoprecipitate by western blot of STIM1 using the same STIM1 antibody as in immunoprecipitation. The STIM1 antibody used in this chapter is same as previous two chapter used.

In Figure 5.1 a, the western blot of STIM1 showed band at the size about 77 kDa on both homozygous lean and fat Zucker rat liver after immunoprecipitating the STIM1 protein. In the input liver lysate, lean and fat Zucker rat liver lysate both displayed the bands at 77 kDa which is the size as same as in STIM1 immunoprecipitation group. No band was observed at negative control of IgG at

the size of 77 kDa. The size of 50 kDa is heavy IgG chain which is pulled down by the same antibody from the same species during immunoprecipitation (Lal et al., 2005). From the result, it indicated that anti-STIM1 antibody can immunoprecipitate STIM1 protein from Zucker rat liver lysate. In future, it is good that the bands intensity for lean and fat lysate can also be quantified, then it can provide an additional information of is that any change on the conformation and influence the binding of the STIM1 antibody.

### 5.2.2 Test the ability of phosphoserine antibody in immunoprecipitating proteins phosphorylated on serine from steatotic liver of obese Zucker rat

In figure 5.1b, it showed the western blot of phosphoserine after immunoprecipitation of phosphorylated proteins on serine from heterozygous lean Zucker liver lysate using same anti-phosphoserine antibody. The result of the western blot indicated that multiple bands were observed from the heterozygous lean Zucker rat liver lysate so the anti-phosphoserine antibody used in the experiment can detect the protein phosphorylated on serine from liver lysate (Figure 5.1b input). Both phosphoserine immunoprecipitation group and IgG control group showed significant bands at 50 kDa and 37 kDa. The band of 50 kDa should be heavy chain of IgG. As it cannot detect multiple bands from immunoprecipitation of phosphoserine group, the pattern is not similar to input liver lysate. Thus, from the result it indicated that no protein phosphorylated on serine was immunoprecipitated from the liver lysate by using phosphoserine antibody.

(a) IP: STIM1, WB: STIM1

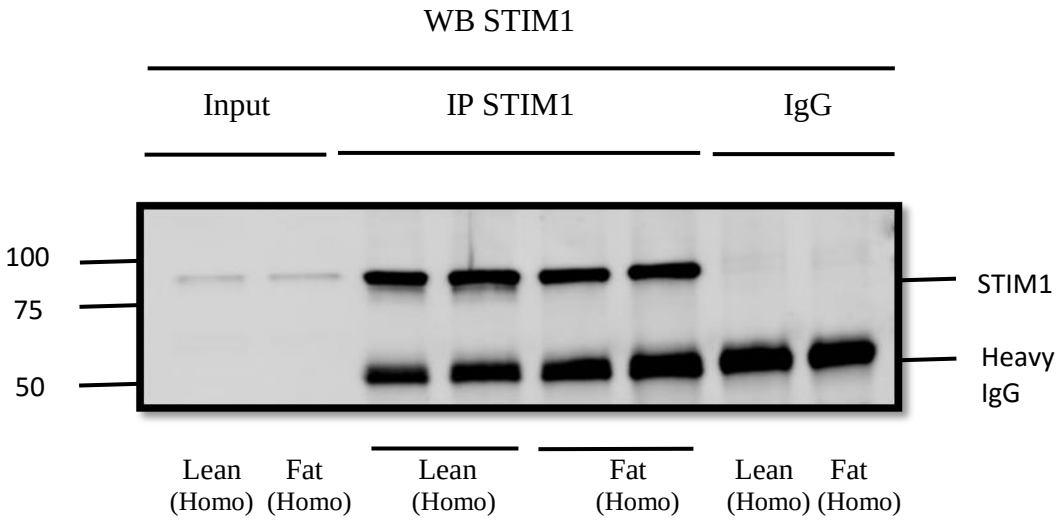


(b) IP: Phosphoserine, WB: Phosphoserine

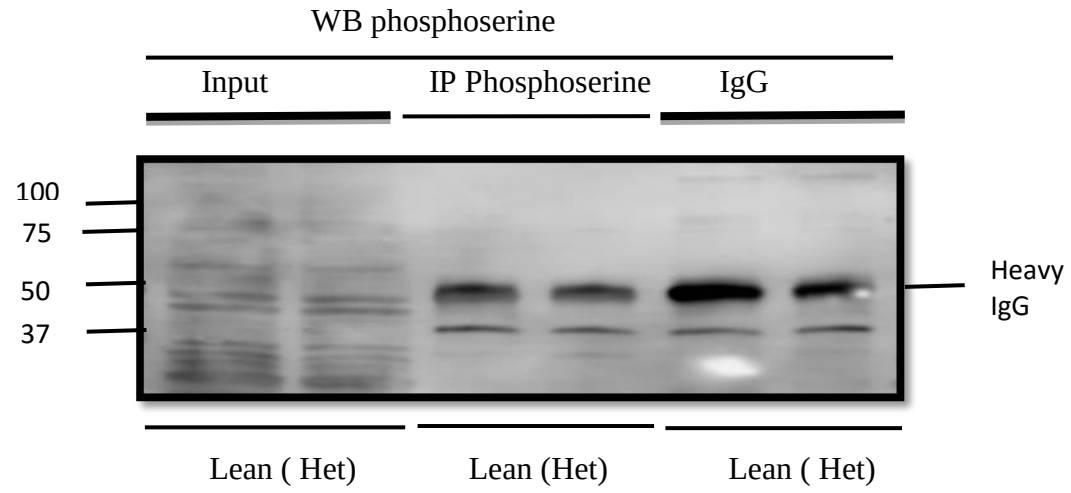

**Figure 5.1 Proteins extracted from Zucker rat liver subject to immunoprecipitation using anti-STIM1 antibody or anti-phosphoserine antibody and subsequent western blot with same anti-STIM1 antibody and anti-phosphoserine antibody.**

(a) Homozygous (Homo) Lean and fat Zucker rat liver lysate were used in immunoprecipitation of STIM1 and western blot with the same anti-STIM1 antibody. The results shown are representative of those obtained from one out of two experiments which give similar results (N=2). (b) Heterozygous (Het) lean Zucker rat liver lysate was used in immunoprecipitating of protein phosphorylated on serine motif and western blot with the same anti-phosphoserine antibody. The bands detected at 77kda is STIM1 protein. The lysate incubated with normal IgG is acted as negative control of immunoprecipitation.

### 5.2.3 Test for the presence of phosphorylated STIM1 in liver extracts from Zucker obese rats using immunoprecipitation with STIM1 antibody and western blot with phosphoserine antibody

After the confirmation of the STIM1 antibody can pull down STIM1 protein from Zucker rat liver lysate, then I used the method of western blot against phosphoserine after the immunoprecipitation of STIM1 to detect whether the phosphorylation happens on STIM1 protein from steatotic liver cells. In figure 5.2, the result showed that multiple bands were detected on the input lysate. Thus, it indicated that the phosphoserine antibody is able to detect the proteins phosphorylated on serine from both lean and fat Zucker input lysate of rat liver. There were no bands observed at about 77 kDa which is the size of STIM1 from lean and fat liver lysate after the immunoprecipitation of STIM1 from the liver lysate. In IgG negative control group, the phosphoserine antibody did not detect any signal at the size about 77 kDa from both lean and fat liver lysate. The bands detected at 50 kDa should be heavy chain of IgG. The results showed that no phosphorylation detected on STIM1.

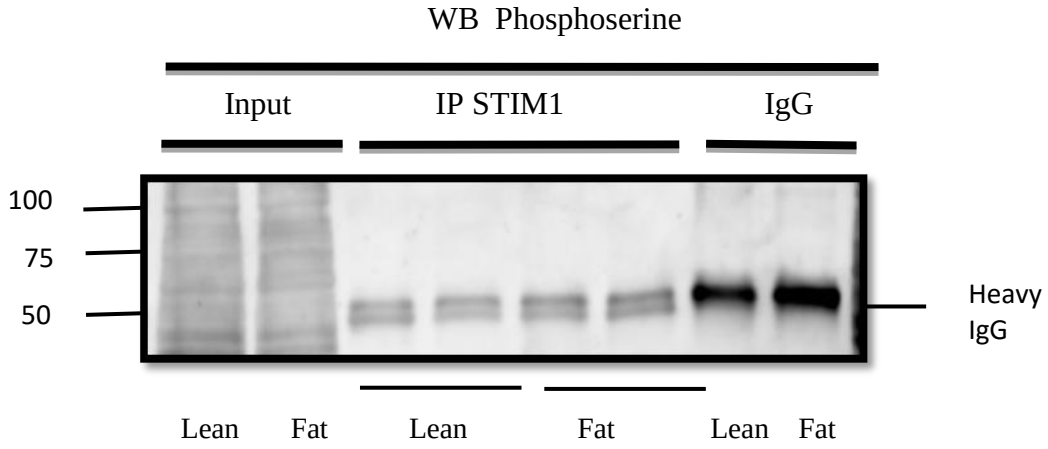


**Fig 5.2 Proteins extracted from Zucker rat liver subject to immunoprecipitation using anti-STIM1 and subsequent western blot with anti-phosphoserine antibody.**

STIM1 was immunoprecipitated from rat liver lysate by anti STIM1 antibody and western blot with anti-phosphoserine antibody on homozygous lean and fat Zucker rat liver lysate. Normal mouse IgG incubated with the lysate is acted as negative control of immunoprecipitation. The results shown are representative of those obtained from one out of two experiments which give similar results (N=2). The size of STIM1 is 77 kDa. The bands of 50 kDa and heavy IgG.

### 5.2.4 Test for the presence of phosphorylated STIM1 in H4IIE cells using immunoprecipitation with STIM1 antibody or phosphoserine antibody and western blot with STIM1antibody and phosphoserine antibody

For using the cells –based lipid loaded models, H4IIE cells were treated with amiodarone for 24 hours to induce lipid accumulation. Total protein was extracted from the H4IIE cells after 24 hours incubation. STIM1 protein was immunoprecipitated from the protein extract by STIM1 antibody from control and amiodarone-treated H4IIE cells and then tested for the phosphorylation of STIM1 by phosphoserine western blot.

The results showed that no STIM1 protein phosphorylated on serine was detected in both control and amiodarone-treated H4IIE cells. In negative control group, it was also no bands detected at the corresponding size of STIM1 at 77 kDa (Figure 5.3). The phosphoserine antibody can detect multiple bands on input cell lysate from control and amiodarone-treated H4IIE cells. Thus, the anti-phosphoserine antibody can detect phosphorylated protein on serine from H4IIE cells.

The protein phosphorylated on serine from H4IIE cells lysate was used to test the phosphorylation on STIM1 by pulling down with phosphoserine antibody to determine is that any difference from Zucker rat liver lysate. In the figure 5.3b, it was the reciprocal immunoprecipitation using anti-phosphoserine antibody to immunoprecipitate the protein phosphorylated on serine followed by STIM1 western blot. The result of western blot did not detect the bands of STIM1 at about 77 kDa from control and amiodarone-treated group after immunoprecipitation of protein phosphorylated on serine. The PBS negative control group displayed no bands at 77 kDa. The band of 50 kDa is heavy IgG

that was observed at STIM1 immunoprecipitation group and PBS group from control and amiodarone-treated H4IIE cells lysate. In input lysate, band at 77kDa was detected at control and amiodarone-treated lysate.

(a) IP: STIM1, WB: Phosphoserine

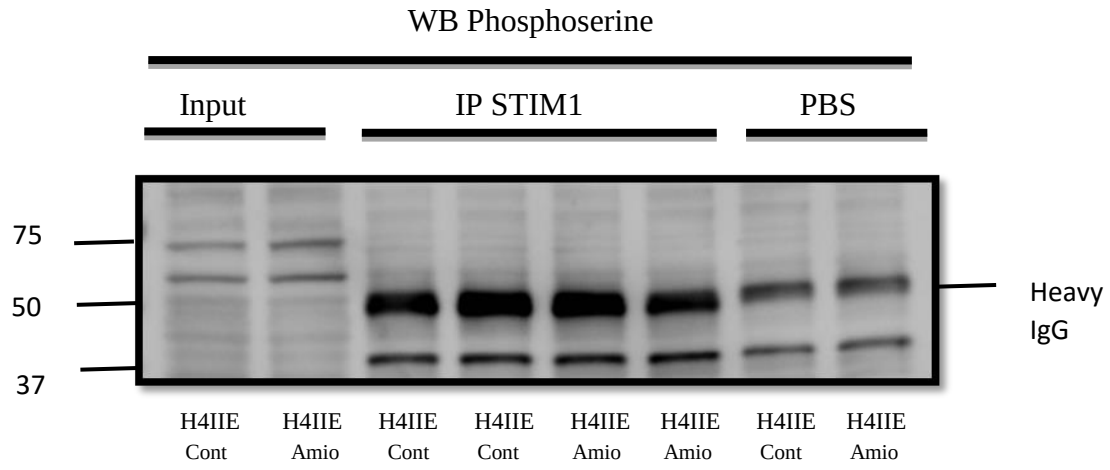


(b) IP:Phosphoserine, WB: STIM1

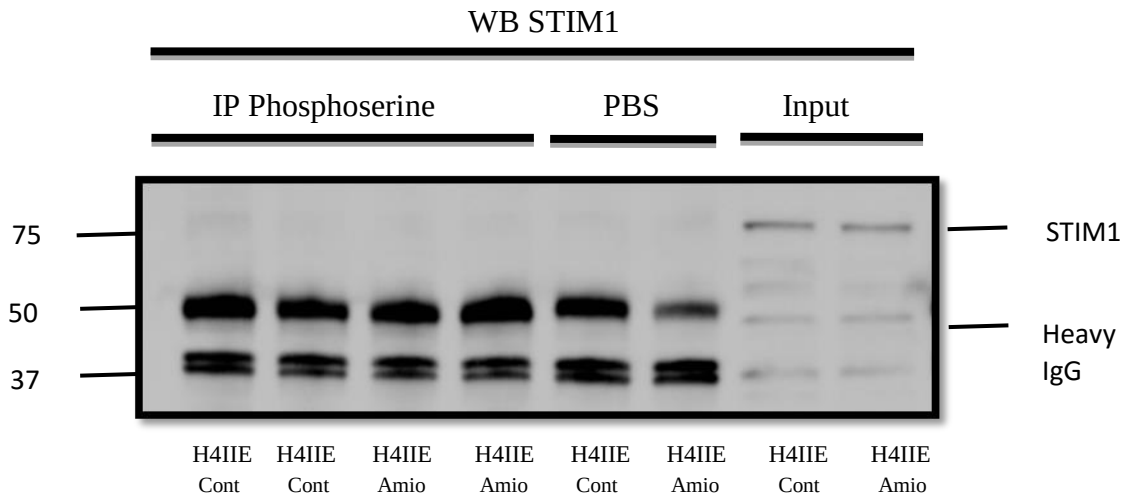

**Figure 5.3 Proteins extracted from H4IIE cells subject to immunoprecipitation using anti-STIM1 antibody and anti-phosphoserine antibody and subsequent western blot with anti- STIM1 antibody or anti-phosphoserine antibody.**

Control(cont) and amiodarone-treated (Amio) H4IIE cells were used to immunoprecipitate (a) STIM1 protein and western blot with anti-phosphoserine antibody. In (b) figure, the phosphorylated proteins on serine were immunoprecipitated from control (cont) and amiodarone-treated (amio) HII4E cells by anti-phosphoserine antibody and western blot with anti-STIM1 antibody. The lysate of control and amiodarone-treated HII4E cells incubated with PBS are acted as negative control of immunoprecipitation. The size of STIM1 is 77 kda. The bands of 50 kDa is heavy IgG.

### 5.2.5 Test of ability of Orai1 antibody from to immunoprecipitate Orai1 protein and protein phosphorylated on serine and western blot with from steatotic liver

In order to detect the phosphorylation of Orai1 from steatotic liver cells, Orai1 protein also needs to be immunoprecipitated from the liver lysate. The rabbit polyclonal Orai1 antibody from Alomone, Jerusalem, Israel was firstly chosen to test its ability to pull down the Orai1 protein from steatotic liver cells. The success of immunoprecipitation of Orai1 was determined by immunoprecipitation of Orai1 using Orai1 antibody and then test the presence of Orai1 in the immunoprecipitate by using western blot of Orai1 with same Orai1 antibody. Two form of Orai1 protein were detected from western blot. Evidence showed that the size of glycosylated Orai1 is 45 kDa and non-glycosylated are 33kDa. (Gwack et al., 2007)

Lean and fat Zucker rat liver lysate was incubated with the Orai1 antibody from Alomone trying to immunoprecipitate Orai1 protein from the liver lysate. In figure 5.4, it is the western blot of Orai1 on the immunoprecipitate. The immunoblot showed that input lysate displayed the bands at 37kDa which is the size of unglycosylated Orai1 (Figure 5.4). In the group of Orai1 immunoprecipitation, the bands at the size of 37 kDa were observed which is similar to input liver lysate. One strong band just above the bands of 37 kDa were also detected on Orai1 immunoprecipitation group. However, the IgG negative control also displayed the similar 37 kDa bands on the Orai1 western blot. Therefore, the result cannot provide good information to determine whether the Orai1 antibody from Alomone could pull down Orai1 protein from the lysate or not.

As we cannot determine the Orai1 antibody from Alomone Jerusalem, Israel is able to immunoprecipitate Orai1 protein from the homozygous lean and fat Zucker rat liver lysate. Then I selected another Orai1 antibody from Santa Cruz Texas USA to test its potential use in immunoprecipitation of Orai1 protein. The result of western bolt of Orai1 by using Santa Cruz Orai1 showed that figure 5.5, two bands at about 37 kDa and 75 kDa were detected on the input lysate (Figure 5.5). These two bands should be glycosylated and unglycosylated Orai1, respectively. The band of 37 kDa may be unglycosylated form of Orai1 and band of 75 kDa may be the glycosylated Orai1. The intensity of 37 kDa is weaker than 75 kDa band. These two bands, 37 kDa and 75 kDa, were also observed from the Orai1 immunoprecipitation group (Figure 5.5). Two faint bands at 37 kDa and 75 kDa were detected in the group of fat lysate incubated with IgG.

Those results indicated that the Orai1 antibodies from Alomone and Santa Cruz seem able to pull down Orai1 protein from the liver lysate as showing bands at immunoprecipitation group but the negative control also showed the same band as the immunoprecipitation group. Therefore, we cannot make a conclusive conclusion about the capability of Orai1 antibody in using at immunoprecipitation.

IP:Orai1 WB: Orai1 (Alomone)

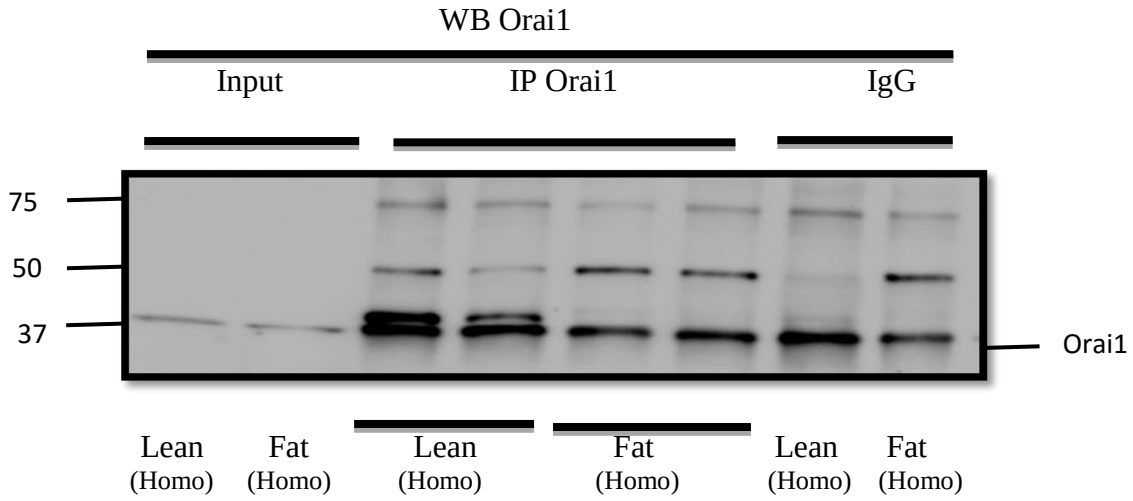


**Figure 5.4 Proteins extracted from Zucker rat liver subject to immunoprecipitation using anti-Orai1 antibody (Alomone) and subsequent western blot with same Orai1 antibody.**

Anti-Orai1 antibody from Alomone Labs (ACC-062) were used in immunoprecipitating Orai1 protein from homozygous lean and fat zucker rat liver lysate and western blot with same Orai1 antibody. The band shown at 37 kDa is unglycosylated from of Orai1. . The results shown are representative of those obtained from one out of two experiments which give similar results (N=2). The liver lysate incubated with normal rabbit IgG was acted as negative control of immunoprecipitation

IP:Orai1 WB: Orai1 (Santa Cruz)

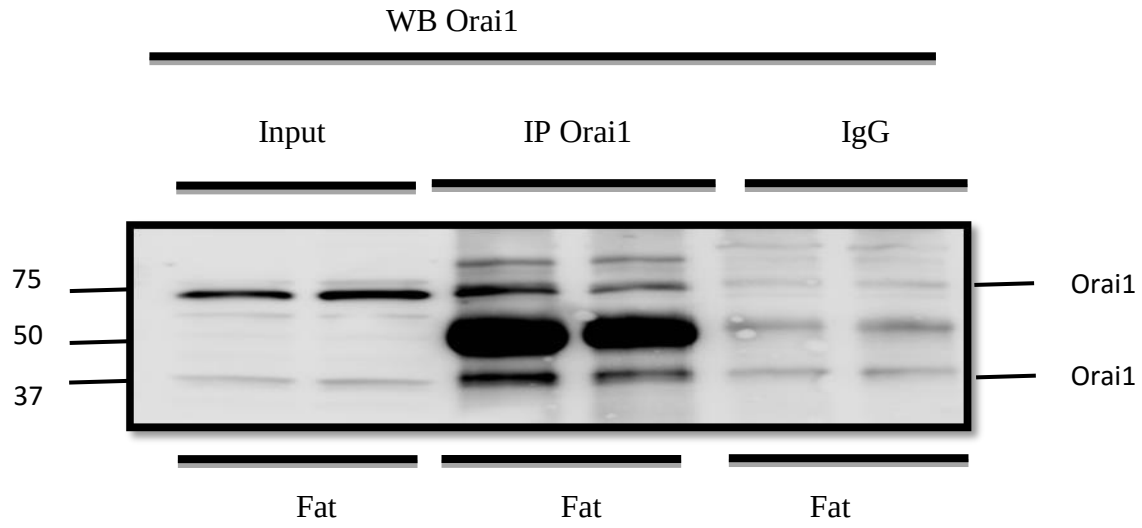


**Figure 5.5 Proteins extracted from Zucker rat liversubject to immunoprecipitation using anti-Orai1 antibody (Santa Cruz) and subsequent western blot with same Orai1 antibody.**

Anti-Orai1 antibody from Santa Cruz (sc68895) was employed in immunoprecipitating Orai1 protein from homozygous fat liver lysate and western blot with the same Orai1 antibody. The band shown at 37 kDa is unglycosylated from of Orai1. The band with higher molecular weight would be glycosylated form of Orai1. The liver lysate incubated with normal rabbit IgG was acted as negative control of immunoprecipitation. The results shown are representative of those obtained from one out of three experiments which give similar results (N=3).

### 5.2.6 Test for the presence of phosphorylated Orai1 in Zucker rat liver using immunoprecipitation with Orai1 antibody and western blot with phosphoserine antibody

The results from section 5.2.5 showed that the Orai1 antibody from Alomone might be able to immunoprecipitate Orai1 protein from the liver lysate. Although the results cannot determine the bands is Orai1 or not, it still possible that the bands showed on the western blot are Orai1 protein from the lysate. Then the experiment in this section was tring to use Alomone antibody to immunoprecipitate Orai1 protein followed by western blot of phosphoserine in order to detect the phosphorylated Orai1 at steatotic liver cells.

In figure 5.6, it was the result of western blot of phosphoserine followed by the immunoprecipitation of Orai1 protein from Zucker rat liver lysate using Orai1 antibody from Alomone. It showed that a weak band at Orai1 immunoprecipitation group at about the size of 50 kDa from lean and fat Zucker rat liver lysate. No bands were observed at PBS negative control sample. One of the Orai1 immunoprecipitation group from lean sample showed weaker band on 50kda and with two other weak bands at about 55 kDa and 60 kDa.

In figure 5.7, the western blot of Orai1 by using Orai1 antibody from Alomone showed the band at about 37kDa on the input lysate but the western of phosphoserine from Orai1 immunoprecipitation showed the bands at about 50kda. As the two results showed two different bands by using same Orai1 antibody from Alomone so it cannot determine the bands detected from phosphoserine western blot is phosphorylated Orai1. Thus it is good to further study what are the proteins at the band of 50 kDa.

IP: Orai1, WB: Phosphoserine

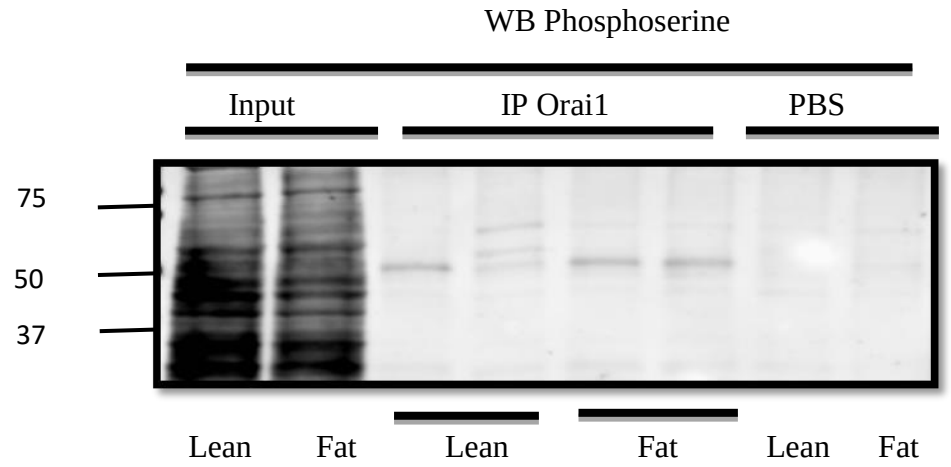


**Fig 5.6 Proteins extracted from Zucker rat liver subject to immunoprecipitation using anti-Orai1 antibody (Alomone) and subsequent western blot with anti-phosphoserine antibody.**

Orai1 protein was immunoprecipitated from lean and fat Zucker rat liver using anti-Orai1 antibody (Alomone) and western blot with anti-phosphoserine antibody. The size of Orai1 are 37 KDa for unglycosylated Orai1 and 47KDa for glycosylated Orai1. The results shown are representative of those obtained from one out of two experiments which give similar results (N=2).

### 5.2.7 Test for the presence of phosphorylated Orai1 in Zucker rat liver using immunoprecipitation with phosphoserine antibody and western blot with Orai1 antibody

The phosphorylated protein on serine was tried to immunoprecipitate by using anti-phosphoserine antibody and detected the phosphorylated Orai1 by western blot of Orai1. As mentioned in chapter 3, Orai1 has two forms, glycosylated Orai1 and unglycosylated Orai1. The western blot of Orai1 showed 37kDa bands which are unglycosylated Orai1 on input liver lysate. After the immunoprecipitation of phosphorylated protein on serine from Zucker rat liver lysate, the western blot of Orai1 on immunoprecipitation showed strong bands at the size about 37kDa on lean and fat liver lysate but the similar bands were also observed at the same size at IgG negative control group (Figure 5.7). Moreover, an additional band with large size was detected in negative IgG control group from fat Zucker rat liver lysate and Orai1 immunoprecipitation group from fat liver lysate.

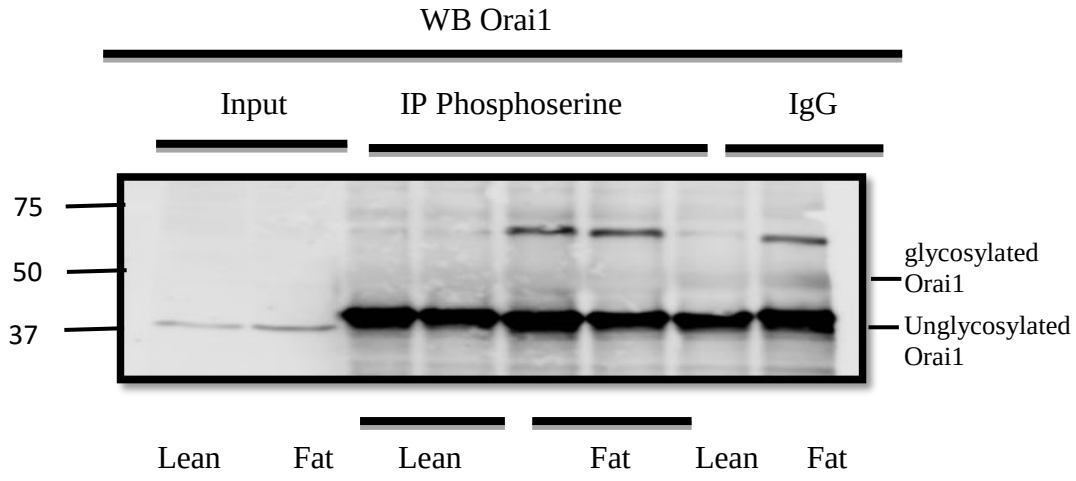


**Fig 5.7 Proteins extracted from Zucker rat liver subject to immunoprecipitation using anti-phosphoserine antibody and subsequent western blot with anti-Orai1 antibody (Alomone).**

Protein phosphorylated on serine was immunoprecipitated from lean and fat Zucker rat live lysate and western blot with anti-phosphoserine antibody. The size of Orai1 are 37 kDa for unglycosylated Orai1 and 47kDa for glycosylated Orai1. The results shown are representative of those obtained from one out of two experiments which give similar results (N=2).

### 5.2.8 Test for the presence of phosphorylated Orai1 in H4IIE cells using immunoprecipitation with Orai1 antibody and phosphoserine antibody

A similar experiment on detecting phosphorylation of Zucker rat liver lysate was also conducted on lipid-loaded H4IIE cells model to further identify the effect of phosphorylation on Orai1 from steatotic liver cells. Immunoprecipitation of Orai1 and protein phosphorylated on serine from lipid-loaded H4IIE cells combined with western blot will be used in detecting the phosphorylation.

In the experiment shown in Figure 5.8a, the H4IIE cells lysate were subjected to immunoprecipitate the Orai1 protein by anti orai1 antibody (Alomone) followed by western blot using anti-phosphoserine antibody. The input lysate showed multiple bands on western blot of phosphoserine. It is most likely to be the proteins phosphorylated on serine. The results of western blot on the immunoprecipitation group showed several strong bands. It has no significant different between control and amiodarone-treated H4IIE cells. The band of 25 kDa is light chain of IgG and 50 kDa is heavy chain of IgG. The PBS negative control group also displayed the bands of 25 kDa and 50 kDa from the phosphoserine western blot result.

The results from figure5.8b showed the reciprocal immunoprecipitation of phosphoserine protein from H4IIE cells lysate followed western blot with Orai1 antibody from Almone. The western blot of Orai1 showed band at about 45 kDa at the input lysate which is glycosylated Orai1. Similarly, no significant difference is observed between control and amiodarone-treated H4IIE cells. The western blot of Orai1 on treat- and untreated group after immunoprecipitation with anti-phosphoserine antibody showed two strong bands at about 37kda and

50kda. In cells lysate incubated with PBS, it also had similar pattern with immunoprecipitation group. Two strong bands at the size of 37kDa and 50kDa were also detected at PBS negative control group. The band at 50kDa should be heavy chain IgG. As the PBS negative control group also present several bands that influence the interpretation of the results. Thus, it is difficult to determine whether phosphorylation occurred on Orai1 or not from the results.

(a)

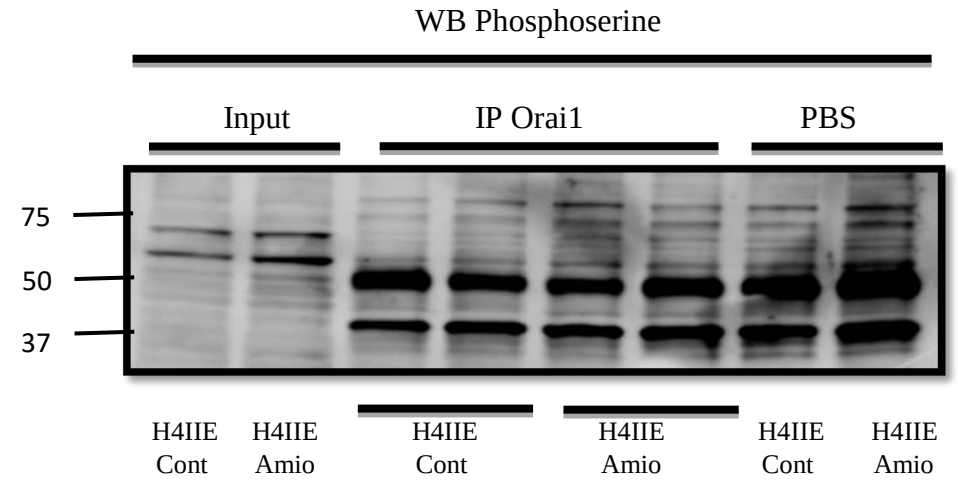
WB Phosphoserine
Input
IP Orai1
PBS
75
50
37
H4IIE Cont
H4IIE Amio
H4IIE Cont
H4IIE Amio
H4IIE Cont
H4IIE Amio

(b)

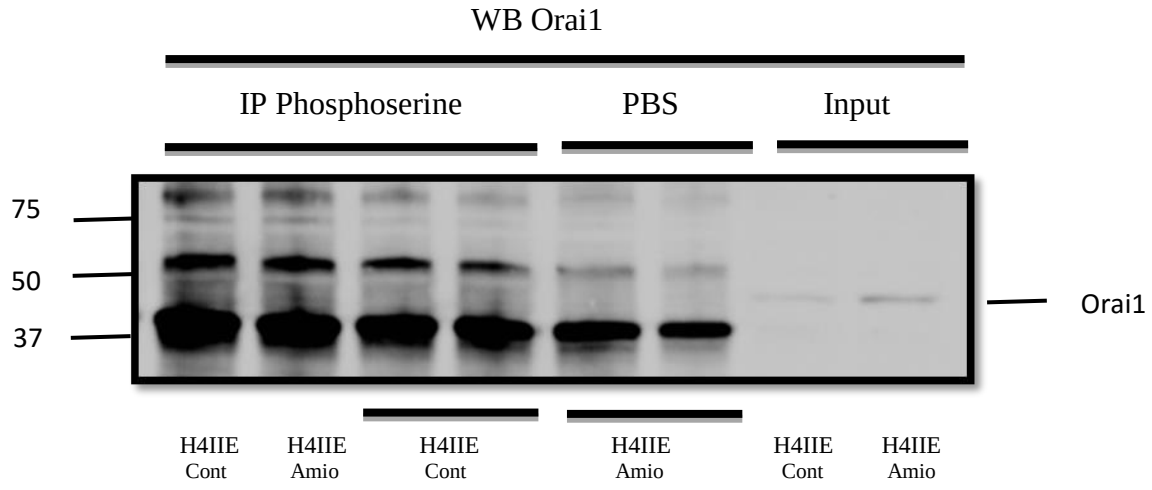
WB Orai1
IP Phosphoserine
PBS
Input
75
50
37
Orai1
H4IIE Cont
H4IIE Amio
H4IIE Cont
H4IIE Amio
H4IIE Cont
H4IIE Amio

**Fig 5.8 Proteins extracted from H4IIE cells subject to immunoprecipitation using anti-Orai1 antibody (Almone) or anti- phosphoserine antibody and subsequent western blot with anti-orai1 (Almone) or anti-phosphoserine antibody.**

(a) Orai1 protein was immunoprecipitated from control (cont) and amiodarone-treated (amio) H4IIE cell and western blot with phosphoserine antibody. In (b) protein phosphorylated on serine were immunoprecipitated from control and amiodarone-treated H4IIE cell and western blot with Orai1 antibody. Orai1 antibody from Alomone Labs (ACC062) was used in immunoprecipitation of Orai1 and western blot. The lysate from control and amiodarone-treated HII4E incubated with PBS were acted as negative control. The size of Orai1 are 37kda for unglycosylated Orai1 and 50kda for glycosylated Orai1. The bands of 50kda and 25kda are heavy and light IgG, respectively.

## 5.3 Discussion

In this chapter the aims are to investigate the role of phosphorylation on STIM1 and Orai1 in steatotic liver cells. I hypothesised that the development of hepatic steatotsis is related to the phosphorylation of STIM1 or Orai1. In order to explore the role of phosphorylation on STIM1 or Orai1 in steatotic cells, immunoprecipitation combined with western blot of phosphoserine were employed as strategy to detect the phosphorylation of STIM1 and Orai1 from steatotic liver cells.

In summary, the anti-STIM1 antibody is able to pull down STIM1 protein from the Zucher rat liver lysates. The phosphorylation of STIM1 cannot be detected by the western blot of phosphoserine after the immunoprecipitation of STIM1 from liver lysate. Two different Orai1 antibodies (from Alomone and Santa Cruz) were used to study the phosphorylation of Orai1 from steatotic liver cells. But the results were difficult to determine whether both the anti-Orai1 antibodies can immunoprecipitate the Orai1 protein from the liver lysate because the IgG negative control also displayed some bands to influence the results interpretation.

No phosphorylated protein were immunoprecipitated from the liver lysate by using anti-phosphoserine antibody. However, the negative result may be caused by the insufficient anti-phosphoserine antibody to pull down protein phosphorylated on serine for detection by western blot. Thus, in next experiment the concentration of anti-phosphoserine antibody need to be increased for the immunoprecipitating the phosphorylated protein on serine. Both PBS and normal IgG were used as negative control form IP experiment in this chapter, as I used

the methods in chapter 4 to set up the experiment, it is easy and quick to set up the IP experiment. However, I also need to use un-immunised normal IgG in IP experiment to exclude the effect of normal IgG from the same species of animal.

### 5.3.1 Phosphorylation of STIM1 from Steatotic cells detected by western blot of phosphoserine

STIM1 protein isolated from liver lysate is an essential step to further study the phosphorylation on STIM1. The capability of anti-STIM1 antibody in pulling down STIM1 protein from the steatotic liver lysate need to be confirmed before the detection of phosphorylation. Although it had been done from chapter 4, in order to avoid any conformation alteration happened on STIM1 protein during the development of steatosis, the conformation of the antibody in immunoprecipitation of STIM1 from Zucker rat liver lysate still need to be done. From our results, the anti-STIM1 antibody used in our experiment is able to immunoprecipitate STIM1 protein from Zucker rat liver lysate. Therefore, the STIM1 antibody used in our experiment is suitable for immunoprecipitation and western blot experiments.

After confirming the capability of STIM1 antibody in immunoprecipitation experiment, the phosphorylation of STIM1 was then examined by phosphoserine western blot on Zucker rat liver lysate and H4IIE cells lysate after immunoprecipitation of STIM1. The western blot of phosphoserine on immunoprecipitate of STIM1 protein showed that no phosphorylation was detected on serine on STIM1 protein from rat liver lysate and cell lysate.

5.3.2 Phosphorylation of Orai1 from steatotic liver

The capability of Orai1 antibody in immunoprecipitating Orai1 protein from the liver lysate was also tested by using same method in previous section. However, we cannot make a good conclusive comments from the results. It has some difficulties in determining the capability of Orai1 antibody in isolating Orai1 protein from the lysate by using immunoprecipitation. Due to the difficulty of using Orai1 antibody in immunoprecipitation, two different commercial Orai1 antibodies from Almone and Santa Cruz had been selected to test its potential use in immunoprecipitating Orai1 protein from liver lysate.

For Orai1 antibody from Almone, this Orai1 antibody seems to be able pulling down Orai1 protein from liver lysate. The immunoprecipitation group of Orai1 showed the same band as in input lysate at 37 kDa which should be unglycosylated Orai1. But the similar bands in the imuunoprecipitation group can also be detected at IgG negative control group. Then we cannot really determine the bands from immunoprecipitation group was Orai1 protein or other protein coimmunoprecipitated from the lysate.

As for the reason mentioned above, we then selected another Orai1 antibody from Santa Cruz which may be potentially immunoprecipitate Orai1 protein from liver lysate. Two bands, 37 KDa and 75 kDa, bands were observed at input lysate from the immunoblot when using Orai1 antibody from Santa Cruz. These two bands were also be detected at immunoprecipitation of Orai1 and only faint bands appeared at corresponding position at negative IgG control group. Thus, the result

seems showing that Orai1 antibody from Santa Cruz could pull down from the liver lysate.

Although the results are not conclusive from the immunoprecipitation of Orai1 and western blot of Orai1 using Alomone Orai1 antibody, it seems that the Alomone Orai1 antibody still could possibly immunoprecipitate Orai1 protein from liver lysate. Then I still tried to perform phosphoserine western blot followed by the immunoprecipitation of Orai1. When used Orai1 antibody from Alomone to immunoprecipitate the Orai1, the western blot of phosphoserine showed band at about 50kDa. However, the result could not be sure it was phosphorylated Orai1. From the result of western blot of Alomone Orai1 antibody on liver lysate, it only displayed unglycosylated form of Orai1 but it showed the bands at about 50kDa from western blot of phosphoserine after the immunoprecipitation of Orai1. Then the higher molecular weight of glycosylated Orai1 would not be the target by the Alomone Orai1 antibody to pull down Orai1 protein. The band could be heavy IgG instead of phosphorylated Orai1. The result of detecting Orai1 phosphorylation from lipid-loaded H4IIE cell also has problem in interpretation. It was observed multi-bands from immunoprecipitation group then we cannot determine which band is phosphorylated Orai1. To sum up, those results cannot show Orai1 is phosphorylated from our experiment and need more study.

5.3.3 Difficulty of using phosphoserine antibody to detect phosphorylation

Although the use of antibody to detect protein phosphorylation has its advantage over other method that no radioisotopes is needed in the detection. From our results in this chapter, it showed that no phosphorylation of STIM1 or Orai1 was detected by using anti-phosphoserine antibody. However, the results from our experiments still cannot exclude the possibility of phosphorylation on STIM1 and Orai1.

Various antibodies detected protein phosphorylated on serine, threonine and tyrosine are commercially available and widely used. However, the affinity and sensitivity of those anti-phosphoamino antibody are the major disadvantages of its usage in detecting phosphorylation site. In eukaryotic cell there are over 90 % of phosphorylation occurred at serine and threonine resident. It is less than 1% found at tyrosine (Hunter, 1998) . Although the higher percentage of phosphorylation is found on serine and threonine residents than on tyrosine, the development of anti-phosphotyrosine antibody is better than anti-phosphoserine/threonine antibody. The reason of the higher sensitivity of anti-phosphotyrosine antibody to anti-phosphoserine/threonine antibodies is that different anti-phosphotyrosine antibody raised from different nature of immunogens can bind to the same protein from western blotting. Secondly steric hindrance of the binding site is another issue in using anti-phosphoamino antibodies especially for anti-phosphoserine/threonine antibodies(Kaufmann et al., 2001).

Motif-specific phosphorylated antibodies that can detect the phosphorylation site on specific sequence is another type of antibodies developed to detect

phosphorylation. These antibodies are very useful tool in studying the signalling kinase related to the phosphorylation(White and Toker, 2001). However the Motif-specific phosphorylated antibodies need the precise sequence of phosphorylation site before the production of the antibodies (Zhang et al., 2002). Therefore, it needs time and afford to identify the precise sequence related to the phosphorylation in order to develop the antibodies. Thus, it only limited amount of motif-specific phosphorylated antibodies available.

In summary, the results from this chapter suggested the methods of immunoprecipitation combined with western blot could not display the phosphorylation on STIM1 on serine from both Zucker rat liver and lipid-load H4IIE cells line. For detecting Orai1 phosphorylation from steatotic liver cells, the Orai1 antibodies cannot show any good results in displaying the Orai1 antibodies could pull down the Orai1 protein. Thus, it cannot be drawn any conclusion from the results and we cannot determine is there any phosphorylation occurred on Orai1. Since there are some disadvantages on using phosphoserine antibody to detect phosphorylation as we discussed above. Therefore, other detection methods such as mass spectrometry may be good to use to detect phosphorylation.

# Chapter VI

# General Discussion

# Chapter VI General Discussion

## 6.1 Summary of the key findings

The key aim of this thesis is to detect the intracellular distribution of endogenous STIM1 and Orai1 from rat liver cells by using subcellular fractionation approach. The previous work from our laboratory showed that a small region of ER rather than the whole ER is thought to be an important region of ER for activating and regulating the function of SOCs and that region should be close to the plasma membrane (Gregory et al., 1999, Castro et al., 2009). By using electron microscopy, Orci and colleagues studied the ultrastructure of ER alongside with the location of STIM1. The results demonstrated that ER can be classified into precortical ER, cortical ER and thin cortical ER. Furthermore, they defined that when $Ca^{2+}$ store depleted, the precortical ER enriched with STIM1 move close to the plasma membrane to form cortical ER.(Orci et al., 2009) In another study, the evidence showed that the rough ER (RER) lose ribosome to form free ribosome RER at the junction of plasma membrane allowing STIM1 to transmit the signal to the plasma membrane in pancreatic acinar cells (Lur et al., 2009). From those results, it implied that STIM1 enriched in the region at cortical ER close to the plasma membrane and that region of ER devoid with the ribosome is an important region of ER for SOCs activation. It is possible that the location of that small region of ER may be located at smooth ER rather than rough ER.

Moreover, most of the results only can provide the evidence about the present of small region of ER in relation to SOCs activity. It is still no clear information about the location, the nature and the molecular compositions of that specific small region of ER. Therefore, the hypothesis is that the small region should be located at smooth ER than in rough ER as the absent of ribosome forming barrier between STIM1 and Orai1. The level of STIM1 or Orai1 should be higher in smooth ER than rough ER as the active small region is at smooth ER. In order to detect the intracellular distribution of STIM1 and Orai1 on a specific region of ER, the technique of subcellular fractionation was employed in this study to isolate rough ER (heavy microsome) and smooth ER (light microsome) from whole liver cells. The location of endogenous STIM1 and Orai1 on those subcellular fractions was detected by western blot. In addition, it also suggests that the region of ER close to plasma membrane is important for SOCs activation, so the plasma membrane fraction was also collected to observe the distribution of STIM1 and Orai1. As most of the studied about the localisation of STIM1 and Orai1 were from overexpressed tagged STIM1 and Orai1 (Prakriya et al., 2006, Ong et al., 2007b). Thus, the results from this study can also provide more information about is there any different between endogenous and exogenous STIM1 and Orai1 at subcellular level from rat liver.

The results from these studies showed that most of the STIM1 and Orai1 are found at heavy microsome, thus it is interesting that do STIM1 protein in heavy microsome require additional binding protein to assist the activation of SOCs. Several STIM1 binding proteins have been identified and reported. The cytoskeleton protein like EB1 can bind to STIM1 to assist the formation of ER-PM junction (Grigoriev et al., 2008). The $Ca^{2+}$ binding proteins like CRACR2A

can regulate the formation of the protein complex of STIM1 and Orai1 (Srikanth et al., 2010a). Ca $^{2+}$ ATPase also the membrane of STIM1 binding protein such as SERCA2. Its function is to assist the refill of the $Ca^{2+}$ store (Manjarrés et al., 2010). Thus, those results suggested that the activation of SOCs not only involves the interaction of STIM1 and Orai1 but also requires other associating proteins. In order to understand more about the protein profiling of STIM1 at the heavy microsome, the strategy of combining immunoprecipitation with western blot or LC/MS was used to identify novel STIM1 binding proteins. The results in chapter 4 showed that peroxiredoxin 4 (Prx4) is a potential STIM1-binding protein located at ER. These results also implicated that redox signalling should play a certain role in regulating the activity of SOCs.

Another major finding from our laboratory was observed the reduction of SOCs activity in steatotic liver and can be reversed by the protein kinase C inhibitor (Wilson et al., 2014). Thus, we assumed that phosphorylation of STIM1 or Orai1 should be involved in the development of hepatic steatosis. The phosphorylation of STIM1 and Orai1 were detected by using immunoprecipitation and western blot method.

In summary, the major findings of my work are summary as follows:

(1) Quantitative method in quantifying the amount of STIM1 and Orai1 on subcellular fractions by western blot was established.

(2) Endogenous STIM1 was mainly located at rough ER (85%) and smooth ER (12.5%). Small amount of STIM1 is found at the plasma membrane (0.09%).

(3) Endogenous Orai1 was found at rough ER (44%) and smooth ER (27%). Less amount was presented at the plasma membrane (0.03%).

(4) Peroxiredoxin 4 (Prx4) was showed to interact with STIM1 from rough ER.

## 6.2 A large proportion of STIM1 is located in the rough ER

In chapter 3, the results showed that a large amount of STIM1 proteins is mainly located at rough ER and less amount of STIM1 in smooth ER. In our hypothesis, STIM1 should mainly locate at smooth ER and less in rough ER. Large amount of STIM1 protein in smooth ER because STIM1 protein should bind easily to Orai1 on plasma membrane due to the absence of ribosome on smooth ER.

The structure of ER is a continuous membrane system that separate ER lumen and cytosol space. Although ER is a continuous structure, it can be identified into different subcompartment according to its morphology (Vertel et al., 1992). ER can be divided into rough ER and smooth ER. Rough ER is a continuous membrane structure bound with ribosomes. The rough ER membrane is mainly located around nucleus and extended from nuclear membrane. Smooth ER appears as a uniformly networking membrane system with a low density of ribosome (Voeltz et al., 2002). Mitochondria is distributed evenly among rough ER and smooth ER. Hepatocytes contain relatively high percentage of smooth ER. It is about 60% of smooth ER, 35% of rough ER and 5% Golgi body in hepatocytes (Sato, 2004). Thus, it cannot explain the unexpected distribution of STIM1 by the different size of the organelles as hepatocytes contain a higher

percentage of smooth ER. Therefore, it could be possible that the function of STIM1 in rough ER is different in smooth ER. It may suggest that a large amount of STIM1 protein in rough ER might act as a $Ca^{2+}$ sensor to detect the change of the $Ca^{2+}$ concentration and STIM1 in smooth ER might function as a transducer to transmit the signal from STIM1 to Orai1 to activate the $Ca^{2+}$ entry through SOCs.

Moreover, exogenous STIM1-tagged protein transfected cells is commonly used methods and materials to observe the distribution of STIM1 in the cells (Luik et al., 2006, Ong et al., 2007b). Thus, it is possible that the transfection of exogenous STIM1 to the cells would cause the change of the nature of cellular distribution of STIM1.

From chapter 1 table 1.1, it is a list of numerous proteins proposed as STIM1 binding partner discovered by other studied. Generally, the STIM1 binding proteins can be classified as four main types according to their function. The first types of binding protein are scaffold protein including actin, α-tubulin, and microtubule-plus-end-tracking protein (EB1). These STIM1 binding may be involved in the movement of STIM1 to the region that activate the $Ca^{2+}$ influx mediated SOCs. The second type is $Ca^{2+}$ channel and $Ca^{2+}$ ATPase like voltage-depend $Ca^{2+}$ channel and SERCA. These types of protein may be involved in regulating $Ca^{2+}$ influx or efflux. The third type is $Ca^{2+}$ binding protein including Calmodulin and calnexin. Those proteins may participate in the regulation of $Ca^{2+}$ affinity to STIM1 protein. The four type is miscellaneous like P-100. Therefore, the involvement of other associating protein with STIM1 at rough ER may have other reason why a large proportion of STIM1 in rough ER. It may form a protein complex retained at rough ER to produce its function.

## 6.3 A large proportion of Orai1 is located in the rough ER

The next experiment after the detection of STIM1 in subcellular fractions was to test the distribution of Orai1 on microsomal fractions and plasma membrane fraction. It has showed in another study that the location of Orai1 is at the plasma membrane and it is the major pore-forming molecule of SOCs. However, the results from the experiments provide interesting and contradicted results on the localisation of Orai1 at the subcellular fractions. The results indicated that most of the Orai1 was found at rough ER and smooth ER. Plasma membrane is presented less amount of Orai1.

There is some possible explanation of why a large amount of Orai1 presents at endoplasmic reticulum rather than in plasma membrane.

Firstly, the morphology of ER is in a dynamic state. The ER membrane can be rearranged by microtubulin-dependent dynamic processor to deform the membrane by some proteins (Pendin et al., 2011). For an instant, the structure of ER can be regulated by activation of Rab GTPase with Rab10 protein (English and Voeltz, 2013). When the cells receive stimuli, the structure of ER undergoes a drastic change. The proliferation of smooth ER was observed when hepatocytes treated with diethylinitrosamine and phenobarbitone to detoxify the drug (Jack et al., 1990). Under ER stress, the ER membrane structure undergo rapid reorganization and the reorganisation of this membrane is related to ion homeostasis of sodium and calcium ions (Varadarajan et al., 2013). Thus, the function of ER would depend on the rearrange the ER membrane structure. In another evidence, the formation of cortical ER (cER) enriched with STIM1 was found at the area close to the plasma membrane and this region is suggested to be

the hub for membrane protein trafficking (Orci et al., 2009, Fox et al., 2013). Thus, Orai1 could be clustered or relocated on ER membrane from the plasma membrane due to the process of ER reorganisation.

Protein trafficking is another reason why ER contains more Orai1. In cells, proteins are transported inside the cell to the target site in order to maintain its normal cellular function. Secretory pathway is a process to traffic the protein between ER and Golgi body. This secretory pathway requires the formation of vesicle containing the proteins that are needed to be transported. The vesicle budded out from the membrane of ER or Golgi complex to transport the protein. According to the protein composition, this vesicle-trafficking system can be divided into three types, Coated protein complex I (COPI), Coated protein complex II (COPII) and Clarthrin-coated vesicle (Lee and Goldberg, 2010). COPI- vesicle is responsible for retrograde transportation of protein from Golgi to ER. Lavier et al using yeast cells to express cortical ER –resident protein, Ist2P, on the mammalian cell to study the formation of cortical ER. The results showed that the formation of cortical ER is induced by COPI, trafficking microtubules and EB1 to cortical ER region (Lavieu et al., 2010). It also suggested that STIM1 has a similar action as Ist2P because STIM1 is recognised as EB1 protein. These results implicated that the cortical ER is the place for initial the retrograde trafficking. Therefore, the role of cortical ER in the regulation of SOCs is important. The cortical ER is not only involved the movement of STIM1 to the region inducing the $Ca^{2+}$ influx via SOCs but also regulate the amount of Orai1 expressed on the plasma membrane.

Secretory pathway $Ca^{2+}$ ATPase (SPCA) is an intracellular $Ca^{2+}$ ATPase which is found at the Golgi and post-Golgi vesicles to sequester $Ca^{2+}$ and $Mn^{2+}$ from the cytosol (Missiaen et al., 2007). The functions of SPCA include protein glycosylation, protein sorting and protein trafficking (Micaroni et al., 2010, Dürr et al., 1998). SPCAs have identified into two isoforms naming SPCA1 and SPCA2. SPCA1 is expressed ubiquitously in higher vertebrates(Missiaen et al., 2007). SPCA2 has limited expression than SPCA1, SPCA2 has detected on neural cell (Xiang et al., 2005) and epithelial cells (Vanoevelen et al., 2005). It has been showed that the trafficking of Orai1 is required the isoform of SPCA2 to transport to the plasma membrane. The binding of Orai1 and SPCA2 induce the $Ca^{2+}$ influx mediated store-independent $Ca^{2+}$ entry (Cross et al., 2013). Taken together, those results implicated that Orai1 should have intracellular function and the expression of Orai1 is tightly controlled by the secretory pathway (Figure 6.2).

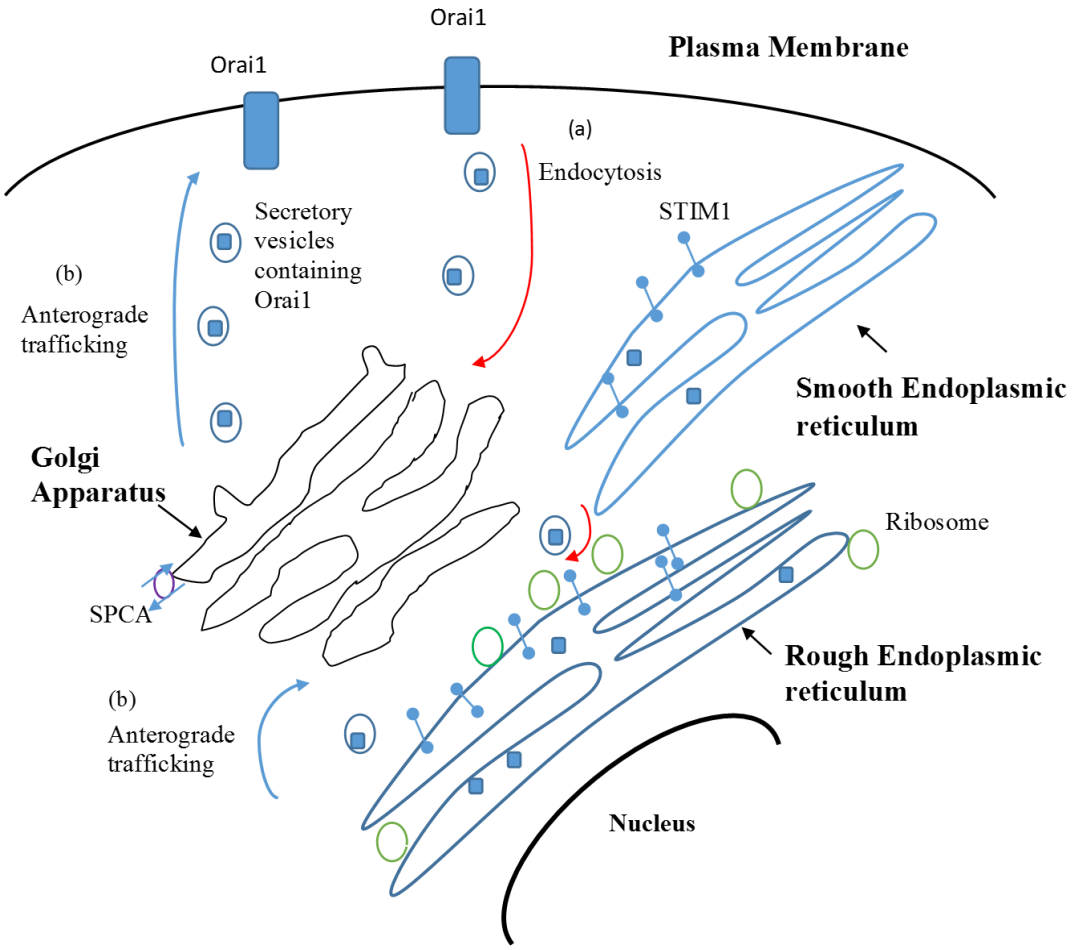


**Figure 6.1 A schematic representation of the distribution of STIM1 and Orai1 in liver cells.**

STIM1and Orai1 is mainly located rough ER and smooth ER. Orai1 protein may mediate two pathways to transport within the cells. **(a)** Endocytosis (red arrow): Orai1 protein on plasma membrane formed secretory vesicles(blue oval containing blue square). The secretory vesicle transport from plasma membrane to Golgi apparatus and then to the endoplasmic reticulum. **(b)** Anterograde trafficking (blue arrow): Orai1 protein budding from the endoplasmic reticulum and transport to Golgi apparatus and then to the plasma membrane. Secretory pathway $Ca^{2+}$ ATPase (SPCA) is located on Golgi apparatus to regulate the $Ca^{2+}$ concentration in the Golgi apparatus and assisted the secretory pathway.

TRPM2 channels is a known plasma membrane protein in liver cells (Kheradpezhouh et al., 2014). Then I used TRPM2 western blot as a model protein to demonstrate the plasma membrane protein transport system is working properly in rat liver. From the result, TRPM2 protein cannot be detected at heavy and light microsome by western blot. Thus, TRPM2 will be transported to the plasma membrane after synthesis. In addition to TRPM2, PMCA is another known plasma membrane protein and it only showed enrichment at plasma membrane fraction not heavy and light microsomes. Therefore, there is no problem in the protein transport system in liver cells. A large amount of Orai1 protein in ER would be mediated by another mechanism.

## 6.4 Preoxiderine 4 (Prx4) is a potential novel STIM1 binding partner

Searching for new STIM1 binding proteins is another main work of this thesis. The results from chapter 4 showed that Prx4 was identified as a new STIM1 binding protein by using the strategy of immunoprecipitation combined with western blot and LC/MS methods. It is interesting that Prx4 is identified as STIM1 binding partner because it may implicate that the redox signalling controlling by Prx4 in liver cells could play a role in STIM1 function.

Prx4 is mainly located at ER and is highly expressed at pancreas, liver and heart cells (Jin et al., 1997). It has demonstrated that Prx4 is a secretory protein and can be released from ER to cell surface under the control of detention mechanism (Okado-Matsumoto et al., 2000, Kakihana et al., 2013). The function of Prx 4 is to detoxify the oxidative stress in ER by oxidation of cysteine residue to reactive

sulfenic acid. The sulfenic then reacts with free thiol to form disulfide. In addition to detoxification of oxidative stress, Prx4 also associates with Ero1-α to facilitate the formation of disulfide bond on the protein to assist and control the oxidative protein folding (Tavender and Bulleid, 2010, Zhu et al., 2014). One of the functions of Prx4 is to control the protein folding in ER mediated oxidation (Zhu et al., 2014). Thus, the identification of the association between STIM1 and Prx4 implicates that Prx4 may be involved in the regulation of protein folding of STIM1 into correct conformation and regulate the function of STIM1 protein.

It has been showed that the $Ca^{2+}$ entry via SOCs is reduced by reactive oxide species (ROS) (Törnquist et al., 2000). The results from this thesis demonstrating Prx4 is STIM1 binding protein in ER region. These results can also provide further information about Prx4 may be one of the regulators in controlling the activity of SOCs. Thus, it suggests that Prx4 may regulate the conformation of STIM1 by mediating the formation of disulfide bond resulting in inference the exposure of the binding site of STIM1 to Orai1 (Figure 6.2).

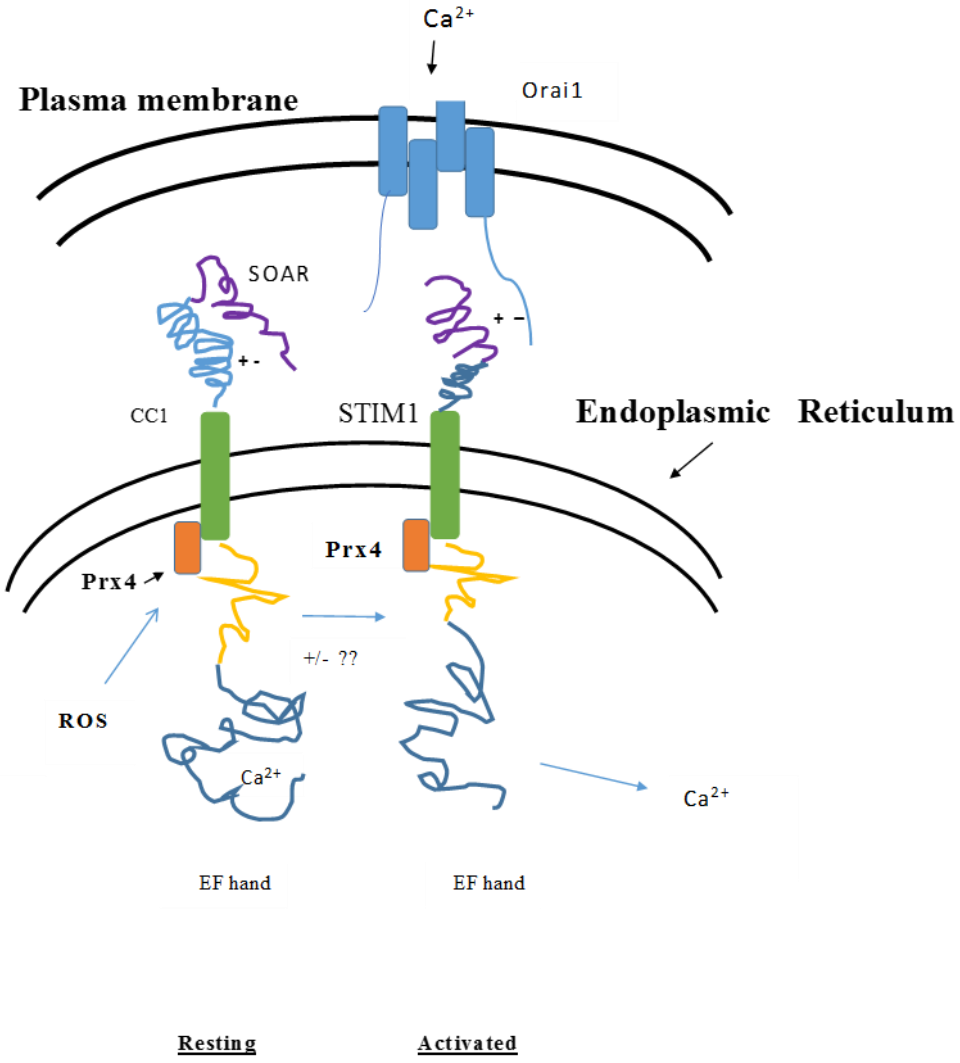


**Figure 6.2 A schematic representation of the possible role of peroxirderin 4 (Prx4) in regulating the activation of SOCs.**

The Prx4 is proposed as an STIM1 binding protein that associated with STIM1 at resting state. When the cells produce reactive oxygen species (ROS), it stimulate the function of Prx4 associated with STIM1, then the conformation of STIM1 is regulated by Prx4. The activity of SOCs is increased or decreased by the changes of the conformation induced by the activation of Prx4.

## 6.5 How the present results relate to recent advances in understanding the actions of Orai1 and STIM1 proteins

One of the main findings in these studies is that STIM1 and Orai1are mainly located at heavy microsome and light microsome, which are derived from rough ER and smooth ER, respectively. These are interesting results why large amount of Orai1 found at heavy and light microsomes but less at plasma membrane. As Orai1 should be similar to other plasma membrane protein like PMCA and TRPM2 that is transported to the plasma membrane after synthesis. Therefore, it suggested that there should present another system for transporting Orai1 to plasma membrane.

A small region of ER is known to be important for SOCs activation. This small region of ER related to SOCs activation should have its specific mechanism and different proteins composition for controlling the transportation of Orai1 to the plasma membrane. Therefore, it is important to identify the location and understand the nature of that small region so as to know more about the mechanism of SOCs activation. As mentioned before, cortical ER, the ER region devoid with ribosome, is enriched with STIM1 in the cell lines after $Ca^{2+}$ store depletion. It implicated that this region of ER absent with ribosome would be the location of that specific small region. Therefore, in order to study the region of ER without the attachment of ribosome, the technique of subcellular fractionation was employed in order to isolate and collect rough ER, smooth ER and plasma membrane from whole rat liver cells and detect the distribution of STIM1 and Orai1 from these subcellular fractions. Moreover, most of the results from other research studying the distribution of STIM1 and Orai1 were using molecular technique to transfect the cell lines with STIM1- or Orai1-tagged with GFP or

other fluorescence proteins. This is the first research trying to study the location and the protein profiling of that small region of ER and *in vivo*

Unlike other plasma membrane proteins which are expressed constitutively on plasma membrane, the expression of Orai1 on plasma membrane seems to be highly dynamic and inducible. Protein trafficking is one of the possible mechanism for controlling the distribution of Orai1. Orai1 trafficking has been discussed at *Xenopus* oocytes before. The results showed that Orai1 is internalised during meiosis and translocated to the plasma membrane after store depletion (Yu et al., 2010). Later, Orai1 trafficking was defined quantitatively by Hodeify et al, the results displayed that it is about 40% of Orai1 located on plasma membrane at resting state and recycling at a high rate between the plasma membrane and intracellular pool. This Orai1 recycling is regulated by STIM1-dependent manner to trap Orai1 in cortical ER and translocated to the plasma membrane when $Ca^{2+}$ store depleted (Hodeify et al., 2015). The movement of Orai1 could also associate with other factors. Evidence showing that STIM1L, the longer isoform of STIM1, is mediated the trapping of Oai1 without influencing the formation of cortical ER (Saüc et al., 2015).

It is interesting that the results from this thesis showed that it is only about 0.03% of Orai1 detected at the plasma membrane. The majority of Orai1 is found at heavy and light microsomes. From the hypothesis of these studied, smooth ER should be the major region for SOCs activation and it should contain higher level of STIM1 or Orai1. However, from the results, there is no significant difference of Orai1 between heavy and light microsomes. Thus, it seems that the small

region of ER for SOCs activation should be scattered over rough ER and smooth ER at resting state.

The use of subcellular fractions of whole rat live cells to detect the distribution of endogenous STIM1 and Orai1 could be the reason causing the difference from other studies. In most of the studies detecting the distribution of STIM1 or Orai1 were used cell lines transfected with exogenous GFP or other fluorescent dyes tagged- STIM1 or -Orai1 to observe the location of these two proteins. During the transfection of the cells with STIM1 or Orai1, it would influence the distribution pattern of STIM1 and Orai1 in the cell lines then in subcellular fractions of whole rat liver. Thus, the different of distribution pattern between endogenous and exogenous of STIM1 and Orai1 could be caused by the use of different methods and materials. Therefore, the results of the higher amount of intracellular Orai1 than in plasma membrane *in vivo* would implicate that the Orai1 trafficking mechanism *in vivo* is a complex process and it should involve various proteins or pathways.

The specific regions of ER - PM junctions are crucial for controlling $Ca^{2+}$ signalling mediated SOCs. It is known that the activation of SOCs requires the formation of STIM1-Orai1 microdomain (Hogan, 2015). The formation may involve the movement of ER mediated the protein complex called tip attachment complex (TAC) to reshape the ER by the movement of the tip at cytoskeleton. When $Ca^{2+}$ store depleted, it causes the relocation of STIM1 from tip attachment complex (TAC) to ER-PM junctions (Westrate et al., 2015). The intact ER-PM junctions from living cell were isolated by using non-disruptive biotin labelling approach on the cell lines and was studied the proteomic mapping of that

junctions followed by LC/MS. The results discovered the ER-resident protein called STIM-activating enhancer (STIMATE) as positive regulator binds with STIM1 to regulate the $Ca^{2+}$ influx (Jing et al., 2015). It is similar to the research from this thesis that both of the studies were exploring the protein profiling at the specific regions of ER, which may relate to the activity of SOCs. However, they are still not able to detect Prx4 as STIM1 binding protein from their results. The reason may be they were using transfected cells to isolate and study the proteomic mapping of ER-PM junctions. Rough and smooth ER isolated by subcellular fractionation of whole rat liver were used in this research to study the protein profiling. The experimental environment of cell lines is different from whole liver cells. It would lose some proteins or molecules during the isolation and transfection. Then it finally would cause the difference of the protein profiling between transfected cells and whole liver cells.

## 6.6 Future Experiment

### 6.5.1 Identification the role of protein trafficking in the distribution of Orai1

As showed in my results, I have indicated that ER contains a large amount of Orai1 and not much is found on the plasma membrane in liver cells. It is becoming interesting and important that what mechanism causes the unexpected Orai1 distribution at the subcellular level. The vesicle-trafficking system is one of the potential mechanism that could explain the usual Orai1 distribution. As mention before, there are present three types of vesicles in the trafficking system. COPI –vesicle or SPCA are considered as a potential candidate in explaining Orai1 distribution from our results because evidence showed the cortical ER

composed with COPI protein and this region is also enriched with STIM1 protein. Then I thought COPI protein would involve in the protein movement in this region. SPCA is another potential molecules involved in transporting Orai1 as evidence has shown Orai1 bind with SPCA. Therefore, in future we have to identify is there any role playing by COPI or SPCA in trafficking Orai1 leading more Orai1 located in ER.

Thus in future experiment, COPI or SPCA could act as secretory granules maker proteins and then determining the distribution of COP1 or SPCA on the subcellular fractions by using western blot. This result would provide the general idea of how the secretory pathway happened among subcellular fractions.

In addition, the previous results from our laboratory were used hepatocytes and H4IIE cells to identify the location of STIM1. However, one of the disadvantages of using hepatocyte and cell lines is the loss of polarity of the cells. It would influence the detection of the distribution as the molecules loss the orientation inside the cells. As for this reasons, using rat liver slices for detection the distribution would be better that hepatocytes and cell lines. Then, using rat liver slices to detect the distribution of Orai1, COPI or SPCA by immunofluorescence is another good evidence for showing the relationship of the secretory pathway and Orai1 by the overlap of the signal.

In addition, we also can detect the interaction between COPI or SPCA and Orai1 by using immunoprecipitation. This result could suggest the requirement of COPI or SPCA in transport Orai1 and also provide the information about these proteins are located at the same site of the cells.

### 6.5.2 The relationship of SOCs and Prx4

Another interesting results from this study is that Prx4 is recognised as a new STIM1 binding protein. This result implicated the potential role of redox signalling pathway may be involved in protein folding of STIM1 or Orai1 and regulated the secretion of the proteins.

In order to understand more about the role of Prx4 in controlling the trafficking pathway, in the next experiment, we could further detect the distribution of STIM1, Orai1 and Prx4 in liver cells by using immunofluorescence method. It is known that a small region of ER is important for the function of SOCs, the western blot of Prx4 on subcellular fraction could be an useful information to understand the signal pathway. As it is still no clear information about the relationship between Prx4 and the function of SOCs, thus it is good to establish the relationship of SOCs and Prx4. To achieve this goal, it can be done by silencing the Prx 4 genes and measure the $Ca^{2+}$ entry by using add-back protocol. In that protocol, the $Ca^{2+}$ concentration of the Prx4 knockdown cells is firstly measured under $Ca^{2+}$ free medium when $Ca^{2+}$ store depleted. The increase of $Ca^{2+}$ via SOCs is measured by replacing $Ca^{2+}$ free medium with medium containing $Ca^{2+}$.

In future, we have to test different condition for immunoprecipitation of STIM1 in order to identify more STIM1 binding proteins. As different types and concentration of detergents should be influence the protein-protein interaction. This is one of the reasons may be why we cannot detect some reported STIM1 binding protein. The phenylephrine-treated liver sample may also need to be

tested in order to determine whether the binding occurred after $Ca^{2+}$ store depletion.

6.5.3 Phosphorylation of STIM1 and Orai1

The use of antibody to detect the phosphorylation is a useful tool to detect the phosphorylation. However, the success of the phosphorylation detection depends on the sensitivity of the antibody detecting the site of the phosphorylation. Thus, it is difficult to say that there is no phosphorylation on STIM1 or Orai1. It may be due to the antibody could not bind to the binding site. As for the reason, the alternative methods for detecting phosphorylation is to incubate of $P^{32}$ phosphate isotope with lipid-loaded H4IIE cells and then detect the radioactivity by running HPLC. If phosphorylation of STIM1 or Orai1 occurs during the development of steatosis, then the $P^{32}$ should be inserted into STIM1 and Orai1 protein.

If we can obtain good Orai1 antibody for immunoprecipitation Orai1 protein from the lysate then using LC/MS instead of the western blot to detect the phosphorylation is one of the possible.

## References


ABDEL-MISIH, S. R. & BLOOMSTON, M. 2010. Liver anatomy. *The Surgical clinics of North America,* 90**,** 643-53.

ABDULLAEV, I. F., BISAILLON, J. M., POTIER, M., GONZALEZ, J. C., MOTIANI, R. K. & TREBAK, M. 2008. Stim1 and Orai1 Mediate CRAC Currents and Store-Operated Calcium Entry Important for Endothelial Cell Proliferation. *Circulation Research* 103**,** 1289-1299.

AGNEW, B. J., MURRAY, D. & PATTON, W. F. 2004. A rapid solid-phase fluorescence-based protein assay for quantitation of protein electrophoresis samples containing detergents, chaotropes, dyes, and reducing agents. *Electrophoresis,* 25**,** 2478-2485.

AMAYA, M. J. & NATHANSON, M. H. 2013. Calcium Signaling in the Liver. *Comprehensive Physiology.* John Wiley & Sons, Inc.

ARGENT, N. B., LILES, J., RODHAM, D., CLAYTON, C. B., WILKINSON, R. & BAYLIS, P. H. 1994. A new method for measuring the blood volume of the rat using 113mIndium as a tracer. *Labratory Animals,* 28**,** 172-5.

AROMATARIS, E. C., CASTRO, J., RYCHKOV, G. Y. & BARRITT, G. J. 2008. Store-operated $Ca^{2+}$ channels and Stromal Interaction Molecule 1 (STIM1) are targets for the actions of bile acids on liver cells. *Biochimica et Biophysica Acta - Molecular Cell Research,* 1783**,** 874-885.

BABA, Y., HAYASHI, K., FUJII, Y., MIZUSHIMA, A., WATARAI, H., WAKAMORI, M., NUMAGA, T., MORI, Y., IINO, M., HIKIDA, M. & KUROSAKI, T. 2006. Coupling of STIM1 to store-operated $Ca^{2+}$ entry through its constitutive and inducible movement in the endoplasmic reticulum. *Proceedings of the National Academy of Sciences,* 103**,** 16704-16709.

BAFFY, G. 2009. Kupffer cells in Non-Alcoholic Fatty Liver Disease: The emerging view. *Journal of hepatology,* 51**,** 212-223.

BAKOWSKI, D. & PAREKH, A. 2002. Monovalent cation permeability and $Ca^{2+}$ block of the store-operated $Ca^{2+}$ current $I_{CRAC}$ in rat basophilic leukemia cells. *Pflügers Archiv European Journal of Physiology,* 443**,** 892-902.

BARRITT, G. J., CHEN, J. & RYCHKOV, G. Y. 2008. $Ca^{2+}$ -permeable channels in the hepatocyte plasma membrane and their roles in hepatocyte physiology. *Biochimica et Biophysica Acta (BBA) - Biomembranes,* 1783**,** 651-72.

BAUER, M. C., O'CONNELL, D., CAHILL, D. J. & LINSE, S. 2008. Calmodulin Binding to the Polybasic C-Termini of STIM Proteins Involved in Store-Operated Calcium Entry†. *Biochemistry,* 47**,** 6089-6091.

BEAR, C. E. 1990. A nonselective cation channel in rat liver cells is activated by membrane stretch. *The American journal of physiology,* 258**,** C421-8.

BERNA-ERRO, A., WOODARD, G. E. & ROSADO, J. A. 2012. Orais and STIMs: physiological mechanisms and disease. *Journal of cellular and molecular medicine,* 16**,** 407-24.

BLOUIN, A., BOLENDER, R. P. & WEIBEL, E. R. 1977. Distribution of organelles and membranes between hepatocytes and nonhepatocytes in the rat liver parenchyma. A stereological study. *The Journal of Cell Biology,* 72**,** 441-455.

BONIFACINO, J. S., DELL'ANGELICA, E. C. & SPRINGER, T. A. 2001. Immunoprecipitation. *Current protocols in immunology,* Chapter 8**,** Unit 8.3.

BOUWENS, L., BAEKELAND, M., DE ZANGER, R. & WISSE, E. 1986. Quantitation, tissue distribution and proliferation kinetics of Kupffer cells in normal rat liver. *Hepatology,* 6**,** 718-22.

BRANDMAN, O., LIOU, J., PARK, W. S. & MEYER, T. 2007. STIM2 Is a Feedback Regulator that Stabilizes Basal Cytosolic and Endoplasmic Reticulum $Ca^{2+}$ Levels. *Cell,* 131**,** 1327-1339.

BRAUN, F.-J., BROAD, L. M., ARMSTRONG, D. L. & PUTNEY, J. W. 2001. Stable Activation of Single $Ca^{2+}$ Release-activated $Ca^{2+}$ Channels in Divalent Cation-free Solutions. *The Journal of Biological Chemistry,* 276**,** 1063-1070.

BROAD, L. M., ARMSTRONG, D. L. & PUTNEY, J. W. 1999. Role of the Inositol 1,4,5-Trisphosphate Receptor in $Ca^{2+}$ Feedback Inhibition of Calcium Release-activated Calcium Current ($I_{crac}$). *The Journal of Biological Chemistry,* 274**,** 32881-32888.

BURK, S. E., LYTTON, J., MACLENNAN, D. H. & SHULL, G. E. 1989. cDNA cloning, functional expression, and mRNA tissue distribution of a third organellar $Ca^{2+}$ pump. *The Journal of biological chemistry,* 264**,** 18561-8.

CALLOWAY, N., HOLOWKA, D. & BAIRD, B. 2010. A Basic Sequence in STIM1 Promotes $Ca^{2+}$ Influx by Interacting with the C-Terminal Acidic Coiled Coil of Orai1. *Biochemistry,* 49**,** 1067-1071.

CAO, Z., TAVENDER, T. J., ROSZAK, A. W., COGDELL, R. J. & BULLEID, N. J. 2011. Crystal Structure of Reduced and of Oxidized Peroxiredoxin IV Enzyme Reveals a Stable Oxidized Decamer and a Non-disulfide-bonded Intermediate in the Catalytic Cycle. *The Journal of Biological Chemistry,* 286**,** 42257-42266.

CARAFOLI, E. & BRINI, M. 2000. Calcium pumps: structural basis for and mechanism of calcium transmembrane transport. *Current Opinion in Chemical Biology,* 4**,** 152-161.

CASTRO, J., AROMATARIS, E. C., RYCHKOV, G. Y. & BARRITT, G. J. 2009. A small component of the endoplasmic reticulum is required for store-operated $Ca^{2+}$ channel activation in liver cells: evidence from studies using TRPV1 and taurodeoxycholic acid. *Biochemical Journal,* 418**,** 553-566.

CHANG, W.-C., DI CAPITE, J., SINGARAVELU, K., NELSON, C., HALSE, V. & PAREKH, A. B. 2008. Local $Ca^{2+}$ Influx through $Ca^{2+}$ Release-activated $Ca^{2+}$ (CRAC) Channels Stimulates Production of an Intracellular Messenger and an Intercellular Pro-inflammatory Signal. *Journal of Biological Chemistry,* 283**,** 4622-4631.

CONLON, F., MITEVA, Y., KALTENBRUN, E., WALDRON, L., GRECO, T. & CRISTEA, I. 2012. Immunoisolation of Protein Complexes from *Xenopus*. *In:* HOPPLER, S. & VIZE, P. D. (eds.) *Xenopus Protocols.* Humana Press.

COVINGTON, E. D., WU, M. M. & LEWIS, R. S. 2010. Essential Role for the CRAC Activation Domain in Store-dependent Oligomerization of STIM1. *Molecular Biology of Cell,* 21**,** 1897-1907.

CROFTS, J. N. & BARRITT, G. J. 1990. The liver cell plasma membrane $Ca^{2+}$ inflow systems exhibit a broad specificity for divalent metal ions. *Biochemical Journal,* 269**,** 579-587.

CROSS, B. M., HACK, A., REINHARDT, T. A. & RAO, R. 2013. SPCA2 Regulates Orai1 Trafficking and Store Independent $Ca^{2+}$ Entry in a Model of Lactation. *PLoS ONE,* 8**,** e67348.

DALLNER, G. & ERNSTER, L. 1968. Subfractionation and composition of microsomal membranes: a review. *The Journal of Histochemistry and Cytochemistry,* 16**,** 611-32.

DARBELLAY, B., ARNAUDEAU, S., KÖNIG, S., JOUSSET, H., BADER, C., DEMAUREX, N. & BERNHEIM, L. 2009. STIM1- and Orai1-dependent Store-operated Calcium Entry Regulates Human Myoblast Differentiation. *Journal of Biological Chemistry,* 284**,** 5370-5380.

DASSO, L. L. & TAYLOR, C. W. 1992. Different calcium-mobilizing receptors share the same guanine nucleotide-binding protein pool in hepatocytes. *Molecular Pharmacology,* 42**,** 453-457.

DE TALAMONI, N., SMITH, C. A., WASSERMAN, R. H., BELTRAMINO, C., FULLMER, C. S. & PENNISTON, J. T. 1993. Immunocytochemical localization of the plasma membrane calcium pump, calbindin-D28k, and parvalbumin in Purkinje cells of avian and mammalian cerebellum. *Proceedings of the National Academy of Sciences,* 90**,** 11949-11953.

DEHAVEN, W. I., SMYTH, J. T., BOYLES, R. R. & PUTNEY, J. W. 2007. Calcium Inhibition and Calcium Potentiation of Orai1, Orai2, and Orai3 Calcium Release-activated Calcium Channels. *The Journal of Biological Chemistry,* 282**,** 17548-17556.

DICKSON, E. J., DUMAN, J. G., MOODY, M. W., CHEN, L. & HILLE, B. 2012. Orai-STIM-mediated $Ca^{2+}$ release from secretory granules revealed by a targeted $Ca^{2+}$ and pH probe. *Proceedings of the National Academy of Sciences of the United States of America,* 109**,** E3539-48.

DONATO, M. T., MARTÍNEZ-ROMERO, A., JIMÉNEZ, N., NEGRO, A., HERRERA, G., CASTELL, J. V., O'CONNOR, J.-E. & GÓMEZ-LECHÓN, M. J. 2009. Cytometric analysis for drug-induced steatosis in HepG2 cells. *Chemico-Biological Interactions,* 181**,** 417-423.

DÜRR, G., STRAYLE, J., PLEMPER, R., ELBS, S., KLEE, S. K., CATTY, P., WOLF, D. H. & RUDOLPH, H. K. 1998. The *medial*-Golgi Ion Pump Pmr1 Supplies the Yeast Secretory Pathway with $Ca^{2+}$ and $Mn^{2+}$ Required for Glycosylation, Sorting, and Endoplasmic Reticulum-Associated Protein Degradation. *Molecular Biology of the Cell,* 9**,** 1149-1162.

DZIADEK, M. A. & JOHNSTONE, L. S. 2007. Biochemical properties and cellular localisation of STIM proteins. *Cell Calcium,* 42**,** 123-132.

EDWARDS, J. N., FRIEDRICH, O., CULLY, T. R., VON WEGNER, F., MURPHY, R. M. & LAUNIKONIS, B. S. 2010. Upregulation of store-operated $Ca^{2+}$ entry in dystrophic mdx mouse muscle. *American journal of physiology. Cell physiology,* 299**,** C42-50.

EL BOUSTANY, C., KATSOGIANNOU, M., DELCOURT, P., DEWAILLY, E., PREVARSKAYA, N., BOROWIEC, A.-S. & CAPIOD, T. 2010. Differential roles of STIM1, STIM2 and Orai1 in the control of cell proliferation and SOCE amplitude in HEK293 cells. *Cell Calcium,* 47**,** 350-359.

ELION, E. A. 2001. Detection of Protein-Protein Interactions by Coprecipitation. *Current Protocols in Immunology.* John Wiley & Sons, Inc.

ENG, J. K., MCCORMACK, A. L. & YATES, J. R. 1994. An approach to correlate tandem mass spectral data of peptides with amino acid sequences in a protein database. *Journal of the American Society for Mass Spectrometry,* 5**,** 976-89.

ENGLISH, A. R. & VOELTZ, G. K. 2013. Rab10 GTPase regulates ER dynamics and morphology. *Nature cell biology,* 15**,** 169-178.

FAHRNER, M., MUIK, M., SCHINDL, R., BUTORAC, C., STATHOPULOS, P., ZHENG, L., JARDIN, I., IKURA, M. & ROMANIN, C. 2014. A Coiled-coil Clamp Controls Both Conformation and Clustering of Stromal Interaction Molecule 1 (STIM1). *The Journal of Biological Chemistry,* 289**,** 33231-33244.

FERNANDO, K. C. & BARRITT, G. J. 1994. Characterisation of the inhibition of the hepatocyte receptor-activated $Ca^{2+}$ inflow system by gadolinium and SK&F 96365. *Biochimica et Biophysica Acta - Molecular Cell Research,* 1222**,** 383-389.

FIERRO, L. & PAREKH, A. B. 1999. On the characterisation of the mechanism underlying passive activation of the $Ca^{2+}$ release-activated $Ca^{2+}$ current $I_{CRAC}$ in rat basophilic leukaemia cells. *The Journal of Physiology,* 520**,** 407-416.

FORCHERON, F., ABDALLAH, P., BASSET, A., DEL CARMINE, P., HAFFAR, G. & BEYLOT, M. 2009. Nonalcoholic Hepatic Steatosis in Zucker Diabetic Rats: Spontaneous Evolution and Effects of Metformin and Fenofibrate. *Obesity,* 17**,** 1381-1389.

FOX, P. D., HABERKORN, C. J., WEIGEL, A. V., HIGGINS, J. L., AKIN, E. J., KENNEDY, M. J., KRAPF, D. & TAMKUN, M. M. 2013. Plasma membrane domains enriched in cortical endoplasmic reticulum function as membrane protein trafficking hubs. *Molecular Biology of the Cell,* 24**,** 2703-2713.

FUKUSHIMA, M., TOMITA, T., JANOSHAZI, A. & PUTNEY, J. W. 2012. Alternative translation initiation gives rise to two isoforms of Orai1 with distinct plasma membrane mobilities. *Journal of Cell Science,* 125**,** 4354-4361.

GALIANO, M., GASPARRE, G., LIPPE, C. & CASSANO, G. 2004. Calcium response after stimulation by substance P of U373 MG cells: inhibition of store-operated calcium entry by protein kinase C. *Cell Calcium,* 35**,** 123-30.

GAO, Y.-D., HANLEY, P. J., RINNÉ, S., ZUZARTE, M. & DAUT, J. 2010. Calcium-activated K+ channel ($K_{Ca}3.1$) activity during $Ca^{2+}$ store depletion and store-operated $Ca^{2+}$ entry in human macrophages. *Cell Calcium,* 48**,** 19-27.

GARCIA-ARCOS, I., RUEDA, Y., GONZÁLEZ-KOTHER, P., PALACIOS, L., OCHOA, B. & FRESNEDO, O. 2010. Association of SND1 protein to low density lipid droplets in liver steatosis. *Journal of Physiology and Biochemistry,* 66**,** 73-83.

GARDAI, S. J., MCPHILLIPS, K. A., FRASCH, S. C., JANSSEN, W. J., STAREFELDT, A., MURPHY-ULLRICH, J. E., BRATTON, D. L., OLDENBORG, P.-A., MICHALAK, M. & HENSON, P. M. 2005. Cell-Surface Calreticulin Initiates Clearance of Viable or Apoptotic Cells through trans-Activation of LRP on the Phagocyte. *Cell,* 123**,** 321-334.

GARY, S. B., OMAR, A., JEAN-PHILIPPE, L., BARBARA, J. W., MOHAMED, T., GUILLERMO, V. & JAMES, W. P., JR. 2004. Mechanisms of Phospholipase C-Regulated Calcium Entry. *Current Molecular Medicine,* 4**,** 291-301.

GEERTS, A. 2001. History, heterogeneity, developmental biology, and functions of quiescent hepatic stellate cells. *Semin Liver Dis,* 21**,** 311-35.

GIACHINI, F. R. C., CHIAO, C.-W., CARNEIRO, F. S., LIMA, V. V., CARNEIRO, Z. N., DORRANCE, A. M., TOSTES, R. C. & WEBB, R. C. 2009. CHBPR: Increased activation of STIM-1/Orai-1 in aorta from hypertensive rats: a novel insight into vascular dysfunction. *Hypertension,* 53**,** 409-416.

GLITSCH, M. D. & PAREKH, A. B. 2000. $Ca^{2+}$ store dynamics determines the pattern of activation of the store-operated $Ca^{2+}$ current $I_{CRAC}$ in response to Ins$P_3$ in rat basophilic leukaemia cells. *The Journal of physiology,* 523 Pt 2**,** 283-90.

GONZÁLEZ NARVÁEZ, A. & CASTILLO, A. 2007. $Ca^{2+}$store determines gating of store operated calcium entry in mammalian skeletal muscle. *Journal of Muscle Research and Cell Motility,* 28**,** 105-113.

GREGORY, R. B. & BARRITT, G. J. 2003. Evidence that $Ca^{2+}$-release-activated $Ca^{2+}$ channels in rat hepatocytes are required for the maintenance of hormone-induced $Ca^{2+}$ oscillations. *The Biochemical journal,* 370**,** 695-702.

GREGORY, R. B., HUGHES, R., RILEY, A. M., POTTER, BARRY V L., WILCOX, R. A. & BARRITT, G. J. 2004. Inositol trisphosphate analogues selective for types I and II inositol trisphosphate receptors exert differential effects on vasopressin-stimulated $Ca^{2+}$ inflow and $Ca^{2+}$ release from intracellular stores in rat hepatocytes. *The Biochemical Journal,* 381**,** 519-526.

GREGORY, R. B., SYKIOTIS, D. & BARRITT, G. J. 2003. Evidence that store-operated $Ca^{2+}$ channels are more effective than intracellular messenger-activated non-selective cation channels in refilling rat hepatocyte intracellular $Ca^{2+}$ stores. *Cell Calcium,* 34**,** 241-51.

GREGORY, R. B., WILCOX, R. A., BERVEN, L. A., VAN STRATEN, N. C., VAN DER MAREL, G. A., VAN BOOM, J. H. & BARRITT, G. J. 1999. Evidence for the involvement of a small subregion of the endoplasmic reticulum in the inositol trisphosphate receptor-induced activation of $Ca^{2+}$ inflow in rat hepatocytes. *The Biochemical Journal,* 341**,** 401-408.

GRESSET, A., SONDEK, J. & HARDEN, T. K. 2012. The Phospholipase C Isozymes and Their Regulation. *In:* BALLA, T., WYMANN, M. & YORK, J. D. (eds.) *Phosphoinositides I: Enzymes of Synthesis and Degradation.* Springer Netherlands.

GRIGORIEV, I., GOUVEIA, S. M., VAN DER VAART, B., DEMMERS, J., SMYTH, J. T., HONNAPPA, S., SPLINTER, D., STEINMETZ, M. O., PUTNEY, J. W., JR., HOOGENRAAD, C. C. & AKHMANOVA, A. 2008. STIM1 is a MT-plus-end-tracking protein involved in remodeling of the ER. *Current Biology,* 18**,** 177-82.

GUIHARD, G., NOEL, J. & CAPIOD, T. 2000. $Ca^{2+}$ Depletion and Inositol 1,4,5-Trisphosphate-evoked Activation of $Ca^{2+}$ Entry in Single Guinea Pig Hepatocyte. *The Journal of Biological Chemistry,* 275**,** 13411-13414.

GUILLEMETTE, G., BALLA, T., BAUKAL, A. J. & CATT, K. J. 1988. Characterization of inositol 1,4,5-trisphosphate receptors and calcium mobilization in a hepatic plasma membrane fraction. *The Journal of Biological Chemistry,* 263**,** 4541-4548.

GUSEV, K., GLOUCHANKOVA, L., ZUBOV, A., KAZNACHEYEVA, E., WANG, Z., BEZPROZVANNY, I. & MOZHAYEVA, G. N. 2003. The store-operated calcium entry pathways in human carcinoma A431 cells: functional properties and activation mechanisms. *The Journal of general physiology,* 122**,** 81-94.

GUZMAN, R., VALENTE, E. G., PRETORIUS, J., PACHECO, E., QI, M., BENNETT, B. D., FONG, D. H., LIN, F.-F., BI, V. & MCBRIDE, H. J. 2014. Expression of ORAI1, a Plasma Membrane Resident Subunit of the CRAC Channel, in Rodent and Non-rodent Species. *Journal of Histochemistry & Cytochemistry*.

GWACK, Y., SRIKANTH, S., FESKE, S., CRUZ-GUILLOTY, F., OH-HORA, M., NEEMS, D. S., HOGAN, P. G. & RAO, A. 2007. Biochemical and Functional Characterization of Orai Proteins. *The Journal of Biological Chemistry,* 282**,** 16232-16243.

HAJKOVA, Z., BUGAJEV, V., DRABEROVA, E., VINOPAL, S., DRABEROVA, L., JANACEK, J., DRABER, P. & DRABER, P. 2011. STIM1-directed reorganization of microtubules in activated mast cells. *The Journal of Immunology,* 186**,** 913-23.

HARLOW, E. & LANE, D. 2006. Lysing Tissue-Culture Cells for Immunoprecipitation. *Cold Spring Harbor Protocols,* 2006**,** pdb.prot4531.

HEALEY, J. E., JR & SCHROY, P. C. 1953. Anatomy of the biliary ducts within the human liver: Analysis of the prevailing pattern of branchings and the major variations of the biliary ducts. *A.M.A. Archives of Surgery,* 66**,** 599-616.

HERNANDEZ, E., FATIMA LEITE, M., GUERRA, M. T., KRUGLOV, E. A., BRUNA-ROMERO, O., RODRIGUES, M. A., GOMES, D. A., GIORDANO, F. J., DRANOFF, J. A. & NATHANSON, M. H. 2007. The Spatial Distribution of Inositol 1,4,5-

Trisphosphate Receptor Isoforms Shapes $Ca^{2+}$Waves. *The Journal of biological chemistry,* 282**,** 10057-10067.

HILFIKER, H., GUERINI, D. & CARAFOLI, E. 1994. Cloning and expression of isoform 2 of the human plasma membrane Ca2+ ATPase. Functional properties of the enzyme and its splicing products. *Journal of Biological Chemistry,* 269**,** 26178-26183.

HIRATA, K., PUSL, T., O'NEILL, A. F., DRANOFF, J. A. & NATHANSON, M. H. 2002. The type II inositol 1,4,5-trisphosphate receptor can trigger $Ca^{2+}$ waves in rat hepatocytes. *Gastroenterology,* 122**,** 1088-1100.

HJORTSJO, C. H. 1951. The topography of the intrahepatic duct systems. *Acta Anat (Basel),* 11**,** 599-615.

HODEIFY, R., SELVARAJ, S., WEN, J., ARREDOUANI, A., HUBRACK, S., DIB, M., AL-THANI, S. N., MCGRAW, T. & MACHACA, K. 2015. A STIM1-dependent 'trafficking trap' mechanism regulates Orai1 plasma membrane residence and $Ca^{2+}$ influx levels. *Journal of Cell Science,* 128**,** 3143-3154.

HODGE, K., HAVE, S. T., HUTTON, L. & LAMOND, A. I. 2013. Cleaning up the masses: Exclusion lists to reduce contamination with HPLC-MS/MS. *Journal of Proteomics,* 88**,** 92-103.

HOFER, A. M., FASOLATO, C. & POZZAN, T. 1998. Capacitative $Ca^{2+}$ Entry Is Closely Linked to the Filling State of Internal $Ca^{2+}$ Stores: A Study Using Simultaneous Measurements of $I_{CRAC}$ and Intraluminal [$Ca^{2+}$]. *The Journal of Cell Biology,* 140**,** 325-334.

HOGAN, P. G. 2015. The STIM1–ORAI1 microdomain. *Cell Calcium,* 58**,** 357-367.

HOTH, M., FANGER, C. M. & LEWIS, R. S. 1997. Mitochondrial Regulation of Store-operated Calcium Signaling in T Lymphocytes. *The Journal of Cell Biology,* 137**,** 633-648.

HOTH, M. & PENNER, R. 1992. Depletion of intracellular calcium stores activates a calcium current in mast cells. *Nature,* 355**,** 353-356.

HOTH, M. & PENNER, R. 1993. Calcium release-activated calcium current in rat mast cells. *The Journal of Physiology,* 465**,** 359-386.

HOU, X., PEDI, L., DIVER, M. M. & LONG, S. B. 2012. Crystal structure of the calcium release-activated calcium channel Orai. *Science (New York, N.Y.),* 338**,** 1308-1313.

HUANG, Y. & PUTNEY, J. W. 1998. Relationship between Intracellular Calcium Store Depletion and Calcium Release-activated Calcium Current in a Mast Cell Line (RBL-1). *Journal of Biological Chemistry,* 273**,** 19554-19559.

HUBBARD, A. L., WALL, D. A. & MA, A. 1983. Isolation of rat hepatocyte plasma membranes. I. Presence of the three major domains. *J Cell Biol,* 96**,** 217-29.

HUNTER, T. 1998. THE CROONIAN LECTURE 1997. The phosphorylation of proteins on tyrosine: its role in cell growth and disease. *Philosophical Transactions of the Royal Society of London. Series B: Biological Sciences,* 353**,** 583-605.

JACK, E. M., STÄUBLI, W., WAECHTER, F., BENTLEY, P., SUTER, J., BIERI, F., MUAKKASSAH-KELLY, S. F. & CRUZ-ORIVE, L. M. 1990. Ultrastructural changes in chemically induced preneoplastic focal lesions in the rat liver: a stereological study. *Carcinogenesis,* 11**,** 1531-1538.

JIN, D.-Y., CHAE, H. Z., RHEE, S. G. & JEANG, K.-T. 1997. Regulatory Role for a Novel Human Thioredoxin Peroxidase in NF-κB Activation. *Journal of Biological Chemistry,* 272**,** 30952-30961.

JING, J., HE, L., SUN, A., QUINTANA, A., DING, Y., MA, G., TAN, P., LIANG, X., ZHENG, X., CHEN, L., SHI, X., ZHANG, S. L., ZHONG, L., HUANG, Y., DONG, M.-Q., WALKER, C. L., HOGAN, P. G., WANG, Y. & ZHOU, Y. 2015. Proteomic mapping of ER-PM junctions identifies STIMATE as a regulator of $Ca^{2+}$ influx. *Nature Cell Biology,* 17**,** 1339-1347.

JOHANSEN, K. & SVENSSON, L. 1998. Immunoprecipitation. *Methods in molecular medicine,* 13**,** 15-28.

JONES, B. F., BOYLES, R. R., HWANG, S.-Y., BIRD, G. S. & PUTNEY, J. W. 2008. Calcium influx mechanisms underlying calcium oscillations in rat hepatocytes. *Hepatology,* 48**,** 1273-1281.

JOSEPH, S. K., COLL, K. E., COOPER, R. H., MARKS, J. S. & WILLIAMSON, J. R. 1983. Mechanisms underlying calcium homeostasis in isolated hepatocytes. *The Journal of Biological Chemistry,* 258**,** 731-741.

JOUSSET, H., FRIEDEN, M. & DEMAUREX, N. 2007. STIM1 Knockdown Reveals That Store-operated $Ca^{2+}$ Channels Located Close to Sarco/Endoplasmic $Ca^{2+}$ ATPases (SERCA) Pumps Silently Refill the Endoplasmic Reticulum. *The Journal of Biological Chemistry,* 282**,** 11456-11464.

KABOORD, B. & PERR, M. 2008. Isolation of proteins and protein complexes by immunoprecipitation. *Methods Mol Biol,* 424**,** 349-64.

KAKIHANA, T., ARAKI, K., VAVASSORI, S., IEMURA, S.-I., CORTINI, M., FAGIOLI, C., NATSUME, T., SITIA, R. & NAGATA, K. 2013. Dynamic Regulation of Ero1α and Peroxiredoxin 4 Localization in the Secretory Pathway. *Journal of Biological Chemistry,* 288**,** 29586-29594.

KAN, A., MOHAMEDALI, A., TAN, S. H., CHERUKU, H. R., SLAPETOVA, I., LEE, L. Y. & BAKER, M. S. 2013. An improved method for the detection and enrichment of low-abundant membrane and lipid raft-residing proteins. *Journal of Proteomics,* 79**,** 299-304.

KASS, G. E., LLOPIS, J., CHOW, S. C., DUDDY, S. K. & ORRENIUS, S. 1990. Receptor-operated calcium influx in rat hepatocytes. Identification and characterization using manganese. *Journal of Biological Chemistry,* 265**,** 17486-17492.

KAUFMANN, H., BAILEY, J. E. & FUSSENEGGER, M. 2001. Use of antibodies for detection of phosphorylated proteins separated by two-dimensional gel electrophoresis. *Proteomics,* 1**,** 194-9.

KAWASAKI, T., UEYAMA, T., LANGE, I., FESKE, S. & SAITO, N. 2010. Protein Kinase C-induced Phosphorylation of Orai1 Regulates the Intracellular Ca2+ Level via the Store-operated Ca2+ Channel. *Journal of Biological Chemistry,* 285**,** 25720-25730.

KEIJI, H., THOMAS, P., ALLISON, F. O. N., JONATHAN, A. D. & MICHAEL, H. N. 2002. The type II inositol 1,4,5-trisphosphate receptor can trigger $Ca^{2+}$ waves in rat hepatocytes. *Gastroenterology,* 122**,** 1088-1100.

KESSLER, F., BENNARDINI, F., BACHS, O., SERRATOSA, J., JAMES, P., CARIDE, A. J., GAZZOTTI, P., PENNISTON, J. T. & CARAFOLI, E. 1990. Partial purification and characterization of the Ca2(+)-pumping ATPase of the liver plasma membrane. *Journal of Biological Chemistry,* 265**,** 16012-9.

KHERADPEZHOUH, E., MA, L., MORPHETT, A., BARRITT, G. J. & RYCHKOV, G. Y. 2014. TRPM2 channels mediate acetaminophen-induced liver damage. *Proc Natl Acad Sci U S A,* 111**,** 3176-81.

KIMURA, S., KUGAI, N., TADA, R., KOJIMA, I., ABE, K. & OGATA, E. 1982. Sources of calcium mobilized by alpha-adrenergic stimulation in perfused rat liver. *Horm Metab Res,* 14**,** 133-8.

KONNO, M., SHIRAKAWA, H., MIYAKE, T., SAKIMOTO, S., NAKAGAWA, T. & KANEKO, S. 2012. Calumin, a Ca2+-binding protein on the endoplasmic reticulum, alters the ion permeability of Ca2+ release-activated Ca2+ (CRAC) channels. *Biochemical and Biophysical Research Communications,* 417**,** 784-789.

KORZENIOWSKI, M. K., SZANDA, G., BALLA, T. & SPÄT, A. 2009. Store-operated Ca2+ influx and subplasmalemmal mitochondria. *Cell Calcium,* 46**,** 49-55.

KOZIEL, K., LEBIEDZINSKA, M., SZABADKAI, G., ONOPIUK, M., BRUTKOWSKI, W., WIERZBICKA, K., WILCZYNSKI, G., PINTON, P., DUSZYNSKI, J., ZABLOCKI, K. & WIECKOWSKI, M. R. 2009. Plasma membrane associated membranes (PAM) from Jurkat cells contain STIM1 protein: Is PAM involved in the capacitative calcium entry? *The International Journal of Biochemistry & Cell Biology,* 41**,** 2440-2449.

KRAPIVINSKY, G., KRAPIVINSKY, L., STOTZ, S. C., MANASIAN, Y. & CLAPHAM, D. E. 2011. POST, partner of stromal interaction molecule 1 (STIM1), targets STIM1 to multiple transporters. *Proceedings of the National Academy of Sciences,* 108**,** 19234-19239.

KRAUSE, E., SCHMID, A., GONZÁLEZ, A. & SCHULZ, I. 1999. Low Cytoplasmic [Ca2+] Activates ICRACIndependently of Global Ca2+ Store Depletion in RBL-1 Cells. *Journal of Biological Chemistry,* 274**,** 36957-36962.

LAL, A., HAYNES, S. R. & GOROSPE, M. 2005. Clean Western blot signals from immunoprecipitated samples. *Mol Cell Probes,* 19**,** 385-8.

LAM, T. K. T., YOSHII, H., HABER, C. A., BOGDANOVIC, E., LAM, L., FANTUS, I. G. & GIACCA, A. 2002. *Free fatty acid-induced hepatic insulin resistance: a potential role for protein kinase C-δ*.

LAVIEU, G., ORCI, L., SHI, L., GEILING, M., RAVAZZOLA, M., WIELAND, F., COSSON, P. & ROTHMAN, J. E. 2010. Induction of cortical endoplasmic reticulum by dimerization of a coatomer-binding peptide anchored to endoplasmic reticulum membranes. *Proceedings of the National Academy of Sciences,* 107**,** 6876-6881.

LEE, C. & GOLDBERG, J. 2010. Structure of Coatomer Cage Proteins and the Relationship among COPI, COPII, and Clathrin Vesicle Coats. *Cell,* 142**,** 123-132.

LEE, K. P., YUAN, J. P., SO, I., WORLEY, P. F. & MUALLEM, S. 2010. STIM1-dependent and STIM1-independent function of transient receptor potential canonical (TRPC) channels tunes their store-operated mode. *J Biol Chem,* 285**,** 38666-73.

LEE, T.-C., SWARTZENDRUBER, D. C. & SNYDER, F. 1969. Zonal centrifugation of microsomes from rat liver: Resolution of rough- and smooth-surfaced membranes. *Biochemical and Biophysical Research Communications,* 36**,** 748-755.

LEITE, M. F., THROWER, E. C., ECHEVARRIA, W., KOULEN, P., HIRATA, K., BENNETT, A. M., EHRLICH, B. E. & NATHANSON, M. H. 2003. Nuclear and cytosolic calcium are regulated independently. *Proceedings of the National Academy of Sciences of the United States of America,* 100**,** 2975-2980.

LI, G., ZHANG, Z., WANG, R., MA, W., YANG, Y., WEI, J. & WEI, Y. 2013. Suppression of STIM1 inhibits human glioblastoma cell proliferation and induces G0/G1 phase arrest. *Journal of Experimental & Clinical Cancer Research : CR,* 32**,** 20-20.

LIÈVREMONT, J. P., HILL, A. M., HILLY, M. & MAUGER, J. P. 1994. The inositol 1,4,5-trisphosphate receptor is localized on specialized sub-regions of the endoplasmic reticulum in rat liver. *Biochemical Journal,* 300**,** 419-427.

LIÈVREMONT, J. P., HILL, A. M., TRAN, D., COQUIL, J. F., STELLY, N. & MAUGER, J. P. 1996. Intracellular calcium stores and inositol 1,4,5-trisphosphate receptor in rat liver cells. *Biochem. J.,* 314**,** 189-197.

LIOU, J., FIVAZ, M., INOUE, T. & MEYER, T. 2007. Live-cell imaging reveals sequential oligomerization and local plasma membrane targeting of stromal interaction molecule 1 after $Ca^{2+}$ store depletion. *Proceedings of the National Academy of Sciences,* 104**,** 9301-9306.

LIOU, J., KIM, M. L., DO HEO, W., JONES, J. T., MYERS, J. W., FERRELL, J. E. & MEYER, T. 2005. STIM Is a $Ca^{2+}$ Sensor Essential for $Ca^{2+}$-Store-Depletion-Triggered $Ca^{2+}$ Influx. *Current Biology,* 15**,** 1235-1241.

LIS, A., PEINELT, C., BECK, A., PARVEZ, S., MONTEILH-ZOLLER, M., FLEIG, A. & PENNER, R. 2007. CRACM1, CRACM2, and CRACM3 are store-operated $Ca^{2+}$ channels with distinct functional properties. *Current Biology,* 17**,** 794-800.

LITJENS, T., HARLAND, M. L., ROBERTS, M. L., BARRITT, G. J. & RYCHKOV, G. Y. 2004. Fast $Ca^{2+}$-dependent inactivation of the store-operated $Ca^{2+}$ current ($I_{SOC}$) in liver cells: a role for calmodulin. *The Journal of Physiology,* 558**,** 85-97.

LITJENS, T., NGUYEN, T., CASTRO, J., AROMATARIS, EDOARDO C., JONES, L., BARRITT, GREG J. & RYCHKOV, GRIGORI Y. 2007. Phospholipase C-γ1 is required for the activation of store-operated $Ca^{2+}$ channels in liver cells. *Biochemical Journal,* 405**,** 269-276.

LÓPEZ, J. J., JARDÍN, I., BOBE, R., PARIENTE, J. A., ENOUF, J., SALIDO, G. M. & ROSADO, J. A. 2008. STIM1 regulates acidic Ca2+ store refilling by interaction with SERCA3 in human platelets. *Biochemical Pharmacology,* 75**,** 2157-2164.

LUIK, R. M., WANG, B., PRAKRIYA, M., WU, M. M. & LEWIS, R. S. 2008. Oligomerization of STIM1 couples ER calcium depletion to CRAC channel activation. *Nature,* 454**,** 538-542.

LUIK, R. M., WU, M. M., BUCHANAN, J. & LEWIS, R. S. 2006. The elementary unit of store-operated Ca2+ entry: local activation of CRAC channels by STIM1 at ER–plasma membrane junctions. *The Journal of Cell Biology,* 174**,** 815-825.

LUR, G., HAYNES, L. P., PRIOR, I. A., GERASIMENKO, O. V., FESKE, S., PETERSEN, O. H., BURGOYNE, R. D. & TEPIKIN, A. V. 2009. Ribosome-free terminals of rough ER allow formation of STIM1 puncta and segregation of STIM1 from $IP_3$ receptors. *Current Biology,* 19**,** 1648-53.

MACLENNAN, D. H., RICE, W. J. & GREEN, N. M. 1997. The mechanism of Ca2+ transport by sarco(endo)plasmic reticulum Ca2+-ATPases. *J Biol Chem,* 272**,** 28815-8.

MALLI, R., NAGHDI, S., ROMANIN, C. & GRAIER, W. F. 2008. Cytosolic Ca2+ prevents the subplasmalemmal clustering of STIM1: an intrinsic mechanism to avoid Ca2+ overload. *J Cell Sci,* 121**,** 3133-3139.

MANDELL, J. W. 2003. Phosphorylation State-Specific Antibodies: Applications in Investigative and Diagnostic Pathology. *The American Journal of Pathology,* 163**,** 1687-1698.

MANJARRÉS, I. M., RODRÍGUEZ-GARCÍA, A., ALONSO, M. T. & GARCÍA-SANCHO, J. 2010. The sarco/endoplasmic reticulum Ca2+ ATPase (SERCA) is the third element in capacitative calcium entry. *Cell Calcium,* 47**,** 412-418.

MANJI, S. S., PARKER, N. J., WILLIAMS, R. T., VAN STEKELENBURG, L., PEARSON, R. B., DZIADEK, M. & SMITH, P. J. 2000. STIM1: a novel phosphoprotein located at the cell surface. *Biochim Biophys Acta,* 1481**,** 147-55.

MARKHAM, K., BAI, Y. & SCHMITT-ULMS, G. 2007. Co-immunoprecipitations revisited: an update on experimental concepts and their implementation for sensitive interactome investigations of endogenous proteins. *Analytical and Bioanalytical Chemistry,* 389**,** 461-473.

MARUYAMA, Y., OGURA, T., MIO, K., KATO, K., KANEKO, T., KIYONAKA, S., MORI, Y. & SATO, C. 2009. Tetrameric Orai1 Is a Teardrop-shaped Molecule with a Long, Tapered Cytoplasmic Domain. *The Journal of Biological Chemistry,* 284**,** 13676-13685.

MASON, M. J., MAHAUT-SMITH, M. P. & GRINSTEIN, S. 1991. The role of intracellular Ca2+ in the regulation of the plasma membrane Ca2+ permeability of unstimulated rat lymphocytes. *Journal of Biological Chemistry,* 266**,** 10872-10879.

MATTEONI, C. A., YOUNOSSI, Z. M., GRAMLICH, T., BOPARAI, N., LIU, Y. C. & MCCULLOUGH, A. J. 1999. Nonalcoholic fatty liver disease: a spectrum of clinical and pathological severity. *Gastroenterology,* 116**,** 1413-9.

MCNALLY, B. A., YAMASHITA, M., ENGH, A. & PRAKRIYA, M. 2009. Structural determinants of ion permeation in CRAC channels. *Proceedings of the National Academy of Sciences,* 106**,** 22516-22521.

MEI, Z.-Z., MAO, H.-J. & JIANG, L.-H. 2006. Conserved cysteine residues in the pore region are obligatory for human TRPM2 channel function. *American journal of physiology. Cell physiology,* 291**,** C1022-C1028.

MELDOLESI, J. & POZZAN, T. 1998. The endoplasmic reticulum Ca2+ store: a view from the lumen. *Trends in Biochemical Sciences,* 23**,** 10-14.

MERCER, J. C., DEHAVEN, W. I., SMYTH, J. T., WEDEL, B., BOYLES, R. R., BIRD, G. S. & PUTNEY, J. W. 2006. Large Store-operated Calcium Selective Currents Due to Co-expression of Orai1 or Orai2 with the Intracellular Calcium Sensor, Stim1. *Journal of Biological Chemistry,* 281**,** 24979-24990.

MICARONI, M., PERINETTI, G., BERRIE, C. P. & MIRONOV, A. A. 2010. The SPCA1 Ca2+ Pump and Intracellular Membrane Trafficking. *Traffic,* 11**,** 1315-1333.

MIGNEN, O., THOMPSON, J. L. & SHUTTLEWORTH, T. J. 2008. Orai1 subunit stoichiometry of the mammalian CRAC channel pore. *The Journal of Physiology,* 586**,** 419-425.

MISSIAEN, L., DODE, L., VANOEVELEN, J., RAEYMAEKERS, L. & WUYTACK, F. 2007. Calcium in the Golgi apparatus. *Cell Calcium,* 41**,** 405-16.

MUIK, M., FAHRNER, M., DERLER, I., SCHINDL, R., BERGSMANN, J., FRISCHAUF, I., GROSCHNER, K. & ROMANIN, C. 2009. A Cytosolic Homomerization and a Modulatory Domain within STIM1 C Terminus Determine Coupling to ORAI1 Channels. *Journal of Biological Chemistry,* 284**,** 8421-8426.

MUIK, M., FAHRNER, M., SCHINDL, R., STATHOPULOS, P., FRISCHAUF, I., DERLER, I., PLENK, P., LACKNER, B., GROSCHNER, K., IKURA, M. & ROMANIN, C. 2011. STIM1 couples to ORAI1 via an intramolecular transition into an extended conformation. *The EMBO Journal,* 30**,** 1678-1689.

MUIK, M., FRISCHAUF, I., DERLER, I., FAHRNER, M., BERGSMANN, J., EDER, P., SCHINDL, R., HESCH, C., POLZINGER, B., FRITSCH, R., KAHR, H., MADL, J., GRUBER, H., GROSCHNER, K. & ROMANIN, C. 2008. Dynamic Coupling of the Putative Coiled-

coil Domain of ORAI1 with STIM1 Mediates ORAI1 Channel Activation. *Journal of Biological Chemistry,* 283**,** 8014-8022.

MULLINS, F. M., CHAN, Y. P., DOLMETSCH, R. E. & LEWIS, R. S. 2009. STIM1 and calmodulin interact with Orai1 to induce Ca(2+)-dependent inactivation of CRAC channels. *Proceedings of the National Academy of Sciences of the United States of America,* 106**,** 15495-15500.

NAGATA, J. U. N., GUERRA, M. T., SHUGRUE, C. A., GOMES, D. A., NAGATA, N. & NATHANSON, M. H. 2007. Lipid Rafts Establish Calcium Waves in Hepatocytes. *Gastroenterology,* 133**,** 256-267.

NAKATANI, K., KANEDA, K., SEKI, S. & NAKAJIMA, Y. 2004. Pit cells as liver-associated natural killer cells: morphology and function. *Med Electron Microsc,* 37**,** 29-36.

NATHANSON, M. H., BURGSTAHLER, A. D. & FALLON, M. B. 1994. Multistep mechanism of polarized Ca2+ wave patterns in hepatocytes. *Am J Physiol,* 267**,** G338-49.

NAVARRO-BORELLY, L., SOMASUNDARAM, A., YAMASHITA, M., REN, D., MILLER, R. J. & PRAKRIYA, M. 2008. STIM1–Orai1 interactions and Orai1 conformational changes revealed by live-cell FRET microscopy. *The Journal of Physiology,* 586**,** 5383-5401.

NEUSCHWANDER-TETRI, B. A. & CALDWELL, S. H. 2003. Nonalcoholic steatohepatitis: summary of an AASLD Single Topic Conference. *Hepatology,* 37**,** 1202-19.

NICOTERA, P., MCCONKEY, D. J., JONES, D. P. & ORRENIUS, S. 1989. ATP stimulates Ca2+ uptake and increases the free Ca2+ concentration in isolated rat liver nuclei. *Proceedings of the National Academy of Sciences of the United States of America,* 86**,** 453-457.

NICOTERA, P., ORRENIUS, S., NILSSON, T. & BERGGREN, P. O. 1990. An inositol 1,4,5-trisphosphate-sensitive Ca2+ pool in liver nuclei. *Proc Natl Acad Sci U S A,* 87**,** 6858-62.

NUNN, D. L. & TAYLOR, C. W. 1990. Liver inositol 1,4,5-trisphosphate-binding sites are the Ca2+-mobilizing receptors. *The Biochemical Journal,* 270**,** 227-32.

OKADO-MATSUMOTO, A., MATSUMOTO, A., FUJII, J. & TANIGUCHI, N. 2000. Peroxiredoxin IV Is a Secretable Protein with Heparin-Binding Properties under Reduced Conditions. *Journal of Biochemistry,* 127**,** 493-501.

ONG, H. L., CHENG, K. T., LIU, X., BANDYOPADHYAY, B. C., PARIA, B. C., SOBOLOFF, J., PANI, B., GWACK, Y., SRIKANTH, S., SINGH, B. B., GILL, D. & AMBUDKAR, I. S. 2007a. Dynamic Assembly of TRPC1-STIM1-Orai1 Ternary Complex Is Involved in Store-operated Calcium Influx: EVIDENCE FOR SIMILARITIES IN STORE-OPERATED AND CALCIUM RELEASE-ACTIVATED CALCIUM CHANNEL COMPONENTS. *Journal of Biological Chemistry,* 282**,** 9105-9116.

ONG, H. L., LIU, X., TSANEVA-ATANASOVA, K., SINGH, B. B., BANDYOPADHYAY, B. C., SWAIM, W. D., RUSSELL, J. T., HEGDE, R. S., SHERMAN, A. & AMBUDKAR, I. S. 2007b. Relocalization of STIM1 for activation of store-operated $^{Ca2+}$ entry is determined by the depletion of subplasma membrane endoplasmic reticulum $Ca^{2+}$ store. *Journal of Biological Chemistry,* 282**,** 12176-85.

ORCI, L., RAVAZZOLA, M., LE COADIC, M., SHEN, W.-W., DEMAUREX, N. & COSSON, P. 2009. STIM1-induced precortical and cortical subdomains of the endoplasmic reticulum. *Proceedings of the National Academy of Sciences,* 106**,** 19358-19362.

PALTY, R., RAVEH, A., KAMINSKY, I., MELLER, R. & REUVENY, E. 2012. SARAF inactivates the store operated calcium entry machinery to prevent excess calcium refilling. *Cell,* 149**,** 425-38.

PANI, B., ONG, H. L., BRAZER, S.-C. W., LIU, X., RAUSER, K., SINGH, B. B. & AMBUDKAR, I. S. 2009. Activation of TRPC1 by STIM1 in ER-PM microdomains involves release of the channel from its scaffold caveolin-1. *Proceedings of the National Academy of Sciences,* 106**,** 20087-20092.

PAREKH, A. B., FLEIG, A. & PENNER, R. 1997. The Store-Operated Calcium Current ICRAC: Nonlinear Activation by InsP3 and Dissociation from Calcium Release. 89**,** 973-980.

PAREKH, A. B. & PUTNEY, J. W., JR. 2005. Store-operated calcium channels. *Physiol Rev,* 85**,** 757-810.

PARK, C. Y., HOOVER, P. J., MULLINS, F. M., BACHHAWAT, P., COVINGTON, E. D., RAUNSER, S., WALZ, T., GARCIA, K. C., DOLMETSCH, R. E. & LEWIS, R. S. 2009. STIM1 Clusters and Activates CRAC Channels via Direct Binding of a Cytosolic Domain to Orai1. *Cell,* 136**,** 876-890.

PARK, C. Y., SHCHEGLOVITOV, A. & DOLMETSCH, R. 2010. The CRAC channel activator STIM1 binds and inhibits L-type voltage-gated calcium channels. *Science,* 330**,** 101-5.

PEINELT, C., BECK, A., MONTEILH-ZOLLER, M. K., PENNER, R. & FLEIG, A. 2009. $IP_3$ receptor subtype-dependent activation of store-operated calcium entry through $I_{CRAC}$. *Cell calcium,* 45**,** 326-330.

PEINELT, C., VIG, M., KOOMOA, D. L., BECK, A., NADLER, M. J. S., KOBLAN-HUBERSON, M., LIS, A., FLEIG, A., PENNER, R. & KINET, J.-P. 2006. Amplification of CRAC current by STIM1 and CRACM1 (Orai1). *Nature Cell Biology,* 8**,** 771-773.

PENDIN, D., MCNEW, J. A. & DAGA, A. 2011. Balancing ER dynamics: shaping, bending, severing, and mending membranes. *Current opinion in cell biology,* 23**,** 435-442.

PENNA, A., DEMURO, A., YEROMIN, A. V., ZHANG, S. L., SAFRINA, O., PARKER, I. & CAHALAN, M. D. 2008. The CRAC channel consists of a tetramer formed by Stim-induced dimerization of Orai dimers. *Nature,* 456**,** 116-120.

PHILLIP KAISER, J., BEIER, J. I., ZHANG, J., DAVID HOETKER, J., MONTFORT, C. V., GUO, L., ZHENG, Y., MONIA, B. P., BHATNAGAR, A. & ARTEEL, G. E. 2009. PKCε plays a causal role in acute ethanol-induced steatosis. *Archives of Biochemistry and Biophysics,* 482**,** 104-111.

POSTIC, C. & GIRARD, J. 2008. Contribution of de novo fatty acid synthesis to hepatic steatosis and insulin resistance: lessons from genetically engineered mice. *The Journal of Clinical Investigation,* 118**,** 829-838.

POTIER, M., GONZALEZ, J. C., MOTIANI, R. K., ABDULLAEV, I. F., BISAILLON, J. M., SINGER, H. A. & TREBAK, M. 2009. Evidence for STIM1- and Orai1-dependent store-operated calcium influx through ICRAC in vascular smooth muscle cells: role in proliferation and migration. *The FASEB Journal,* 23**,** 2425-2437.

POZO-GUISADO, E., CAMPBELL, D. G., DEAK, M., ÁLVAREZ-BARRIENTOS, A., MORRICE, N. A., ÁLVAREZ, I. S., ALESSI, D. R. & MARTÍN-ROMERO, F. J. 2010. Phosphorylation of STIM1 at ERK1/2 target sites modulates store-operated calcium entry. *Journal of Cell Science,* 123**,** 3084-3093.

POZO-GUISADO, E., CASAS-RUA, V., TOMAS-MARTIN, P., LOPEZ-GUERRERO, A. M., ALVAREZ-BARRIENTOS, A. & MARTIN-ROMERO, F. J. 2013. Phosphorylation of STIM1 at ERK1/2 target sites regulates interaction with the microtubule plus-end binding protein EB1. *Journal of Cell Science,* 126**,** 3170-3180.

PRAKRIYA, M., FESKE, S., GWACK, Y., SRIKANTH, S., RAO, A. & HOGAN, P. G. 2006. Orai1 is an essential pore subunit of the CRAC channel. *Nature,* 443**,** 230-233.

PRPIĆ, V., GREEN, K. C., BLACKMORE, P. F. & EXTON, J. H. 1984. Vasopressin-, angiotensin II-, and alpha 1-adrenergic-induced inhibition of $Ca^{2+}$ transport by rat liver plasma membrane vesicles. *Journal of Biological Chemistry,* 259**,** 1382-1385.

PUTNEY JR, J. W. 1986. A model for receptor-regulated calcium entry. *Cell Calcium,* 7**,** 1-12.

PUTNEY, J. W. & TOMITA, T. 2012. Phospholipase C Signaling and Calcium Influx. *Advances in biological regulation,* 52**,** 152-164.

RAMSEY, I. S., DELLING, M. & CLAPHAM, D. E. 2006. An Introduction to TRP Channels. *Annual Review of Physiology,* 68**,** 619-647.

ROBB-GASPERS, L. D. & THOMAS, A. P. 1995. Coordination of Ca2+ Signaling by Intercellular Propagation of $Ca^{2+}$ Waves in the Intact Liver. *Journal of Biological Chemistry,* 270**,** 8102-8107.

ROOS, J., DIGREGORIO, P. J., YEROMIN, A. V., OHLSEN, K., LIOUDYNO, M., ZHANG, S., SAFRINA, O., KOZAK, J. A., WAGNER, S. L., CAHALAN, M. D., VELIÇELEBI, G. & STAUDERMAN, K. A. 2005. STIM1, an essential and conserved component of store-operated $Ca^{2+}$ channel function. *The Journal of Cell Biology,* 169**,** 435-445.

RYCHKOV, G. & BARRITT, G. J. 2007. TRPC1 $Ca^{2+}$-permeable channels in animal cells. *Handb Exp Pharmacol***,** 23-52.

RYCHKOV, G., BRERETON, H. M., HARLAND, M. L. & BARRITT, G. J. 2001. Plasma membrane $Ca^{2+}$ release–Activated $Ca^{2+}$ channels with a high selectivity for $Ca^{2+}$ identified by patch-clamp recording in rat liver cells. *Hepatology,* 33**,** 938-947.

RYCHKOV, G. Y., LITJENS, T., ROBERTS, M. L. & BARRITT, G. J. 2005a. Arachidonic acid inhibits the store-operated $Ca^{2+}$ current in rat liver cells. *The Biochemical Journal,* 385**,** 551-556.

RYCHKOV, G. Y., LITJENS, T., ROBERTS, M. L. & BARRITT, G. J. 2005b. ATP and vasopressin activate a single type of store-operated $Ca^{2+}$ channel, identified by patch-clamp recording, in rat hepatocytes. *Cell Calcium,* 37**,** 183-91.

SABBIONI, S., BARBANTI-BRODANO, G., CROCE, C. M. & NEGRINI, M. 1997. GOK: A Gene at 11p15 Involved in Rhabdomyosarcoma and Rhabdoid Tumor Development. *Cancer Research,* 57**,** 4493-4497.

SAHA, J. K., XIA, J., GRONDIN, J. M., ENGLE, S. K. & JAKUBOWSKI, J. A. 2005. Acute hyperglycemia induced by ketamine/xylazine anesthesia in rats: mechanisms and implications for preclinical models. *Exp Biol Med (Maywood),* 230**,** 777-84.

SAITOH, N., ORITANI, K., SAITO, K., YOKOTA, T., ICHII, M., SUDO, T., FUJITA, N., NAKAJIMA, K., OKADA, M. & KANAKURA, Y. 2011. Identification of functional domains and novel binding partners of STIM proteins. *Journal of Cellular Biochemistry,* 112**,** 147-156.

SAMPIERI, A., ZEPEDA, A., ASANOV, A. & VACA, L. 2009a. Visualizing the store-operated channel complex assembly in real time: identification of SERCA2 as a new member. *Cell Calcium,* 45**,** 439-46.

SAMPIERI, A., ZEPEDA, A., ASANOV, A. & VACA, L. 2009b. Visualizing the store-operated channel complex assembly in real time: Identification of SERCA2 as a new member. *Cell Calcium,* 45**,** 439-446.

SAMUEL, V. T., LIU, Z.-X., WANG, A., BEDDOW, S. A., GEISLER, J. G., KAHN, M., ZHANG, X.-M., MONIA, B. P., BHANOT, S. & SHULMAN, G. I. 2007. Inhibition of protein kinase Cε prevents hepatic insulin resistance in nonalcoholic fatty liver disease. *The Journal of Clinical Investigation,* 117**,** 739-745.

SANCHEZ-BUENO, A., GREENWOOD, M. R., VARELA-NIETO, I., MARRERO, I., GIL, B., MATO, J. M. & COBBOLD, P. H. 1997. Inositol-phosphoglycan inhibits calcium oscillations in hepatocytes by reducing calcium entry. *Cell Calcium,* 21**,** 125-133.

SANCHEZ-MIRANDA, E., IBARRA-SANCHEZ, A. & GONZALEZ-ESPINOSA, C. 2010. Fyn kinase controls FcεRI receptor-operated calcium entry necessary for full degranulation in mast cells. *Biochemical and Biophysical Research Communications,* 391**,** 1714-1720.

SATO, S. 2004. Ultrastructural and morphometric studies of normal rat hepatocytes. *Journal of submicroscopic cytology and pathology,* 36**,** 131-140.

SAÜC, S., BULLA, M., NUNES, P., ORCI, L., MARCHETTI, A., ANTIGNY, F., BERNHEIM, L., COSSON, P., FRIEDEN, M. & DEMAUREX, N. 2015. STIM1L traps and gates Orai1 channels without remodeling the cortical ER. *Journal of Cell Science,* 128**,** 1568-1579.

SAWANOBORI, T., TAKANASHI, H., HIRAOKA, M., IIDA, Y., KAMISAKA, K. & MAEZAWA, H. 1989. Electrophysiological properties of isolated rat liver cells. *Journal of Cellular Physiology,* 139**,** 580-585.

SCHINDL, R., FRISCHAUF, I., BERGSMANN, J., MUIK, M., DERLER, I., LACKNER, B., GROSCHNER, K. & ROMANIN, C. 2009. Plasticity in $Ca^{2+}$ selectivity of Orai1/Orai3 heteromeric channel. *Proceedings of the National Academy of Sciences,* 106**,** 19623-19628.

SCRIMGEOUR, N., LITJENS, T., MA, L., BARRITT, G. J. & RYCHKOV, G. Y. 2009. Properties of Orai1 mediated store-operated current depend on the expression levels of STIM1 and Orai1 proteins. *The Journal of Physiology,* 587**,** 2903-2918.

SHEARS, S. B. & KIRK, C. J. 1984. Determination of mitochondrial calcium content in hepatocytes by a rapid cellular fractionation technique. Vasopressin stimulates mitochondrial Ca2+ uptake. *Biochemical Journal,* 220**,** 417-421.

SHI, Y., SONG, M., GUO, R., WANG, H., GAO, P., SHI, W. & HUANG, L. 2010. Knockdown of stromal interaction molecule 1 attenuates hepatocyte growth factor-induced endothelial progenitor cell proliferation. *Exp. Biol. Med.,* 235**,** 317-325.

SKANDALAKIS, J. E., SKANDALAKIS, L. J., SKANDALAKIS, P. N. & MIRILAS, P. 2004. Hepatic surgical anatomy. *Surgical Clinics of North America,* 84**,** 413-435.

SMITH, M. J. & KOCH, G. L. 1989. Multiple zones in the sequence of calreticulin (CRP55, calregulin, HACBP), a. *Embo J,* 8**,** 3581-6.

SMYTH, J. T., DEHAVEN, W. I., BIRD, G. S. & PUTNEY, J. W. 2008. $Ca^{2+}$-store-dependent and -independent reversal of Stim1 localization and function. *Journal of cell science,* 121**,** 762-772.

SMYTH, J. T., DEHAVEN, W. I., BIRD, G. S. & PUTNEY, J. W., JR 2007. Role of the microtubule cytoskeleton in the function of the store-operated Ca2+ channel activator STIM1. *J Cell Sci,* 120**,** 3762-3771.

SMYTH, J. T., PETRANKA, J. G., BOYLES, R. R., DEHAVEN, W. I., FUKUSHIMA, M., JOHNSON, K. L., WILLIAMS, J. G. & PUTNEY JR, J. W. 2009. Phosphorylation of STIM1 underlies suppression of store-operated calcium entry during mitosis. *Nature Cell Biology,* 11**,** 1465-1472.

SOBOLOFF, J., SPASSOVA, M. A., TANG, X. D., HEWAVITHARANA, T., XU, W. & GILL, D. L. 2006. Orai1 and STIM Reconstitute Store-operated Calcium Channel Function. *Journal of Biological Chemistry,* 281**,** 20661-20665.

SPASSOVA, M. A., HEWAVITHARANA, T., FANDINO, R. A., KAYA, A., TANAKA, J. & GILL, D. L. 2008. Voltage Gating at the Selectivity Filter of the Ca2+ Release-activated

Ca2+ Channel Induced by Mutation of the Orai1 Protein. *Journal of Biological Chemistry,* 283**,** 14938-14945.

SRIKANTH, S., JEW, M., KIM, K.-D., YEE, M.-K., ABRAMSON, J. & GWACK, Y. 2012. Junctate is a $Ca^{2+}$-sensing structural component of Orai1 and stromal interaction molecule 1 (STIM1). *Proceedings of the National Academy of Sciences,* 109**,** 8682-8687.

SRIKANTH, S., JUNG, H.-J., KIM, K.-D., SOUDA, P., WHITELEGGE, J. & GWACK, Y. 2010a. A novel EF-hand protein, CRACR2A, is a cytosolic $Ca^{2+}$ sensor that stabilizes CRAC channels in T cells. *Nature cell biology,* 12**,** 436-446.

SRIKANTH, S., JUNG, H.-J., RIBALET, B. & GWACK, Y. 2010b. The Intracellular Loop of Orai1 Plays a Central Role in Fast Inactivation of $Ca^{2+}$ Release-activated $Ca^{2+}$ Channels. *Journal of Biological Chemistry,* 285**,** 5066-5075.

STATHOPULOS, P. B., LI, G.-Y., PLEVIN, M. J., AMES, J. B. & IKURA, M. 2006a. Stored $Ca^{2+}$ Depletion-induced Oligomerization of Stromal Interaction Molecule 1 (STIM1) via the EF-SAM Region. *AN INITITATION MECHANISM FOR CAPACITIVE $Ca^{2+}$ ENTRY*. *Journal of Biological Chemistry,* 281**,** 35855-35862.

STATHOPULOS, P. B., LI, G.-Y., PLEVIN, M. J., AMES, J. B. & IKURA, M. 2006b. Stored $Ca^{2+}$ Depletion-induced Oligomerization of Stromal Interaction Molecule 1 (STIM1) via the EF-SAM Region: AN INITIATION MECHANISM FOR CAPACITIVE $Ca^{2+}$ ENTRY. *Journal of Biological Chemistry,* 281**,** 35855-35862.

STEINCKWICH, N., FRIPPIAT, J.-P., STASIA, M.-J., ERARD, M., BOXIO, R., TANKOSIC, C., DOIGNON, I. & NÜßE, O. 2007. Potent inhibition of store-operated $Ca^{2+}$ influx and superoxide production in HL60 cells and polymorphonuclear neutrophils by the pyrazole derivative BTP2. *Journal of Leukocyte Biology,* 81**,** 1054-1064.

SUNDIVAKKAM, P. C., NATARAJAN, V., MALIK, A. B. & TIRUPPATHI, C. 2013. Store-operated $Ca^{2+}$ Entry (SOCE) Induced by Protease-activated Receptor-1 Mediates STIM1 Protein Phosphorylation to Inhibit SOCE in Endothelial Cells through AMP-activated Protein Kinase and p38β Mitogen-activated Protein Kinase. *The Journal of Biological Chemistry,* 288**,** 17030-17041.

TAKAHASHI, Y., MURAKAMI, M., WATANABE, H., HASEGAWA, H., OHBA, T., MUNEHISA, Y., NOBORI, K., ONO, K., IIJIMA, T. & ITO, H. 2007. Essential role of the N-terminus of murine Orai1 in store-operated $Ca^{2+}$ entry. *Biochemical and Biophysical Research Communications,* 356**,** 45-52.

TAKEMURA, H., HUGHES, A. R., THASTRUP, O. & PUTNEY, J. W. 1989. Activation of calcium entry by the tumor promoter thapsigargin in parotid acinar cells. Evidence that an intracellular calcium pool and not an inositol phosphate regulates calcium fluxes at the plasma membrane. *Journal of Biological Chemistry,* 264**,** 12266-12271.

TANAKA, M., ITOH, T., TANIMIZU, N. & MIYAJIMA, A. 2011. Liver stem/progenitor cells: their characteristics and regulatory mechanisms. *J Biochem,* 149**,** 231-9.

TAVENDER, T. J. & BULLEID, N. J. 2010. Peroxiredoxin IV protects cells from oxidative stress by removing H2O2 produced during disulphide formation. *Journal of Cell Science,* 123**,** 2672-2679.

TAVENDER, T. J., SHEPPARD, A. M. & BULLEID, N. J. 2008. Peroxiredoxin IV is an endoplasmic reticulum-localized enzyme forming oligomeric complexes in human cells. *Biochem J,* 411**,** 191-199.

TAVENDER, T. J., SPRINGATE, J. J. & BULLEID, N. J. 2010. Recycling of peroxiredoxin IV provides a novel pathway for disulphide formation in the endoplasmic reticulum. *EMBO J,* 29**,** 4185-4197.

THOMAS, A. P., ALEXANDER, J. & WILLIAMSON, J. R. 1984. Relationship between Inositol Polyphosphate Production and the Increase of Cytosolic Free $Ca^{2+}$ Induced by Vasopressin in Isolated Hepatocyte. *Journal of Biological Chemistry,* 259**,** 5574-5584.

THOMAS, A. P., RENARD, D. C. & ROONEY, T. A. 1991. Spatial and temporal organization of calcium signalling in hepatocytes. *Cell Calcium,* 12**,** 111-126.

TOJYO, Y., TANIMURA, A. & MATSUMOTO, Y. 1995a. Suppression of capacitative $Ca^{2+}$ entry by serine/threonine phosphatase inhibitors in rat parotid acinar cells. *The Japanese Journal of Pharmacology,* 69**,** 381-9.

TOJYO, Y., TANIMURA, A., MATSUMOTO, Y. & SUGIYA, H. 1995b. Staurosporine enhances $Ca^{2+}$ entry induced by depletion of intracellular $Ca^{2+}$ stores in rat parotid acinar cells. *Cell Calcium,* 17**,** 32-40.

TÖRNQUIST, K., VAINIO, P. J., BJÖRKLUND, S., TITIEVSKY, A., DUGUÉ, B. & TUOMINEN, R. K. 2000. Hydrogen peroxide attenuates store-operated calcium entry and enhances calcium extrusion in thyroid FRTL-5 cells. *The Biochemical Journal,* 351**,** 47-56.

TRINKLE-MULCAHY, L., BOULON, S., LAM, Y. W., URCIA, R., BOISVERT, F.-M., VANDERMOERE, F., MORRICE, N. A., SWIFT, S., ROTHBAUER, U., LEONHARDT, H. & LAMOND, A. 2008. Identifying specific protein interaction partners using quantitative mass spectrometry and bead proteomes. *The Journal of Cell Biology,* 183**,** 223-239.

VACA, L. 2010. SOCIC: the store-operated calcium influx complex. *Cell Calcium,* 47**,** 199-209.

VANOEVELEN, J., DODE, L., VAN BAELEN, K., FAIRCLOUGH, R. J., MISSIAEN, L., RAEYMAEKERS, L. & WUYTACK, F. 2005. The Secretory Pathway $Ca^{2+}/Mn^{2+}$-ATPase 2 Is a Golgi-localized Pump with High Affinity for $Ca^{2+}$ Ions. *Journal of Biological Chemistry,* 280**,** 22800-22808.

VARADARAJAN, S., TANAKA, K., SMALLEY, J. L., BAMPTON, E. T., PELLECCHIA, M., DINSDALE, D., WILLARS, G. B. & COHEN, G. M. 2013. Endoplasmic reticulum membrane reorganization is regulated by ionic homeostasis. *PLoS One,* 8**,** e56603.

VÁRNAI, P., TÓTH, B., TÓTH, D. J., HUNYADY, L. & BALLA, T. 2007. Visualization and Manipulation of Plasma Membrane-Endoplasmic Reticulum Contact Sites Indicates the Presence of Additional Molecular Components within the STIM1-Orai1 Complex. *Journal of Biological Chemistry,* 282**,** 29678-29690.

VERTEL, B. M., WALTERS, L. M. & MILLS, D. 1992. Subcompartments of the endoplasmic reticulum. *Semin Cell Biol,* 3**,** 325-41.

VIG, M., BECK, A., BILLINGSLEY, J. M., LIS, A., PARVEZ, S., PEINELT, C., KOOMOA, D. L., SOBOLOFF, J., GILL, D. L., FLEIG, A., KINET, J.-P. & PENNER, R. 2006a. CRACM1 Multimers Form the Ion-Selective Pore of the CRAC Channel. *Current biology : CB,* 16**,** 2073-2079.

VIG, M., PEINELT, C., BECK, A., KOOMOA, D. L., RABAH, D., KOBLAN-HUBERSON, M., KRAFT, S., TURNER, H., FLEIG, A., PENNER, R. & KINET, J. P. 2006b. CRACM1 is a plasma membrane protein essential for store-operated $Ca^{2+}$ entry. *Science,* 312**,** 1220-3.

VOELTZ, G. K., ROLLS, M. M. & RAPOPORT, T. A. 2002. Structural organization of the endoplasmic reticulum. *EMBO Reports,* 3**,** 944-950.

WALSH, C. M., DOHERTY, M. K., TEPIKIN, A. V. & BURGOYNE, R. D. 2010. Evidence for an interaction between Golli and STIM1 in store-operated calcium entry. *Biochemical Journal,* 430**,** 453-460.

WANG, H.-J., GUAY, G., POGAN, L., SAUVÉ, R. & NABI, I. R. 2000. Calcium Regulates the Association between Mitochondria and a Smooth Subdomain of the Endoplasmic Reticulum. *The Journal of Cell Biology,* 150**,** 1489-1498.

WANG, J. Y., SUN, J., HUANG, M. Y., WANG, Y. S., HOU, M. F., SUN, Y., HE, H., KRISHNA, N., CHIU, S. J., LIN, S., YANG, S. & CHANG, W. C. 2014. STIM1 overexpression promotes colorectal cancer progression, cell motility and COX-2 expression. *Oncogene*.

WANG, X., WANG, L., WANG, X. E., SUN, F. & WANG, C. C. 2012. Structural insights into the peroxidase activity and inactivation of human peroxiredoxin 4. *Biochemical Journal,* 441**,** 113-118.

WEIDINGER, C., SHAW, P. J. & FESKE, S. 2013. STIM1 and STIM2-mediated $Ca^{2+}$ influx regulates antitumour immunity by $CD8^{+}$ T cells. *EMBO molecular medicine,* 5**,** 1311-21.

WESTRATE, L. M., LEE, J. E., PRINZ, W. A. & VOELTZ, G. K. 2015. Form follows function: the importance of endoplasmic reticulum shape. *Annual review of biochemistry,* 84**,** 791-811.

WHITE, C. D. & TOKER, A. 2001. Using Phospho-Motif Antibodies to Determine Kinase Substrates. *Current Protocols in Molecular Biology.* John Wiley & Sons, Inc.

WILSON, C. H., ALI, E. S., SCRIMGEOUR, N., MARTIN, A. M., HUA, J., TALLIS, G. A., RYCHKOV, G. Y. & BARRITT, G. J. 2014. Steatosis inhibits liver cell store-operated $Ca^{2+}$ entry and reduces ER $Ca^{2+}$ through a protein kinase C dependent mechanism. *Biochem J*.

WOODS, N. M., CUTHBERTSON, K. S. R. & COBBOLD, P. H. 1986. Repetitive transient rises in cytoplasmic free calcium in hormone-stimulated hepatocytes. *Nature,* 319**,** 600-602.

WOODWARD, O. M., LI, Y., YU, S., GREENWELL, P., WODARCZYK, C., BOLETTA, A., GUGGINO, W. B. & QIAN, F. 2010. Identification of a polycystin-1 cleavage product, P100, that regulates store operated Ca entry through interactions with STIM1. *PLoS One,* 5**,** e12305.

WU, M. M., BUCHANAN, J., LUIK, R. M. & LEWIS, R. S. 2006. $Ca^{2+}$ store depletion causes STIM1 to accumulate in ER regions closely associated with the plasma membrane. *The Journal of Cell Biology,* 174**,** 803-813.

XIANG, M., MOHAMALAWARI, D. & RAO, R. 2005. A Novel Isoform of the Secretory Pathway Ca2+,Mn2+-ATPase, hSPCA2, Has Unusual Properties and Is Expressed in the Brain. *Journal of Biological Chemistry,* 280**,** 11608-11614.

XIE, R., XU, J., WEN, G., JIN, H., LIU, X., YANG, Y., JI, B., JIANG, Y., SONG, P., DONG, H. & TUO, B. 2014. The P2Y2 Nucleotide Receptor Mediates the Proliferation and Migration of Human Hepatocellular Carcinoma Cells Induced by ATP. *The Journal of Biological Chemistry,* 289**,** 19137-19149.

XU, P., LU, J., LI, Z., YU, X., CHEN, L. & XU, T. 2006. Aggregation of STIM1 underneath the plasma membrane induces clustering of Orai1. *Biochemical and Biophysical Research Communications,* 350**,** 969-976.

YANG, L., ZHANG, H. & BRUCE, J. E. 2009. Optimizing the detergent concentration conditions for immunoprecipitation (IP) coupled with LC-MS/MS identification of interacting proteins. *Analyst,* 134**,** 755-762.

YE, R. D. 2014. STIM1 for stimulation of phagocyte NADPH oxidase. *Blood,* 123**,** 2129-2130.

YU, F., SUN, L. & MACHACA, K. 2010. Constitutive recycling of the store-operated $Ca^{2+}$ channel Orai1 and its internalization during meiosis. *The Journal of Cell Biology,* 191**,** 523-535.

YUAN, J. P., ZENG, W., DORWART, M. R., CHOI, Y. J., WORLEY, P. F. & MUALLEM, S. 2009. SOAR and the polybasic STIM1 domains gate and regulate Orai channels. *Nature cell biology,* 11**,** 337-43.

ZÁMBÓ, V., SIMON-SZABÓ, L., SZELÉNYI, P., KERESZTURI, É., BÁNHEGYI, G. & CSALA, M. 2013. Lipotoxicity in the liver. *World Journal of Hepatology,* 5**,** 550-557.

ZHANG, H., CLEMENS, R. A., LIU, F., HU, Y., BABA, Y., THEODORE, P., KUROSAKI, T. & LOWELL, C. A. 2014. STIM1 calcium sensor is required for activation of the phagocyte oxidase during inflammation and host defense. *Blood,* 123**,** 2238-49.

ZHANG, H., ZHA, X., TAN, Y., HORNBECK, P. V., MASTRANGELO, A. J., ALESSI, D. R., POLAKIEWICZ, R. D. & COMB, M. J. 2002. Phosphoprotein analysis using antibodies broadly reactive against phosphorylated motifs. *The Journal of Biological Chemistry*.

ZHANG, S. L., YEROMIN, A. V., ZHANG, X. H.-F., YU, Y., SAFRINA, O., PENNA, A., ROOS, J., STAUDERMAN, K. A. & CAHALAN, M. D. 2006a. Genome-wide RNAi screen of $Ca^{2+}$ influx identifies genes that regulate $Ca^{2+}$ release-activated $Ca^{2+}$ channel activity. *Proceedings of the National Academy of Sciences,* 103**,** 9357-9362.

ZHANG, S. L., YU, Y., ROOS, J., KOZAK, J. A., DEERINCK, T. J., ELLISMAN, M. H., STAUDERMAN, K. A. & CAHALAN, M. D. 2005. STIM1 is a $Ca^{2+}$ sensor that activates CRAC channels and migrates from the $Ca^{2+}$ store to the plasma membrane. *Nature,* 437**,** 902-905.

ZHANG, W., HIRSCHLER-LASZKIEWICZ, I., TONG, Q., CONRAD, K., SUN, S. C., PENN, L., BARBER, D. L., STAHL, R., CAREY, D. J., CHEUNG, J. Y. & MILLER, B. A. 2006b. TRPM2 is an ion channel that modulates hematopoietic cell death through activation of caspases and PARP cleavage. *American journal of physiology. Cell physiology,* 290**,** C1146-59.

ZHAO, B., ZHONG, X., BAI, X., WANG, Q., SONG, B. & LI, L. 2014. Changes in Store-operated Calcium Channels in Rat Bladders With Detrusor Overactivity. *Urology,* 84**,** 491.e1-491.e6.

ZHENG, L., STATHOPULOS, P. B., LI, G.-Y. & IKURA, M. 2008. Biophysical characterization of the EF-hand and SAM domain containing $Ca^{2+}$ sensory region of STIM1 and STIM2. *Biochemical and Biophysical Research Communications,* 369**,** 240-246.

ZHOU, Y., MANCARELLA, S., WANG, Y., YUE, C., RITCHIE, M., GILL, D. L. & SOBOLOFF, J. 2009. The Short N-terminal Domains of STIM1 and STIM2 Control the Activation Kinetics of Orai1 Channels. *Journal of Biological Chemistry,* 284**,** 19164-19168.

ZHOU, Y., RAMACHANDRAN, S., OH-HORA, M., RAO, A. & HOGAN, P. G. 2010. Pore architecture of the ORAI1 store-operated calcium channel. *Proceedings of the National Academy of Sciences,* 107**,** 4896-4901.

ZHU, L., YANG, K., WANG, X. E., WANG, X. & WANG, C.-C. 2014. A Novel Reaction of Peroxiredoxin 4 towards Substrates in Oxidative Protein Folding. *PLoS ONE,* 9**,** e105529.

ZWEIFACH, A. & LEWIS, R. S. 1995a. Rapid inactivation of depletion-activated calcium current (ICRAC) due to local calcium feedback. *The Journal of General Physiology,* 105**,** 209-226.

ZWEIFACH, A. & LEWIS, R. S. 1995b. Slow Calcium-dependent Inactivation of Depletion-activated Calcium Current. STORE-DEPENDENT AND -INDEPENDENT MECHANISMS. *The Journal of Biological Chemistry,* 270**,** 14445-14451.